Rendiconti Lincei. Scienze Fisiche e Naturali (2023) 34:369–413
https://doi.org/10.1007/s12210-023-01153-5

REVIEW

Egyptian blue, Chinese blue, and related two-dimensional silicates: from antiquity to future technologies. Part A: general properties and historical uses

Marco Nicola[1,2] · **Roberto Gobetto**[1] · **Admir Masic**[3]

Received: 4 November 2022 / Accepted: 2 March 2023 / Published online: 10 April 2023

Abstract
The ancient Egyptian blue pigment was developed over 5000 years ago and was used extensively for around four millennia until its use mysteriously declined dramatically during the Early Middle Ages. It recently attracted a lot of attention along with some related materials, leading to a fast-growing number of applications in fields, such as sensors, solar concentrators, energy-saving, and medicine. The new surge in interest began in 1996 with the discovery of their intense NIR photoluminescence that surprisingly can be triggered even by visible light. In 2013, the possibility of exfoliating them and producing NIR luminescent nanosheets was established, expanding the family of 2D nanomaterials. More recently, the discovery of their high antibacterial effects and biocompatibility, and very promising optical, electric and magnetic properties, has further boosted their applications. The characteristics of Egyptian blue are due to its main component: the very stable crystalline compound $CaCuSi_4O_{10}$. This tetragonal sheet silicate is the synthetic analogous of the rare cuprorivaite mineral. In Part A of this review, we summarize the historical uses and main properties (i.e., composition, structure, color, stability, luminescence, and biological activity) of cuprorivaite and related 2D silicates, i.e., $BaCuSi_4O_{10}$ (the main constituent of the ancient pigment Chinese Blue), $BaCuSi_2O_6$ (the main constituent of the ancient pigment Chinese Purple), $SrCuSi_4O_{10}$ (synthetic analogous of wesselsite) and $BaFeSi_4O_{10}$ (synthetic analogous of gillespite). The Part B of the review will focus on the modern rediscovery of these materials, their modern synthesis and exfoliation, and the innovative applications based on their properties.

Keywords Egyptian blue · Han blue · Han purple · Cuprorivaite · Wesselsite · Gillespite · Luminescence

1 Egyptian blue, Chinese blue, and related 2D silicates

Egyptian Blue (EB) is an artificial blue pigment of mineral origin used also to mold small objects thanks to its vitreous ceramic nature (Lucas and Harris 1962; Chase 1971; Delamare 1997). It was developed in Egypt during the Early Bronze Age, more than 5000 years ago (Corcoran 2016), and is considered to be the first true synthetic pigment ever produced by humans (Riederer 1997; Warner 2011; Corcoran 2016; Greco 2022).

EB largely owes its color and its extraordinary features to the crystals of $CaCuSi_4O_{10}$ (also $CaO{\cdot}CuO{\cdot}4SiO_2$ or calcium copper tetrasilicate) that form during its manufacturing. This compound is the artificial analogous of a mineral very rare in nature, i.e., cuprorivaite (Mazzi and Pabst 1962). Natural cuprorivaite (see Fig. 1) forms likely under hydrothermal conditions, i.e., high temperature and high-pressure conditions that occur beneath the Earth's surface in the presence of water (Giester and Rieck 1994; Warner 2011; Johnson-McDaniel et al. 2015; Cairncross and Rumsey 2022). It was identified as a new mineral by Minguzzi in 1938 on a rock specimen from Mount Vesuvius (Minguzzi 1938). Some 20 years later, it has been correlated to the chemical composition of EB (Schippa and Torraca 1957; Pabst 1959; Mazzi

✉ Marco Nicola
nicola@adamantionet.com

✉ Roberto Gobetto
roberto.gobetto@unito.it

[1] Department of Chemistry, University of Torino, Via Giuria, 7, 10125 Turin, Italy

[2] Adamantio Srl, Science in Conservation, Via Napione, 29/A, 10124 Turin, Italy

[3] Department of Civil and Environmental Engineering, Massachusetts Institute of Technology, Cambridge, MA 02139, USA

Fig. 1 Natural cuprorivaite from Nickenicher Weinberg, Nickenich, Andernach, Eifel, Rhineland-Palatinate, Germany. Metric reference: 50 µm. Reproduced with permission from mindat.org © Christof Schäfer (finder of the mineral). Photo by Marko Burkhardt

and Pabst 1962), and since then, the terms «cuprorivaite» and «Egyptian blue» have been often used as synonymous (Mazzi and Pabst 1962; Gaines et al. 1997).

However, artificially produced EB, unlike natural cuprorivaite, is a multicomponent material (Ullrich 1979; Tite et al. 1984; Hatton et al. 2008) and generally contains a certain amount of amorphous silicate glass (Pradell et al. 2006) as well as some minor amounts of other crystalline phases relative to silica (quartz, cristobalite, or tridymite), silicates (e.g., wollastonite), and oxides (e.g., tenorite) (Jaksch et al. 1983; Etcheverry et al. 2001; Pradell et al. 2006; Aliatis et al. 2010). Due to its rarity, natural cuprorivaite has never been considered a blue pigment or a raw material (Riederer 1997; Berke and Wiedemann 2000). However, artificial EB was widely used in antiquity, although in those times and places other natural mineral alternatives were known and occasionally have been reported, e.g., azurite, lapis lazuli, and glaucophane (Kakoulli 2009). Countless archaeological finds show that for over 3000 year EB was nearly the only blue pigment used in North Africa, Western Asia, and Europe until it was almost abandoned during the Early Middle Ages (see Sect. 4) (Scott 2016; Nicola et al. 2019; Švarcová et al. 2021; Sgamellotti and Anselmi 2022).

There are some other materials closely related to EB that often show similar intriguing features. Two of them, analogously to EB, have been used in antiquity as pigments and have been named «Chinese Purple» (CP) and «Chinese Blue» (CB), since they were developed in ancient China (Berke et al. 2009). The main constituents of CP and CB are two layered barium and copper silicates, $BaCuSi_2O_6$ and $BaCuSi_4O_{10,}$ respectively. The main constituent of CB has a structure analogous to that of $CaCuSi_4O_{10}$ in EB, the only difference being the presence of Ba^{2+} instead of Ca^{2+}. The main constituent of CP is strictly related to $BaCuSi_4O_{10}$ in CB but has a different framework within a layer (Wiedemann and Berke 2001) (see Sect. 3.2). Although CP and CB have a composition and production technology quite similar to that of EB, they were developed in China more than two thousand years later, most likely independently of EB (Berke 2007; Qin et al. 2016). Quite recently the two extremely rare natural analogs of the main constituents of CB and CP have been also identified, both in the Wessels mine, Kalahari Manganese Field, South Africa (Giester and Rieck 1994; Rieck et al. 2015). They were named, respectively, effenbergerite and colinowensite and are sometimes reported in association with the mineral wesselsite ($SrCuSi_4O_{10}$) which is the structural analogous of cuprorivaite with Ca^{2+} replaced by Sr^{2+} (Giester and Rieck 1996). Cuprorivaite, effenbergerite, and wesselsite share a similar structure and the same formula $MCuSi_4O_{10}$ (M=Ca, Sr, and Ba) and belong to the wider gillespite-type group of minerals $MQSi_4O_{10}$ (Pabst 1959; Salguero et al. 2014; Chen et al. 2016), where Q is an appropriate divalent cation that is basically in square planar coordination (Burzo 2009). The gillespite mineral that gives its name to the whole group is $BaFeSi_4O_{10}$ and was described for the first time by Schaller in 1922 as a new mineral present in a rock specimen from the glacial moraine near the head of Dry Delta, Alaska (Schaller 1922; Pabst 1943). It is analogous to effenbergerite with Cu^{2+} replaced by Fe^{2+}.

Some other compounds that show the structure of gillespite-group minerals are known. They are $MCrSi_4O_{10}$ with M=Ca, Sr and Ba (Belsky et al. 1984; Miletich et al. 1997), and probably also $BaMgSi_4O_{10}$ (Yuan et al. 2012; Zhong et al. 2020). However, it seems that so far, they have not yet been found as natural minerals.

Some attempts to replace Fe^{2+} with Co^{2+}, Ni^{2+}, and Mn^{2+} to produce other compounds with gillespite structure have been reported (Hassanein 1969; Nicolini and Porta 1970; Masse et al. 1999; Lee et al. 2013; Szubka et al. 2022) as well as to produce isostructural members with Ge replacing Si (Hassanein 1969; Riederer 1997).

Furthermore, the production of roughly monoatomic sheets of pure crystalline hydrated silica starting from leached gillespite has been pioneered by Schaller (1929) and by Pabst (1958), and in the near future, it may become more attractive due to the recent improvement in the synthesis of artificial gillespite (Bloise 2018). This kind of intriguing 2D hydrated silica could be very promising for some new technologies, such as for the production of zeolites (Frondel

1979; Marler and Gies 2012) and in many other fields (Fang et al. 2015).

2 Nomenclature

EB is listed in the Colour Index with the Generic Name PB31 and the Constitution Number 77437 (colour-index.com). Some common names other than «Egyptian Blue» in use for EB include «Alexandrian Blue», «Pozzuoli Blue», «Vestorian Blue», and «Pompeian Blue» (Riederer 1997). Those names are overall related to the production and use of EB in Roman times (see Sect. 4). In the literature, EB is also widely referred to as «blue frit» (Hatton et al. 2008; Warner 2011; Lazzarini and Verità 2015; Grifa et al. 2016). However, some scholars pointed out that referring to EB as «blue frit» could be misleading, since it seems that there is some disagreement about the proper use of the term «frit» (Lee and Quirke 2000; Nicholson and Henderson 2000; Clegg 2014). To avoid ambiguity in terminology, in this work «Egyptian blue» (shortened «EB») will be used to refer to artificially produced modern or archaeological specimens of pigment or ceramic material (i.e., mainly constituted by $CaCuSi_4O_{10}$ but overall containing also other amorphous or crystalline phases), while «cuprorivaite» will be used for the natural or artificial pure crystalline $CaCuSi_4O_{10}$. May be worth noting that the terminology "Egyptian blue" has also been used as a way to identify a web color (Wenerstrom and Kantardzic 2011) or a specific tone of blue, e.g., with the following standardized set of values in different color coordinates systems: Hex Code: #1034A6; RGB: 16, 52, 166; CMYK: 90%, 69%, 0%, 35%; HSV/HSB: 226°, 90%, 65%; Closest Pantone: 286 C (color-name.com). However, such kind of standardizations should be used carefully and are possibly misleading, since EB does not have a specific color but is associated with a range of colors (see also Sect. 3.3).

CP and CB pigments, unlike EB, have no Generic Name in the Colour Index nor they have been in general standardized in color coordinates systems. CP and CB are widely known also with their previous names, i.e., «Han purple» and «Han blue» but it has been pointed out that those terminologies could be misleading (Berke et al. 2009). Indeed, the former names of these two ancient artificial pigments based on barium–copper silicates derive from a proposal by FitzHugh and Zycherman that related them to the Han dynasty, since the finds in which they were initially identified mainly belong to that period, i.e., 206 BCE–220 CE (FitzHugh and Zycherman 1983, 1992). However, more recently it turned out that both pigments were highly widespread even long before the times of the Han Dynasty (Ma et al. 2006), thus the renaming (Berke et al. 2009). Analogously to EB, in this work «Chinese Purple» (shortened «CP») and «Chinese Blue» (shortened «CB») will refer to the respective archaeological specimens or modern products obtained by artificial syntheses (i.e., overall containing also amorphous or crystalline phases other than $BaCuSi_2O_6$ and $BaCuSi_4O_{10,}$ respectively). The terms «colinowensite» and «effenbergerite» will be, instead, reserved for the natural or artificial pure crystalline compounds $BaCuSi_2O_6$ and $BaCuSi_4O_{10,}$ respectively.

Artificial wesselsite ($SrCuSi_4O_{10}$) has been occasionally found in anthropogenic ancient blue pigments. It can be argued that its presence occurred unintentionally due to difficulties in distinguishing the relatively rare Sr-containing minerals from Ca analogs (Berke and Wiedemann 2000). $BaFeSi_4O_{10}$ (gillespite), $MCrSi_4O_{10}$ (M=Ca, Sr or Ba), and $BaMgSi_4O_{10}$ have not been so far found as a component of any ancient pigment. Wesselsite, gillespite, and the remaining two-dimensional silicates related to EB are not commonly used as pigments and have no common names being generally known only by their own mineralogical or chemical names.

3 General properties

3.1 Composition

3.1.1 Composition of Egyptian blue

EB is mainly constituted by cuprorivaite and it commonly contains some other minor components mainly due to incomplete reaction, unbalanced reagents, additives (i.e., fluxes, see Sect. 4.2), impurities from the reactants, and contamination from the crucibles or the production technique utilized. Furthermore, although EB is a very stable material, some compounds within it can also be the results of deterioration processes, e.g., due to overheating during the production (e.g., cristobalite or tridymite) or severe and prolonged harsh conditions as reported, i.e., in some archaeological findings (see also Sects. 3.4 and 3.3.11).

In EB produced through the traditional melt-flux synthesis (see Sect. 3.3.4), the impurities are often concentrated in a glassy matrix surrounding practically pure cuprorivaite crystals (Delamare 1997). However, the occurrence of minor amounts of other crystalline phases is common, i.e., oxides or silicates (Tite et al. 1984; Bouherour et al. 2001; Nicola et al. 2019; Seymour et al. 2020). Overall the presence of excess silica (10–30%) above that necessary to produce cuprorivaite has been commonly reported in archaeological specimens as well as a slight excess of Ca or Cu, associated with the presence of $CaSiO_3$ (wollastonite) or black copper oxide CuO (tenorite), respectively (Jaksch et al. 1983; Tite et al. 1984; Pagès-Camagna et al. 1999; Hatton et al. 2008;

Fontana et al. 2020). The composition of the glassy matrix consists mainly of Si from excess silica, Ca and Cu from unreacted reagents, and Na and K from the fluxing agent (see Sect. 4.2.3). Al, Mg, and Fe, and to a minor extent Mn, Cr, and Ti are common impurities (Hatton et al. 2008; Lazzarini and Verità 2015; Baraldi et al. 2017; Fontana et al. 2020). Along with some Na and K, they could likely derive from silicate impurities (e.g., feldspar) present in the silica source (Hatton et al. 2008), or from the terracotta crucibles traditionally used for the production process (Mazzocchin et al. 2004; Warner 2011; Grifa et al. 2016; Nicola et al. 2019). Cl, S, and P impurities can derive from specific contaminants in the reactants (e.g., chlorides, sulfates, phosphates, etc.) and are generally considered to be mainly associated with fluxes (Jaksch et al. 1983; Giménez et al. 2017; Dariz and Schmid 2022) but their presence can be as well due to other features, e.g., S from Cu_2S ores used as a source of copper (Dariz and Schmid 2021). The presence of As, Sn, Pb (El Goresy et al. 1998), and Zn (Ingo et al. 2013; Nicola et al. 2019) in the glass matrix or as oxides and silicates have been correlated with the copper source (i.e., copper alloys). The presence of Pb and Zn has been thought to be possibly also intentional and has been correlated with their function as fluxes (Nicola et al. 2019; Rodler and Kostomitsopoulou Marketou 2022). Traces of Co, Pt, Ni, Mg, Sr, Ba, Sb, Ag, Rb, Y, Zr, Nb, Sc, V, La, Ce, and C have also been considered in archaeological specimens (Jaksch et al. 1983; Tite et al. 1984; Riederer 1997; Ingo et al. 2013; Clegg 2014; Grifa et al. 2016; Zaina et al. 2019; Oudbashi and Hessari 2020). For example, the sporadic presence of a minor amount of Co has been investigated by Tite et al. to assess a possible intentional adding to improve the color of EB (Tite et al. 1984), while the content of Pt has been taken into account by Zaina et al. to obtain information on the provenance of EB, since Pt presence might suggest that EB was produced and imported from Eastern Desert of Egypt or Nubia (Zaina et al. 2019). Indeed, in archaeological science, the characterization of impurities in EB is extensively used as a method to try to trace its provenance and production technique (Nicola et al. 2019; Fontana et al. 2020; Martín et al. 2020; Seymour et al. 2020; Coccato et al. 2021; Dariz and Schmid 2021, 2022). For this purpose also isotopic techniques have been used on lead impurities and also on copper (Rodler et al. 2017, 2021).

3.1.2 Composition of Chinese blue and Chinese purple

EB has been by far more studied in comparison to its Chinese counterpart CB and the related CP. It could be roughly argued that archaeological CB and CP are quite similar to EB except for the fact that, instead of $CaCuSi_4O_{10}$ (cuprorivaite), their main constituents are, respectively, $BaCuSi_4O_{10}$ (effenbergerite) and $BaCuSi_2O_6$ (colinowensite). However, the system $BaO–CuO–SiO_2$ is much more complex than the $CaO–CuO–SiO_2$ one (Wiedemann and Berke 2001), and thus some other differences are present between the average composition of EB and that of CB and CP. The main difference is that at least four different stoichiometric barium–copper silicates can form during the production of CB and CP. Besides $BaCuSi_4O_{10}$ and $BaCuSi_2O_6$, they are $BaCu_2Si_2O_7$ and $Ba_2CuSi_2O_7$.

- $BaCu_2Si_2O_7$ has been named Chinese dark blue (Berke et al. 2009). It is a dull blue compound corresponding to the mineral scottyite. It has been first identified in nature only recently, analogously to effenbergerite, colinowensite, and wesselsite in the Wessels mine, Kalahari Manganese Field, South Africa (Yang et al. 2013). It has been synthesized with modern hydrothermal synthesis to be used as a pigment (Chen et al. 2014b; Rendón-Angeles et al. 2021) and has been extensively studied as an intriguing example of a spin $S = 1/2$ quasi-one-dimensional antiferromagnet (Tsukada et al. 1999; Glazkov et al. 2005, 2011).
- $Ba_2CuSi_2O_7$ has been seldomly referred to as Chinese light blue (Ma et al. 2016). It is a whitish compound that has not yet been found as a natural mineral. It exists generally in two slightly different forms, i.e., α- and β-$Ba_2CuSi_2O_7$ differing in the solid state structure just in the rotational orientation of the disilicate anions (Du et al. 2003; Berke et al. 2009). Only β-$Ba_2CuSi_2O_7$ can be produced via solid-state synthesis, while α-$Ba_2CuSi_2O_7$ can be produced only via hydrothermal synthesis (Du et al. 2003). β-$Ba_2CuSi_2O_7$ is produced at around 600 °C and seems to show a higher thermal sensitivity in comparison to the other three barium–copper silicates.

$BaCu_2Si_2O_7$ and $Ba_2CuSi_2O_7$ similar to cuprorivaite (EB) and related two-dimensional silicates have a layered structure but unlike them they are sorosilicates, i.e., less condensed silicates characterized by the presence of isolated double tetrahedral groups $Si_2O_7^{6-}$ (Berke et al. 2009) (see also the following 3.2). For this reason, $BaCu_2Si_2O_7$ and $Ba_2CuSi_2O_7$ will not be a focus of this work, and will not be further detailed. However, it has to be noted that $BaCu_2Si_2O_7$ has been occasionally found along with CB and CP in archaeological specimens (Berke et al. 2009; Xia et al. 2014; Ma et al. 2016; Zhang et al. 2019), while $Ba_2CuSi_2O_7$ has not yet been identified in any archaeological findings (Lin 2018) and it is unlikely that has ever been historically used as a pigment due to its poor color features and the difficulties in its preparation (Berke et al. 2009).

Other important features that differentiate CB and CP from EB are the following:

- other barium silicates can be present within CB and CP, e.g., $BaSiO_3$ and $Ba_4Si_6O_{16}$ (Sheptyakov et al. 2012;

Chen et al. 2014a). They can form also from impurities, e.g., $BaSnSi_3O_9$ (Zhang et al. 2019)

- Pb has been historically largely preferred as fluxing agent for CP and CB (Bouherour et al. 2001; Li et al. 2015a; Zhang et al. 2019)
- $BaSO_4$ is sometimes present and has been associated with the source of Ba (Li et al. 2015b)
- red Cu_2O can be present (especially in CP) and has been considered responsible for a possible shift in the color of the pigments toward purple or red (Berke 2007) (see also Sect. 3.3.8).

3.1.3 Other 2D silicates related to Egyptian blue

The other EB-related 2D silicates of the gillespite group (i.e., wesselsite, gillespite, $MCrSi_4O_{10}$ (M=Ca, Sr, or Ba), and $BaMgSi_4O_{10}$) have only recently been artificially produced and have been obtained in fairly pure form, with minor impurities only due to the specific synthetic route employed. For further details, it is suggested to consult the specific sources in the literature (Belsky et al. 1984; Miletich et al. 1997; Inoue et al. 2009; Bloise 2018; Zhong et al. 2020).

3.2 Structure

3.2.1 Cuprorivaite and other MCuSi4O10 (M=Ca, Sr, Ba)

Cuprorivaite ($CaCuSi_4O_{10}$) and the other two alkaline-earth copper tetrasilicates (i.e., effenbergerite or $BaCuSi_4O_{10}$ and wesselsite or $SrCuSi_4O_{10}$) are phyllosilicates that belong to the gillespite-group and crystallize in the tetragonal system, space group *P4/ncc*, $Z=4$ (Gaines et al. 1997; Kendrick et al. 2007).

Their structure was first established by single-crystal X-Ray Diffraction in 1959 (Pabst 1959) and subsequently reexamined and refined several times (Janczak and Kubiak 1992a; Bensch and Schur 1995; Mirti et al. 1995; Kendrick et al. 2007; Burzo 2009; Barbar et al. 2017) using also Rietveld refinement of powder neutron diffraction (Chakoumakos et al. 1993; Hughes et al. 1997; Knight et al. 2010), Cu K-edge XAFS, EXAFS, and XANES (Hughes et al. 1997; Pagès-Camagna et al. 2006), Electron Paramagnetic Resonance (EPR) (Ford and Hitchman 1979; Mirti et al. 1995; Orsega et al. 2006; Binet et al. 2021) and high-resolution magic angle spinning (MAS) ^{29}Si Nuclear Magnetic Resonance (NMR) (Stebbins 2017). Vibrational

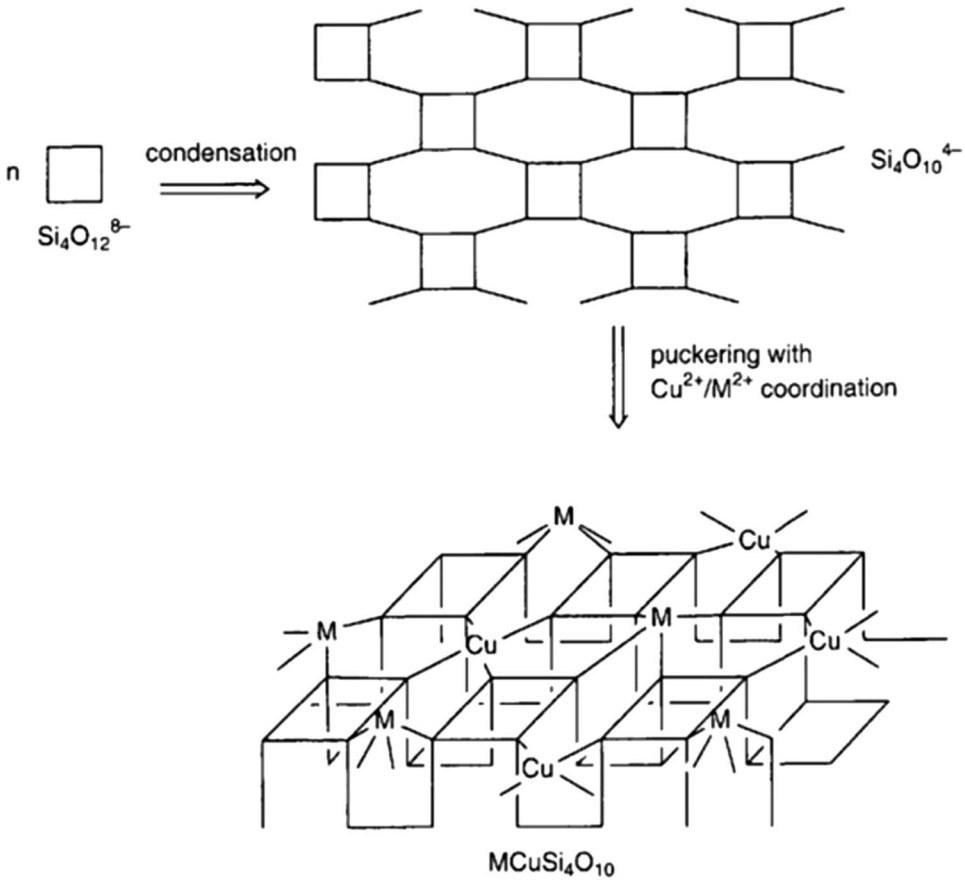

Fig. 2 Schematic sketch of the condensation process of a four-membered silicate ring ($Si_4O_{12}^{8-}$) to build up a $Si_4O_{10}^{4-}$ layer and its puckering induced by coordination of Cu^{2+} and M^{2+} (M=Ca, Sr, Ba). Adapted from Bouherour et al. (2001)

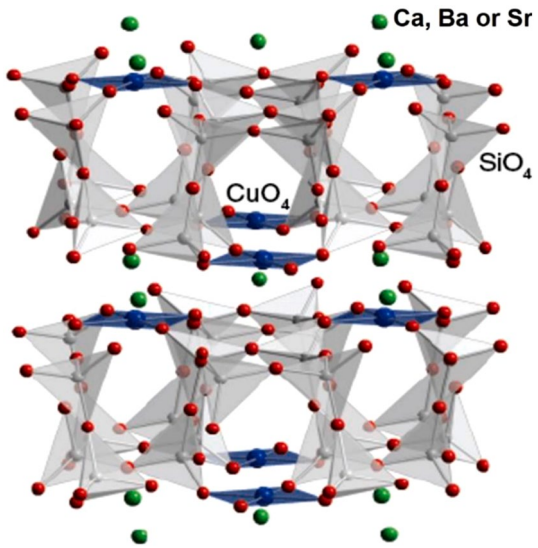

Fig. 3 Crystal structure of $MCuSi_4O_{10}$. In blue are shown Cu^{2+} ions, in gray the silicate tetrahedra. Reproduced with permission from Sgamellotti and Anselmi (2022). Original source: chemtube3d.com

and spectroscopic properties have also been studied, mainly using UV–Vis, FT-IR, and Raman spectroscopies (Mirti et al. 1995; McKeown and Bell 1997; Bruni et al. 1999; Baraldi et al. 2001a, 2006; Bouherour et al. 2001; Edreira et al. 2003; Ma et al. 2006; Pagès-Camagna et al. 2006; Barbar et al. 2017; Seymour et al. 2020). In this regard, it may be worth noting that spectroscopic details about EB, CB, and CP bulk commercial pigments (Kremer Pigmente) can be found in public databases, such as the CCR Pictorial Material Database (i.e., FORS spectra in the range 350–2200 nm, ATR–FTIR, and XRF) (Cavaleri et al. 2017), the FTIR and Raman IRUG Spectral Database (irug.org), and the FORS Spectral Database of Historical Pigments in Different Binders (Cosentino 2014).

The layered structure of cuprorivaite, effenbergerite, and wesselsite is sketched in Figs. 2, 3, and 4. It is built up of analogous nanosheets each constituted by a virtually endless layout of four and eight-membered rings of corner-shared SiO_4 tetrahedra (Berke 2007). Each SiO_4 tetrahedron is connected to two neighboring tetrahedra in the same square ring through two identical bridging oxygens O2 and to a third tetrahedron belonging to a different square ring through a different bridging oxygen O1 (Knight and Henderson 2007; Warner 2011). The fourth oxygen is a non-bridging oxygen anion O3 (Knight and Henderson 2007). Within each square ring, the four apical anions O3 all point in the same direction. Each square ring of tetrahedra is connected through the four O1 to four other identical square rings whose apical oxygen anions O3 all point in the opposite direction (Warner 2011).

The nanosheet of tetrahedra is puckered by Cu^{2+} ions that form CuO_4 groups by linking four oxygen anions O3 pointing in the same direction and belonging to four different (and thus non-directly adjacent) square-rings (Berke et al. 2009; Warner 2011). The Cu–O bonds are all equal in length (i.e., about 1.91 Å) and Cu^{2+} in the CuO_4 groups are in an almost perfect D_{4h} square planar geometry of coordination due both to lattice constraints and the Jahn–Teller effect (Mirti et al. 1995; Hughes et al. 1997; Kendrick et al. 2007; Berke et al. 2009; Knight et al. 2010; Sgamellotti and Anselmi 2022). Indeed, the stability of Cu^{2+} in square planar coordination is favored by the Jahn–Teller effect, since for some specific electronic configurations (and especially the d^9 in Cu^{2+}), the square planar symmetry often turns to be the preferred

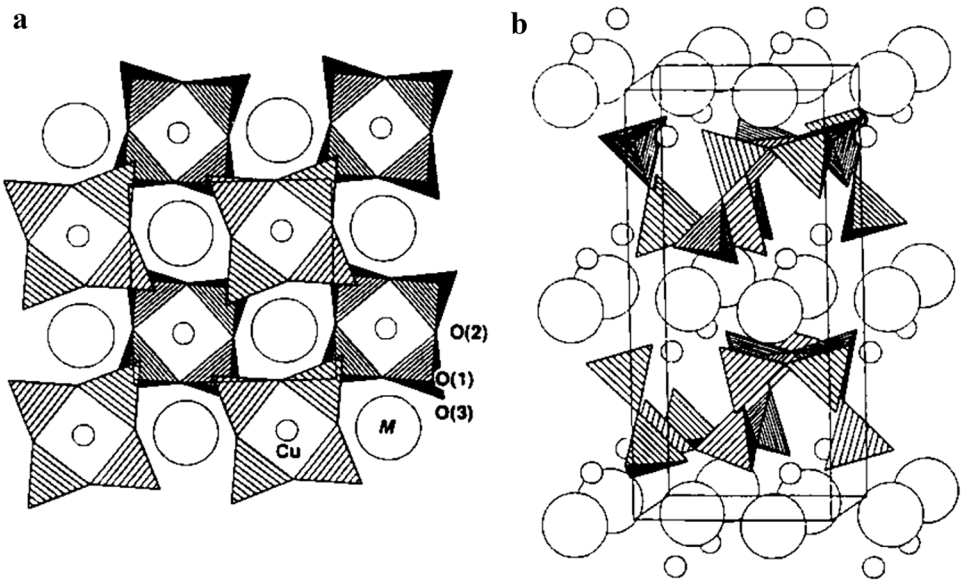

Fig. 4 Projections of: **a** one-half of the cell (outlined) thickness viewed along [001] and **b** axiometric view with c vertical. The shaded tetrahedra represent SiO_4 units, the large circles, alkaline-earth ions, and the small circles, Cu atoms. Reproduced with permission from Chakoumakos et al. (1993)

one in comparison with the elongated tetragonal (T_d) coordination (Huheey 1978). The square-planar coordination descends as an extreme case of the progressive distancing of negatively charged ligands orthogonal to the square plane and their ultimate removal, as is the case of the oxygen coordinating Cu^{2+} ion in $MCuSi_4O_{10}$ (M=Ca, Sr, Ba) (Warner 2011). Indeed, in this case, there are no anions of any sort on the normal of the CuO_4 square groups, and this might be considered an ideal case (Pabst 1959).

Due to the puckering produced by Cu^{2+}, each $[CuSi_4O_{10}]^{2-}$ nanosheet results in a virtually infinite double layer of square rings of SiO_4 tetrahedra. The two layers forming each nanosheet are internally strongly connected via the bridging oxygens O1. It has to be noted that the square rings of SiO_4 tetrahedra and the CuO_4 groups display specific rotations and tilting within the double layer (Chakoumakos et al. 1993; Knight et al. 2010). The nanosheets $[CuSi_4O_{10}]^{2-}$ are joined together by alkaline earth M^{2+} (M = Ca, Sr, or Ba) in a distorted cubic geometry (Knight and Henderson 2007). The M^{2+} ions are in eightfold coordination with four coordination sites in each neighboring nanosheet. Two of them are oxygen anions O3 also coordinated to Cu^{2+} in different CuO_4 groups, while the other two are O2 bridging SiO_4 tetrahedra belonging to distinct square rings (Giester and Rieck 1994; Knight and Henderson 2007; Warner 2011).

The distance between two neighboring nanosheets depends largely on the dimension of the M^{2+} ions. It increases in the series Ca^{2+}, Sr^{2+}, and Ba^{2+} reaching a maximum of about 4.5 Å for Ba^{2+} (Burzo 2009). The shortest Cu^{2+}–Cu^{2+} distance is between adjacent layers and is about 5.73 Å for cuprorivaite and 6.08 Å for effenbergerite. Within a layer, each Cu^{2+} ion has, instead, 8 neighbors at 7.25–7.30 Å (Binet et al. 2021). Despite their high concentration, Cu^{2+} ions are weakly antiferromagnetically coupled and can be roughly considered independent Cu^{2+} ions (Warner 2011; Binet et al. 2021). The weak coupling occurs within a single $[CuSi_4O_{10}]^{2-}$ nanosheet, since the anion sublattice transmitting the super-exchange interactions is disrupted between the neighboring nanosheets (Binet et al. 2021). The type of M^{2+} (i.e., Ca^{2+}, Sr^{2+}, or Ba^{2+}) produces only minor variations in the double layer arrangement of SiO_4 tetrahedra within the $[CuSi_4O_{10}]^{2-}$ nanosheets (Miletich et al. 1997; Kendrick et al. 2007). However, Knight et al. point out that a slight increase in the magnitude of rotation and tilting of tetrahedra and in the rotation of CuO_4 groups occurs to accommodate the larger and more electropositive Ba^{2+} within the crystal structure (Knight et al. 2010).

According to Hughes et al. (1997), the refined characteristic unit cell parameters for the three alkaline-earth copper tetrasilicates are the following:cuprorivaite $a = b = 7.30128(4)$ Å and $c = 15.12370(15)$ Åwesselsite $a = b = 7.36964(3)$ Å and $c = 15.57986(9)$ Åeffenbergerite $a = b = 7.44534(6)$ Å and $c = 16.13971(22)$ Å

Small deviations from these values are reported by different authors (Janczak and Kubiak 1992a; Chakoumakos et al. 1993; Giester and Rieck 1994, 1996; Mirti et al. 1995; Kendrick et al. 2007; Knight et al. 2010; Masunaga et al. 2015).

The parameters of mixed alkaline-earth systems have been studied by Kendrick et al. in M^1_{1-x} $M^2_x CuSi_4O_{10}$, where M^1, M^2=Ca, Sr and Ba. They report that it is possible to successfully form a solid solution across the whole series of x when M^1 and M^2 are both $Ca^{2+}$and Sr^{2+} or else $Sr^{2+}$and Ba^{2+} but it is not possible to produce a solid solution when Ca^{2+} and Ba^{2+} are chosen together as M^1 and M^2. They explain this feature by assuming that the excessive difference in ionic radii between Ca^{2+} and Ba^{2+} prevents the occurrence of a solid solution and, instead, leads to the formation of the two distinct endmembers, i.e., cuprorivaite and effenbergerite (Kendrick et al. 2007). Knight and colleagues accurately studied the system $Sr_{1-x}Ba_xCuSi_4O_{10}$ (Knight et al. 2010) accounting also for the minor structural variations occurring at cryogenic temperatures (Knight and Henderson 2007). Masunaga et al. point out that at least for effenbergerite, two minor phase transitions occur at low temperatures (i.e., 87 K and 103 K) slightly differing the lengths of the a and b lattice parameters, thus breaking the tetragonal symmetry (Masunaga et al. 2015).

3.2.2 Structure of gillespite and its other group members

The structure of gillespite (i.e., $BaFeSi_4O_{10}$) was first described by Pabst in 1943 (Pabst 1943) and was used by the same author as a model for the analogous structure of the three alkaline earth copper tetrasilicates described in the previous paragraph (Pabst 1959). The structure has been refined and studied several times and has been reviewed by Burzo (2009). Unlike the three alkaline earth copper tetrasilicates, gillespite undergo an intriguing reversible first-order phase transition induced by an increase in applied pressure. The transformation begins in the range of 1.2–2.6 GPa and has been first described by Strens (Strens 1966). It is associated with a shift in color from red to blue and it is due to a change in the iron coordination from square-planar to flattened tetrahedral (Knight and Henderson 2007). Single crystal, high-pressure X-ray diffraction measurements showed that the phase transformation is associated with a structural phase transition from the tetragonal space group *P4/ncc* to the orthorhombic space group $P2_12_12$. The two distinct phases are called, respectively, Gillespite I (tetragonal) and Gillespite II (orthorhombic) (Hazen and Burnham 1974; Hazen and Finger 1983). Gillespite shows a rare pattern of isolated Fe^{2+} in square-planar coordination with a high-spin $S = 2$ state (Schofield et al. 1998; Pascualini et al. 2015).

All the three alkaline earth chromium tetrasilicate $MCrSi_4O_{10}$ (M=Ca, Sr, Ba) have been synthesized, although they have not yet been found in nature (Belsky et al. 1984;

Miletich et al. 1997). They have a structure completely analogous to that of the minerals of the gillespite-group with only minor variation in the unit cell parameters. Analogously to what happens in alkaline earth copper silicates, the type of M^{2+} (Ca^{2+}, Sr^{2+}, Ba^{2+}) affects mainly the c lattice parameter. The substitution of the Q^{2+} in the $MQSi_4O_{10}$ series ($Q=Cu^{2+}$, Cr^{2+}, Fe^{2+}) leads, instead, to only small changes in cell unit, equally influencing the a and b parameters, without any significant change in symmetry. Analogously to what happens for $MCuSi_4O_{10}$, also in $MCrSi_4O_{10}$ the relatively high stability of the compound is favored by the Jahn–Teller effect (Belsky et al. 1984; Miletich et al. 1997). The Cr^{2+} cation in $MCrSi_4O_{10}$ occupies a square-planar coordinated site unique in oxide crystal chemistry (Miletich et al. 1997).

$BaMgSi_4O_{10}$ seems to be another gillespite-group member that has not yet been found as a natural mineral. It has been first described by Toropov et al. to crystallize in the tetragonal space group *P4/ncc* and to be isostructural with gillespite (Toropov 1962). More recently, different authors synthesized and characterized it (Inoue et al. 2009; Yuan et al. 2012; Zhong et al. 2020). However, there is some debate about the exact structure of this compound relying on a different route of synthesis and some diffractograms discrepancies (Inoue et al. 2009; Zhong et al. 2020). Zhong et al. point out that more work is needed to reveal the exact crystal structure of this compound that if confirmed should contain a peculiar and intriguing Mg^{2+} in roughly square-planar coordination (Zhong et al. 2020).

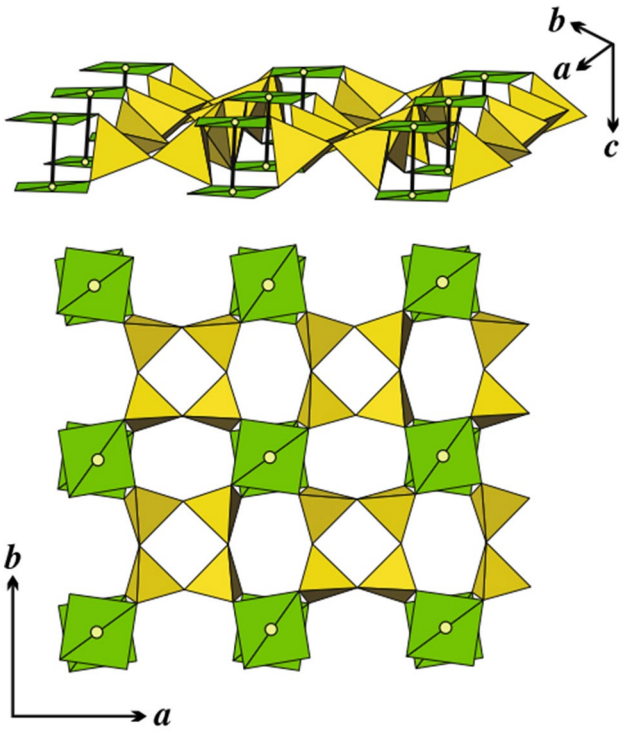

Fig. 5 Crystal structure of $BaCuSi_2O_6$. Different projections of a single bilayer of Cu atoms, which is equivalent to one layer of spin dimers. Si atoms are in the yellow tetrahedra and coupled to both upper and bottom sites of a dimer (colour figure online). Reproduced with permission from Stern et al. (2014)

3.2.3 Structure of $BaCuSi_2O_6$, i.e., colinowensite

The main constituent of CP, i.e., $BaCuSi_2O_6$ (colinowensite) also crystallizes in the tetragonal system but unlike the other 2D alkaline-earth copper silicate described so far, is not a member of the gillespite-group and is not a phyllosilicate. Indeed, it is a cyclosilicate (Rieck et al. 2015). Its crystal structure has been at first assigned to space group $I\,\overline{4}\,m2$ ($Z=4$) (Finger et al. 1989; Janczak and Kubiak 1992b) but Sparta and Roth in 2004 proposed an improved model placing it in the space group $I4_1/acd$ with $Z=16$ ($a=10.009(2)$, $c=22.467(6)$ Å) (Sparta and Roth 2004). Their model has been confirmed by further studies (Chen et al. 2014b; Stern et al. 2014; Rieck et al. 2015). Sparta and Roth also described a first-order phase transition at high temperature (610 K) when superstructure reflections disappear and the structure model shifts to space group *I4/mmm* with $Z=4$. Another first-order phase transition occurs at low temperature (~ 107 K) and is associated with an incommensurately modulated orthorhombic structure with space group *Ibam* (Samulon et al. 2006; Sheptyakov et al. 2012; Chen et al. 2014b). Low-Temperature High-Resolution Solid-State (cryoMAS) NMR has been used to investigate this structure that results composed of two different kinds of CuO_4–CuO_4 dimers (Stern et al. 2014) (see below within this paragraph).

The low-temperature phase transition can be avoided down to about 1.5 K stabilizing the structure of $BaCuSi_2O_6$ with a partial replacement of Ba with Sr in $Sr_xBa_{1-x}CuSi_2O_6$ ($x<0.3$) (Puphal et al. 2016; van Well et al. 2016; Song et al. 2019). It may be worth noting that the existence of other compounds isostructural with CP, e.g., pure $SrCuSi_2O_6$ has so far not been reported (Puphal et al. 2016; Song et al. 2019). The non-existence of $CaCuSi_2O_6$ has been related to its instability (Berke and Wiedemann 2000; Bouherour et al. 2001). Compounds such as $CaMgSi_2O_6$ (diopside), $CaFeSi_2O_6$ (hedenbergite), $CaCoSi_2O_6$ (copside) and $CaNiSi_2O_6$ (niopside) exist but display pyroxene structure (Masse et al. 1999; Szubka et al. 2022). They, thus, are not 2D materials and, therefore, will not be a focus of this work.

Interestingly, there appears to be no known mineral or compound that exhibits a similar structure to that of colinowensite. However, colinowensite shares some structural similarities with alkaline-earth copper tetrasilicates and especially with effenbergerite. Indeed, also $BaCuSi_2O_6$ has a layered structure built up by nanosheets intercalated by Ba^{2+} ions, and its nanosheets are composed of square rings of silica tetrahedra linked together by Cu^{2+} forming CuO_4

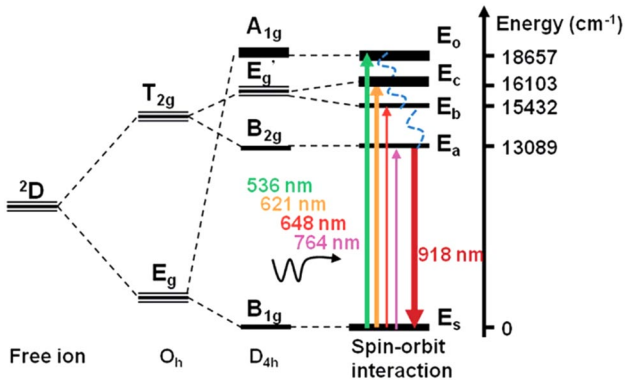

Fig. 6 Simplified energy level diagram of Cu^{2+} ion in tetragonally distorted octahedral crystal field environment in cu-prorivaite lattice. Reproduced with permission from Li et al. (2014)

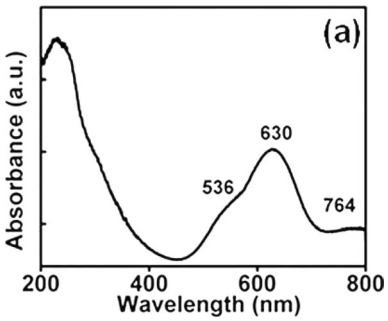

Fig. 7 Absorption spectra of cu-prorivaite at room temperature. Reproduced with permission from Li et al. (2014)

groups in almost perfect square planar coordination (Rieck et al. 2015) and with almost identical Cu–O bond length, i.e., about 1.92 Å (Pozza et al. 2000). The main difference between the structure of $BaCuSi_2O_6$ and that of the other 2D alkaline earth copper silicates is that in $BaCuSi_2O_6$ the square rings of tetrahedra are isolated and they are connected only by the CuO_4 groups. Berke et al. point out that the difference between $BaCuSi_2O_6$ and the structures of compounds in the gillespite-group can be viewed as the condensation of the square rings of tetrahedra in the latter one, as sketched also in Fig. 2 (Berke et al. 2009). In $BaCuSi_2O_6$, the lack of this condensation precludes the formation of a virtually infinite network of silica tetrahedra. Indeed, the isolated square rings $[Si_4O_{12}]^{8-}$ need Cu^{2+} ions to constitute a virtually infinite nanosheet $[Cu_2Si_4O_{12}]^{4-}$. CuO_4 groups link together four non-bridging oxygen anions from four different square rings of silica tetrahedra. As represented in Fig. 5, CuO_4 groups face directly two by two, forming, therefore, a nanosheet composed of single square rings of silica tetrahedra connected in each corner by two parallel CuO_4 groups. The nanosheets are then joined together by Ba^{2+} in tenfold coordination.

Within the layer, at room temperature the distance between two opposite Cu^{2+} is quite small, i.e., 2.73–2.75 Å (Chen et al. 2014b; Stern et al. 2014; Rieck et al. 2015), which is close to the Cu–Cu distance in nanometer scale metallic clusters, i.e., 2.55–2.70 Å (Bazin and Rehr 2003). Actually, the Cu^{2+} ions ($S = 1/2$) form a square lattice of CuO_4–CuO_4 dimers parallel to the c axis with antiferromagnetic coupling. Each dimer is roughly isolated from the others being the interdimer distance ~ 7 Å in the same layers and ~ 5.75 Å between dimers in adjacent layers (Sheptyakov et al. 2012; Stern et al. 2014). This unique feature has made $BaCuSi_2O_6$ a choice material to study Bose–Einstein condensation (BEC) of magnons in high magnetic fields and to study quasi-two dimensional isolated spin dimer systems (Jaime et al. 2004; Sebastian et al. 2006a, 2006b; Harrison et al. 2006; Batista et al. 2007; Krämer et al. 2007; Rösch and Vojta 2007; Chen et al. 2014a; Mazurenko et al. 2014; van Well et al. 2016; Allenspach et al. 2020, 2021). $BaCuSi_2O_6$ has also been used as a model to study the behavior of isolated square rings of silica tetrahedra (McKeown and Bell 1997, 1998).

3.3 Color

3.3.1 Color of cuprorivaite and related 2D-silicates

The three alkaline earth copper silicates owe their vivid blue color to their chromophores, i.e., Cu^{2+} ions in square-planar coordination, and the effect of the internal electric field created by the entire crystal on them (García-Fernández et al. 2015, 2016). (Stern et al. 2014).

The geometry around Cu^{2+} ions induces the descent of symmetry from O_h to D_{4h}, thus resolving the degeneracy within the E_g and T_{2g} orbitals that resulted from the splitting of the octahedral crystal field. In this way, four energy levels are formed (see also Fig. 6). A further minor splitting is due to spin–orbit interactions (Li et al. 2014).

Three fundamental broad absorption bands associated with d–d transition thus exist, two of them in the visible and one in the NIR. The overall blue color of the three alkaline earth copper silicate is basically a consequence of the two absorption broad bands in the visible which are centered in the red and the green regions, while no absorption takes place in the blue region (see Fig. 7).

In cuprorivaite, according to Li et al., the absorption bands are, respectively, in green at 536 nm ($^2B_{1g} \rightarrow {}^2A_{1g}$), in red at 630 nm ($^2B_{1g} \rightarrow {}^2E_g$), and in NIR at 764 nm ($^2B_{1g} \rightarrow {}^2B_{2g}$) (Li et al. 2014). Slight differences are reported by other authors, especially for the NIR band that is often reported at a little longer wavelength, i.e., around 780 nm (Pagès-Camagna et al. 2006; Accorsi et al. 2009; Warner 2011; Borisov et al. 2013; García-Fernández et al. 2015; King et al. 2016; Binet et al. 2021).

Fig. 8 Image of modern EB and related pigments marketed by Kremer Pigmente. From the left: 10,064 Egyptian green, 100,601 Egyptian blue (particles < to 10 µm), 10,060 Egyptian blue (particles < 120 µm), 10,072 Han blue (i.e., CB) and 10,075 Han purple (i.e., CP) (colour figure online). Adapted from Nicola (2019)

Only minor differences are reported to occur among the three $MCuSi_4O_{10}$ species (Kendrick et al. 2007). However, Borisov et al. point out that on going from $CaCuSi_4O_{10}$ to $BaCuSi_4O_{10}$ a shift is noticeable (~36 nm) in the NIR absorption band associated with $^2B_{1g}$—> $^2B_{2g}$, although in the visible region just a limited bathochromic shift (~10 nm) of the $^2B_{1g}$—> $^2A_{1g}$ band is observed (Borisov et al. 2013). Kendrik et al. report some slight shift in color properties in the $M^1{}_{1-x}M^2{}_xCuSi_4O_{10}$ series, where M^1, M^2=Ca and Sr or else Sr and Ba. Overall, they point out that only a very limited whitening takes place with the replacement of Ca^{2+} by $Sr^{2+,}$ while a more appreciable effect is associated with the replacement of Sr^{2+} by Ba^{2+} (Kendrick et al. 2007).

May be worth noting that the three $MCuSi_4O_{10}$ as well as the other $MQSi_4O_{10}$ (M=Ca, Sr or Ba and Q=Cu, Fe, Cr and possibly Mg) and also $BaCuSi_2O_6$ all show dichroism, i.e., they show two distinct colors when they are observed in different orientation under polarized light (Belsky et al. 1984; Miletich et al. 1997; Schofield et al. 1998; Wiedemann and Berke 2001; Eastaugh et al. 2004; Warner 2011; Johnson-Mcdaniel et al. 2012; Skovmøller et al. 2016). In cuprorivaite, e.g., the ordinary ray, ω is deep blue, and the extraordinary ray, ε is pale pink (Fouqué 1889; Warner 2011).

The overall color of the other members in the gillespite group $MQSi_4O_{10}$ is also due to the Q^{2+} atom in roughly square-planar coordination that acts as a chromophore and to lattice constraints. $MCrSi_4O_{10}$ has tones in the range of pink, magenta, and salmon-red (Belsky et al. 1984; Miletich et al. 1997). It has three broadband absorptions that show some resemblance with those of $MCuSi_4O_{10}$ but seem blue-shifted. In $CaCrSi_4O_{10}$ the most intense absorption reaches a maximum at 511 nm for light polarized in (001). For light polarized parallel to the *c*-axis, an absorption maximum occurs at 453 nm. A broad, weak absorption also occurs centered at 670 nm in (001) (Belsky et al. 1984).

Gillespite is normally red but, unlike the other members of the group, it changes its color at high pressure, turning blue as a consequence of its phase transition (see Sect. 3.2.2). $BaMgSi_4O_{10}$ is white (Zhong et al. 2020) due to the absence of any possible d–d transition.

Like other alkaline-earth copper silicates, $BaCuSi_2O_6$ also owes its color to Cu^{2+} in square-planar coordination but García-Fernández et al. point out that a significative difference exists in comparison to $MCuSi_4O_{10}$ in the contribution from the internal electric field created by the crystal (García-Fernández et al. 2016). Berke et al. report that $BaCuSi_2O_6$ in its pure state (degree of purity 99.5%), obtained through melt-flux synthesis, seems to be not purple, but dark blue. A purple shade in $BaCuSi_2O_6$ has been suggested to be the result of the formation of impurities of red Cu_2O (cuprite), as a consequence of the high temperature reached in the production process (Berke 2007). However, Chen et al. point out that $BaCuSi_2O_6$ produced through hydrothermal synthesis is markedly purple even when no Cu_2O phase is detected through XRD analysis (Chen et al. 2014b). The exact color of $BaCuSi_2O_6$ specimens seems, indeed, to be related to the dimension of the crystals (Wiedemann and Berke 2001). In fact, also $BaCuSi_2O_6$ found as natural colinowensite appears dark blue when in large crystals, while it seems distinctively purple when crystals are smaller than 40 µm (Rieck et al. 2015).

3.3.2 Egyptian blue, Chinese blue, and Chinese purple

EB, CB, and CP pigments are not single phases of their main constituents and it has to be said that they owe a color that can take on different tones due to many factors.

EB commonly ranges in color from ashy or pale blue to intense deep blue. Sometimes, it can also get blackish or greenish shades. When pure and in the same particle sizes, the color of CB is in general very similar to that of EB (Berke 2007). However, CB can often get a purplish shade, and less commonly than EB, it gets blackish or greenish. The tone of CP is generally purple but can also have shades of

blue, pink, and red, and can get blackish. Some commercial EB, CB, and CP are shown in Fig. 8 also in comparison with Egyptian green, a vitreous material related to EB and better detailed in Sect. 4.1.1 The main features that can influence the color of EB, CB, and CP are listed in the following paragraphs.

3.3.3 Effect of particle size

Coarse EB, CB, and CP are generally deep blue if constituted of clusters of large crystals (Augusti 1967; Tite et al. 1987; Berke and Wiedemann 2000; Canti and Heathcote 2002). If ground to less than 15 µm EB gets quite pale but can stay deep blue if kept greater than 30 µm (Pagès-Camagna et al. 2010). The effect is evident in Fig. 8. The pale aspect of thin particles of EB and CB is generally due to the increase in the scattering of light (Kakoulli 2002). This seems true especially if the EB particles are the result of the grinding of pigments with high amounts of glass matrix. The pigments produced with a limited amount of glass matrix or via sol–gel, seem less affected by the whitening due to grinding (Chopin and Macaudiere 1994). However, pigments with a low amount of glass matrix are in general constituted of fine-textured agglomerate of particles, therefore, of relatively light tones, but, especially the sol–gels ones, can be produced in very thin particles of few µm or less without losing their quite brilliant blue tone (Chopin and Macaudiere 1994). The possibility of producing EBs made up of particles of different sizes has historically been widely exploited to obtain a series of pigments with different tones of blue as suggested by *Theophrastus* (Eichholz 1965; Katsaros et al. 2010; Kostomitsopoulou Marketou et al. 2020). CP is different from EB and CB in the fact that the crushing of large blue crystals of CP does not produce a simple whitening but turns it to a purplish color as does its streak (Rieck et al. 2015). May be worth noting that the exfoliation in nanosheets of cuprorivaite (i.e., EB), effenbergerite (i.e., CB), and wesselsite generally induces an ashy tone (Johnson-McDaniel and Salguero 2014) that has been related to their dichroic properties and the reversible weakening of the 536 nm ($^2B_{1g} \rightarrow {}^2A_{1g}$) absorption in the green (Johnson-Mcdaniel et al. 2012).

3.3.4 Effect of the amount of flux and the route of synthesis

The traditional way to produce EB, CB, and CP consists of a high-temperature synthesis involving a flux that promotes the melting of silica in a liquid phase of silicates and the formation of crystals within it through nucleation and growth (see also Sect. 4.2). For this reason, it is often referred to as melt-flux synthesis or salt-flux synthesis (Warner 2011; Johnson-McDaniel and Salguero 2014). If the amount of

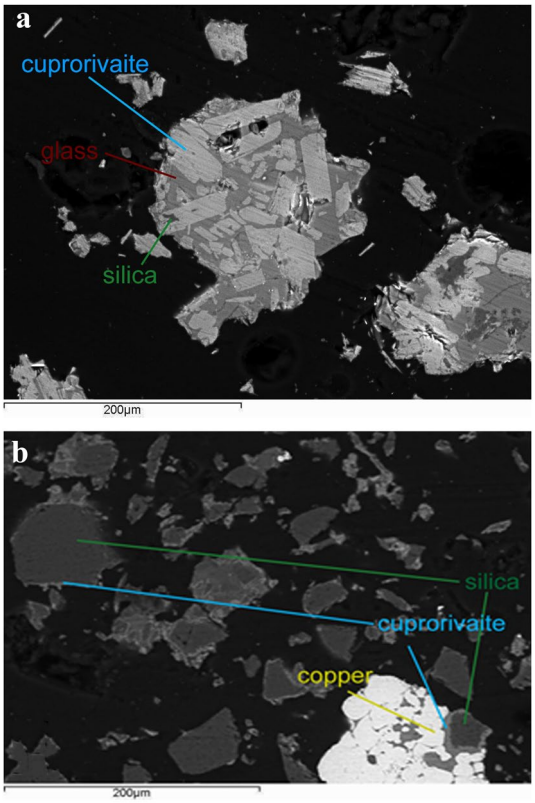

Fig. 9 SEM–EDS images showing cross sections of EB particles included in resin: **A** melt-flux synthesis and **B** solid-state synthesis. Reproduced with permission from Nicola et al. (2019)

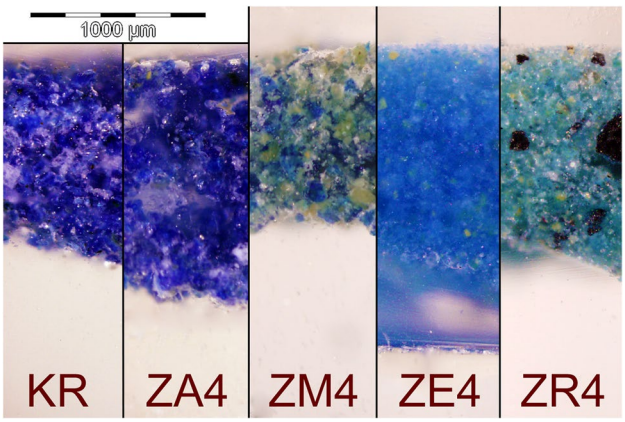

Fig. 10 Images acquired through optical microscopy of powders of different EB pigment modernly synthetized. The powders have been embedded in polyester resin and lapped. KR is from Kremer Pigmente; ZA4 is obtained through high-temperature melt-flux synthesis using zinc as a secondary flux; ZM4 is analogous to ZA4 containing excess of Ca, Zn and silica; ZE4 is obtained with conventional solid-state synthesis (i.e., without any flux), and ZR4 is analogous to ZE4 but contain unreacted reagents due to different raw materials used. Reproduced with permission from Nicola et al. (2019)

flux is enough (e.g., above 2% w/w in the final product), then the crystals of cuprorivaite, effenbergerite, or colinowensite will end up being embedded into quite an extensive silicate glass matrix (Tite et al. 1987; Delamare 1997; Wiedemann and Berke 2001). An example of EB obtained via melt-flux synthesis is shown in Fig. 9A. The glass matrix contains copper and has its own color that in general ranges between blue and green, and takes part in the overall color of the pigments (Onoratini et al. 1987; Etcheverry et al. 2001; Pagès-Camagna et al. 2006). Melt-flux synthesis generally produces the quick growth of large crystals of $MCuSi_4O_{10}$ (Delamare 1997; Johnson-McDaniel and Salguero 2014) and, therefore, gives the pigments an overall intense and deep color (Ullrich 1979; Wiedemann and Bayer 1982). This feature is evident in Fig. 10, where ZA4 is a sample of EB produced via high-temperature melt-flux synthesis with zinc as secondary flux and KR is a sample of commercial EB, arguably obtained by conventional melt-flux synthesis using sodium or potassium compounds as fluxing agents. However, if the amount of glass formed is very large and there is little copper within it, or if some colorless glass has been deliberately added in certain steps of the production, then the EB obtained will be diluted and the color will be pale blue even for solid masses of EB obtained via melt-flux synthesis (Jaksch et al. 1983; Lee and Quirke 2000).

If the flux present in the high-temperature synthesis is close to zero then the glass phase will be limited or almost absent (Pradell et al. 2006). In this case, the temperature required for an efficient synthesis will be higher, e.g., 975 °C instead of 875 °C (Johnson-McDaniel and Salguero 2014), the synthesis will be possibly governed mainly by diffusion laws (Delamare 1997), and will be in general defined as solid-state synthesis (Johnson-McDaniel and Salguero 2014). However, Pradell et al. point out that EB crystals are formed through nucleation and growth within a liquid phase, even for flux content as low as 0.3 wt%, i.e., arguably in any ancient EB (Pradell et al. 2006).

As shown in Fig. 9B, the crystals of cuprorivaite formed by solid-state synthesis (i.e., without the adding of any flux) are not embedded in a glass matrix and are smaller, producing an overall lighter color of the pigment (Delamare 1997; Nicola et al. 2019). In fact, they consist of fine-textured crystals in small clusters uniformly interspersed on the surface of unreacted quartz grains (Tite et al. 1987; Nicola et al. 2019). ZE4 in Fig. 10 is an example of EB produced without any flux, i.e., via solid-state synthesis. It is evident its lighter color if compared with pigments produced via melt-flux synthesis (e.g., ZA4 and KR).

When hydrothermal synthesis is used to produce crystals of cuprorivaite, effenbergerite, and wesselsite they have been reported to be bright blue (Chen et al. 2014a; Johnson-McDaniel et al. 2015; Zhang et al. 2018), while those of colinowensite looks purple (Chen et al. 2014b). Solution combustion synthesis has been reported to produce EB pigments with a color that depends on the preheating temperature and that ranges between midnight blue (700 °C), teal (750 °C), dark cyan (800 °C), and dark turquoise (850 °C) (Panagopoulou et al. 2016). Sol–gel syntheses of alkaline earth copper silicates can produce pigments in a wide range of colors in blue and violet tones. It is claimed that such pigments are very easily ground in mild conditions reaching a much thinner grain size, without altering the color of the products unacceptably. They would also have excellent coloring power and excellent hiding power (Chopin and Macaudiere 1994).

3.3.5 Effect of non-stoichiometric or unreacted reagents

The excess of copper or its incomplete reaction often leads to the formation of colored impurities (see, e.g., ZR4 in Fig. 10). In EB they are often present as black CuO (Johnson-McDaniel and Salguero 2014; Bloise et al. 2016). CuO is a common occurrence when EB is produced with stoichiometric ratios of reagents, since in this case part of the silica in the mix of reagents cannot take part in the reaction that is forming cuprorivaite. In fact, some SiO_2 reacts, e.g., with sodium from the flux to form the glass matrix or stays unreacted forming grains in the core of particles of cuprorivaite. The lack of silica leads to the formation of byproducts such as CuO and $CaSiO_3$ instead of $CaCuSi_4O_{10}$. Arguably, this side effect has been historically countered using the excess of 10–30% SiO_2 that has been reported in archaeological samples by almost any author (see Sect. 3.1.1). When CuO is present, it gives an overall gray-blackish unpleasant color to the pigment. CuO can be removed from EB by washing the product with a strong acid, e.g., HCl, in general with subsequent annealing of the pigment, which will turn to bright blue (Canti and Heathcote 2002; Moussa and Ali 2013; Johnson-McDaniel and Salguero 2014; Berdahl et al. 2018; Fontana et al. 2020).

In the case of CB, a lack of silica during manufacturing can lead to the formation of a wider range of byproducts, since the BaO–CuO–SiO_2 system is more complex than CaO–CuO–SiO_2. Indeed, at least four stoichiometric ternary phases exist, i.e., $BaCuSi_4O_{10}$ (effenbergerite, blue), $BaCuSi_2O_6$ (colinowensite, purple), $BaCu_2Si_2O_7$ (scottyite, dark blue), and $Ba_2CuSi_2O_7$ (light blue) (see also Sect. 3.1.2). Although only one of them is generally largely predominant, a mix of the first two (or occasionally three) compounds generally occurs in CB and CP pigments obtained via melt-flux synthesis. The exact ratio influences the specific color of each CB or CP pigment produced (Berke and Wiedemann 2000; Wiedemann and Berke 2001). A limited excess of silica seems not to impact heavily the overall color of EB and CB. On the contrary, during CP manufacturing, it can promote the formation of impurities

constituted by CB, giving it a bluish tone. A slight excess of alkaline earth can produce some whitening due to the formation of barium or calcium compounds such as $CaSiO_3$ (wollastonite) in EB. It may be worth noting that $CaSiO_3$ is also produced from EB in presence of a high amount of flux and temperatures overall higher than its thermal stability. In this case, it is generally associated with a greenish copper-bearing glass phase, see also Sects. 3.4.2 and 4.1.1 (Pagès-Camagna and Colinart 2003; Hatton et al. 2008; Grifa et al. 2016; Kostomitsopoulou Marketou et al. 2020).

3.3.6 Effect of the raw materials used

The synthesis of EB, CB, and CP can be accomplished with a wide variety of reagents. Many different sources of silica, copper, and alkaline earth can be exploited as well as other additives commonly used, i.e., fluxes. In general, pure metals or alloys, oxides, carbonates, nitrates, and (seldom) sulfates, sulfides, and chlorides are the preferred ones (Riederer 1997; Qin et al. 2016; Zhang et al. 2016; Lin 2018; Nicola et al. 2019; Dariz and Schmid 2021; Kiss et al. 2022). However, the exact type of each reagent can promote the formation of specific impurities in the final product or can influence the dynamic of the reaction impacting thus the overall final color of the pigments. The large white particle in the bottom-right corner of Fig. 9B and ZR4 in Fig. 10 show, e.g., how the use of pure copper metal powder as a source of copper could be not recommended in solid-state synthesis. Indeed, even if the copper powder is effective in melt-flux synthesis, it became detrimental if flux is not present, originating a lot of unreacted particles that will impact the general color (Nicola et al. 2019). The use of chlorides and sulfates (or sulfides) can instead produce the formation of separate melt systems called *galle* (Rehren 2008; Dariz and Schmid 2022). Some effects on the color due to different reagents have been described, e.g., for the melt-flux synthesis of EB (Tite et al. 1984; Bianchetti et al. 2000; Mazzocchin et al. 2004; Hatton et al. 2008; Bloise et al. 2016; Rodler and Kostomitsopoulou Marketou 2022) and for CB and CP (Berke and Wiedemann 2000; Wiedemann and Berke 2001; Corbiere 2009; Qin et al. 2016; Lin 2018). It has been reported that the chemical nature of the flux can influence the tone of the blue (Warner 2011). It may be worth noting that the final result not only depends on the chemical nature of each reagent but is also influenced by the size and shape of the grains, since, e.g., thin silica particles will result in a minor amount of unreacted reagents (Schippa and Torraca 1957; Ullrich 1979; Mazzocchin et al. 2004; Kakoulli 2009).

3.3.7 Effect of impurities

Some impurities in the reactants, e.g., NaCl (Giménez et al. 2017), Fe (Bianchetti et al. 2000), or a high amount of Zn and Ca (Nicola et al. 2019) can promote the formation of greenish byproducts in EB (see, e.g., ZM4 in Fig. 10). Limited amounts of As, Sn, Pb, and Zn have instead not been reported to alter significantly the color of EB even if more work on this topic is needed (Kakoulli 2002). However, some of them (i.e., Pb and Zn) can act as fluxing agents and have effects similar to those described in Sect. 3.3.4 Effect of the amount of flux and the route of synthesis (Nicola et al. 2019; Rodler and Kostomitsopoulou Marketou 2022). Kostomitsopoulou Marketou et al. extensively describe the effects of some common impurities on a large group of archaeological pellets of EB (Kostomitsopoulou Marketou et al. 2020, 2021). The chromatic effects of impurities in CB and CP have also been studied even if they are more difficult to describe, since the $BaO–CuO–SiO_2$ system is more complex than $CaO–CuO–SiO_2$. Some detailed discussions are however available in the literature (Wiedemann and Bayer 1997; Berke and Wiedemann 2000; Bouherour et al. 2001; Berke et al. 2009; Corbiere 2009; Lin 2018).

3.3.8 Effect of the temperature and length of production

If the temperature of the reaction in the traditional synthesis is too high, e.g., above 1050–1100 °C, cuprorivaite may start to decompose (Mazzocchin et al. 2004) turning EB into a greenish concoction containing wollastonite, high-temperature polymorphs of silica (i.e., tridymite and cristobalite), and a copper-bearing glassy phase (Grifa et al. 2016). Furthermore, if a large amount of flux is present, then the process takes place more markedly and an extensive green glassy matrix is formed. These conditions have historically been used to deliberately produce a green pigment known as Egyptian green or green frit (Pagès-Camagna and Colinart 2003; Hatton et al. 2008; Grifa et al. 2016). A modernly produced commercial Egyptian green is shown in Fig. 8, for further details on it see also Sect. 4.1.1.

In the synthesis of CB, analogous decomposing effects take place at a similar or possibly higher temperature, i.e., above 1200 °C (Wiedemann and Bayer 1997). CP is instead more temperature sensitive than EB. Wiedemann and Berke report that CP already at 1000 °C can decompose according to the general route: $3BaCuSi_2O_6 \rightarrow BaCuSi_4O_{10} + 2BaSiO_3 + 2CuO$ turning thus partly in CB and getting blackish due to the formation of CuO. They also argued that if the temperature is above 1050 °C, CP can turn also reddish-purple as a consequence of the transformation of CuO (black) into Cu_2O (red) and oxygen (Wiedemann and Berke 2001). CP melts with decomposition at around 1100 °C (Berke and Wiedemann 2000).

Also in hydrothermal syntheses the temperature of the reaction impact the color of the pigments produced (Johnson-McDaniel et al. 2015; Sun et al. 2021). In this case,

the final color arguably depends also on other aspects, such as pH and concentrations of reactants (Chen et al. 2014a, b; Rendón-Angeles et al. 2021). The effects of temperature in solution combustion synthesis have been described in Sect. 3.3.4.

Overall, the duration of the high-temperature production processes and the cooling rate can induce some changes in the final color of the pigments produced in each type of synthesis. In melt-flux synthesis, longer duration and slow cooling can promote, e.g., the formation of larger crystals of more intense color (Schippa and Torraca 1957; Riederer 1997; Warner 2011), while a short time of reaction and a fast cooling can lead to smaller crystals and thus to a paler color of the pigments. A short time of production can lead also to large amounts of unreacted reagents. May be worth noting that the span in the length of synthesis reported in the literature can be very wide, ranging from a few minutes (Pradell et al. 2006; Kiss et al. 2022) to more than 300 h (Schippa and Torraca 1957; Riederer 1997; Warner 2011).

3.3.9 Refractive Index and mixing with binding media

The presence of binding media is another factor that can modify the aspect of the pigments. Indeed, the hiding power and the saturation of pigments depend on the difference between their refractive index (RI) and that of the binder (Cosentino 2015). EB has refractive indices of 1.636 w (ordinary ray, electric field perpendicular to the *c*-axis) and 1.591 e (extraordinary ray) (Berdahl et al. 2018; Sobik et al. 2021). CB has almost identical values (i.e., 1.633 w and 1.593 e), while CP has higher values of 1.72 and 1.74 (Eastaugh et al. 2004). The RI values of the pigments are quite different from the ones of many water-based binding media. For this reason, EB, CB, and CP pigments are in general light and opaque when used, e.g., with gum arabic, simply showing a slight effect of whitening due to dilution. Oils, waxes, and many polymeric resins have RIs closer to that of EB, CB, and CP. If they are used as binding media for the three pigments, they decrease the scattering effect of the powders and produce more intense and deep colors. However, they decrease also the hiding power of the pigments and increase transparency effects (Kakoulli 2002; Daniels et al. 2004). EB has been used to paint not only on walls or wood but also on terracotta. Osanna and Rescigno report that for this purpose lime is used as binding media (Osanna and Rescigno 2022) arguably leading to light blue tones.

3.3.10 Interaction with other pigments

EB, CB, and CP are generally considered to be compatible with any other pigment. The mixing with pigments (or any other extraneous material) can be used to modify their color. However, the careful exploitation of partial transparency allows the production of color effects even simply by superimposing thin layers of, e.g., EB on layers containing other pigments (Osanna and Rescigno 2022). Historically, EB has been used to produce green tones by mixing it with, e.g., orpiment or iron-oxide yellows (Scott 2016) or to improve the tone of green pigments by adding it, e.g., to green earth or Egyptian green (Mazzocchin et al. 2003; Perez-Rodriguez et al. 2015; Nicola et al. 2018b; Bracci et al. 2022). It was also used to obtain gray, brown, purple, ocher, and skin colors by adding, e.g., iron-oxides or cinnabar (i.e., vermilion) (Edreira et al. 2003; Aliatis et al. 2010; Fermo et al. 2013; Skovmøller et al. 2016; AIRPA 2021; Bracci et al. 2022; Osanna and Rescigno 2022).

In general, EB has been lightened by mixing it with white pigments (Osanna and Rescigno 2022), such as calcium carbonate, calcareous clay (Augusti 1967), or lead white (Aliatis et al. 2010). Sometimes, EB has been added only in very small amounts, likely to optically achieve a perceived higher intensity of the white sensation (Edreira et al. 2003; Hallmann et al. 2021). Early uses of EB to improve the whiteness of white pigments predate Roman times. G. Chiari reported, e.g., it in paintings within the tomb of Tutankhamun (personal communication, December 3, 2016).

CP and CB have also been mixed with other pigments, e.g., lapis lazuli blue in beads of the eighth century BCE (see Fig. 19). In polychromies of the Qin Shi Huang Terracotta Army, CP has been found mixed, e.g., with vermilion, azurite, and iron oxide (Herm et al. 1995; Bouherour et al. 2001; Berke 2007), while in a Western Han dynasty Terracotta Army, CP has been reported mixed with chalk (Wei et al. 2012).

The possibility to add organic dyes to improve or modify the color of EB, CB and CP should not be ruled out. In this regard, it may be worth noting that, in *Book XXXIII* of *Naturalis Historia,* Pliny the Elder reports a practice consisting in boiling EB with plant juice to improve its color (Bostock and Riley 1857). However, no organic dyes have been reported so far in any archaeological specimen of EB, CB, or CP, likely due to their labile nature (Augusti 1967).

3.3.11 Effects of deterioration processes

In some circumstances also very stable pigments such as EB, CB and CP have been reported to suffer some decay that can impact their color (see also Sect. 3.4.3). More specifically, a color alteration toward green has been reported in many EB of Egyptian origin (Schiegl et al. 1989, 1992; Abadir 2014; Giménez 2015a, b; Scott 2016; Moussa et al. 2021), while an example in EB of Roman times has been, e.g., reported in the coastal city of Formia, in a hypogeum environment with a very high relative humidity and high level of dissolved calcium carbonate and possibly calcium bicarbonate

and chlorides (Nicola et al. 2006). In general, such color alterations have been attributed to the copper chloride cancer mechanism (Schiegl et al. 1989, 1992; Abadir 2014; Giménez 2015a, b; Scott 2016; Moussa et al. 2021) and the consequent formation of green basic copper chlorides. However, there is some debate about basic copper chlorides found in EB of archaeological sources. The general consensus is that they generally are signs of degradation of sensitive pigments, such as azurite and malachite, and possibly even of more stable pigments, such as EB (Scott 2016; Blom-Böer and Warburton 2020; Hallmann et al. 2021). Nevertheless, it seems not possible to rule out that at least occasionally basic copper chlorides have been used as synthetically prepared green pigments (El Goresy et al. 1986; Hedegaard et al. 2019; Švarcová et al. 2021). It seems that it cannot be ruled out that chloride impurities in natron or other reactants used in the production of EB have a role in its decay. However, in some specific experimental syntheses, Giménez et al. report that adding NaCl among the reactants does not induce the formation of copper chlorides in products, but rather produces a mixture with features similar to Egyptian green (see also Sect. 4.1.1) (Giménez et al. 2017).

Another mechanism of decay that can turn EB, CB, and CP toward green (or brown) is the very common phenomenon of the yellowing of paints, binders, or coatings (Scott 2016).

The blackening of painting layers containing EB is a common occurrence in many archaeological findings and has been reported already in 1934 by Lucas (Lucas 1934, Lucas and Harris 1962 and Scott 2016). Daniels et al. concluded that it can be due to two main causes. The first seems prevalent and is the darkening of the organic materials used as pictorial binders and varnishes. In this regard, it may be worth noting that possibly the natural photooxidation of many organic compounds could be intensified by the presence of EB due to its catalytic effects (Coccato et al. 2017; Gao et al. 2022). The second hypothesis of Daniels et al. regarding the blackening of EB is that it can be due to the deposition of dirt followed by the formation of gypsum-rich black crusts over the rough surface of the coarse pigment (Daniels et al. 2004). The effect seems accentuated by the fact that EB has often been used coarser than the other pigments to preserve its deep blue tone (see Sect. 3.3.3). This produces thicker pictorial layers that require more binding media than those containing other pigments and that show a rough surface that can easily trap dust and deposits. The blackening of EB has been at first argued to be linked to the formation of black CuO, maybe also mixed with other degradation products (Lucas 1934; Scott 2016). Kendrick et al. point out a possible light sensitivity of cuprorivaite, wesselsite, and effenbergerite that could lead to the blackening of EB and CB due to the local formation of black CuO (Kendrick et al. 2007). However, Lee and Daniels et al. reported that no significant presence of CuO is detectable in EB from blackened areas, concluding that the blackening of EB in archaeological samples is not due to the presence of CuO (Green 2001; Daniels et al. 2004). For further details see also Sect. 3.4.5. It has to be noted that also other chromatic alterations can be commonly observed in many samples of EB of archaeological sources, e.g., toward brown, or dark green. They can be explained as a combination of some of the mechanisms already discussed (Scott 2016).

CB has been reported to be much more stable than CP (Wiedemann and Bayer 1997) and even more stable than EB (Salguero et al. 2014). It is so stable that it can be argued that CP could get bluish and blackish over time due to the at least partial transformation into the more stable CB along with CuO (Wiedemann and Bayer 1997; Berke et al. 2009; Xia et al. 2014). CP fades rapidly and decomposes when exposed to diluted strong acids. Contact with aqueous oxalic acid can result in the formation of a turquoise-bluish residue. Since lichens excrete oxalates or even oxalic acid, this is a possible threat to the conservation of CP in archaeological sites (Wiedemann and Bayer 1997). It has been argued that for this reason, the light blue color of the trousers of some Terracotta Warriors may not be the original color, but rather an alteration of CP due to the presence of oxalic acid (Wiedemann and Berke 2001). Nevertheless, the conservation issues of CP and CB on archaeological finds are overall not particularly a matter of concern in comparison to those of the other ancient blue pigments such as azurite or lapis lazuli which can easily fade even in humid or slightly acidic environments (Plesters 1966; Berke et al. 2010). The ancient organic artistic materials used to apply EB, CB, and CP are generally far more sensitive to color alteration or conservation issues than the pigments themself. For example, the greenish tone observed in the so-called blue room in Ariadne's House in Pompei is due to the collapsing of the painting layer and not to EB alteration (Prieto-Taboada et al. 2021), while the darkening of many statues of the Terracotta Army of Emperor Qin Shi Huang has overall been due to the flaking of the ground layer of Qi lacquer behind the polychromies and not to the alteration of CP (Blänsdorf and Xia 2006; Bonaduce et al. 2008).

3.4 Stability

3.4.1 Overview

Alkaline earth copper tetrasilicates are very stable over time as suggested by the very high number of archeological findings of EB and CB produced thousands of years ago and in excellent conditions (Wiedemann and Bayer 1997; Li et al. 2014). CP is more sensitive than EB and CB (Berke et al.

2010). However, CP is still overall stable and is generally found sound in archaeological findings (Wei et al. 2012).

3.4.2 Thermal stability

EB is extremely stable over a wide range of temperatures (Li et al. 2014) starting to decompose around 1050–1100 °C (Mazzocchin et al. 2004). CB seems to be even more stable, decomposing around 1200 °C (Wiedemann and Bayer 1997). The 2D materials related to EB and CB are arguably all stable from cryogenic temperatures to 1000 °C or more. Among the copper-containing members, CP is the most sensitive to high temperatures starting to decompose at about 1000 °C (Wiedemann and Berke 2001). For further details on thermal stability see also Sect. 3.3.8. May be worth noting that the specific thermal stability of the pigments produced through traditional synthesis seems to be influenced by the presence in the glass matrix of elements such as Na^+ and K^+ originating from fluxes. A high amount of fluxes, could arguably decrease the thermal stability of the pigments produced, and in any case can prevent their formation (Mazzocchin et al. 2004). The different amounts of fluxes in the specimens analyzed by different authors could possibly account for the discrepancies in the range of thermal stability reported in the literature and emphasized, e.g., by Jaksch et al. (1983), Mazzocchin et al. (2004) and Warner (2011).

3.4.3 Stability in the acid environment

Cuprorivaite, effenbergerite, and wesselsite have been reported and confirmed to be very resistant to acid attacks, even against concentrated, hot, and strong acids, such as HCl (Pabst 1959; Riederer 1997; Wiedemann and Bayer 1997; Berke and Wiedemann 2000; Johnson-McDaniel and Salguero 2014; Berdahl et al. 2018; Fontana et al. 2020). On the contrary, $BaCuSi_2O_6$ (i.e., colinowensite) and $BaFeSi_4O_{10}$ (i.e., gillespite) have been reported to be readily leached and/or decomposed when in contact with acids (Pabst 1958, 1959; Wiedemann and Bayer 1997). It seems unknown whether $MCrSi_4O_{10}$ (M=Ca, Sr or Ba) and $BaMgSi_4O_{10}$ are resistant to acids but they are likely more sensitive than Cu members of the gillespite-group, since it has been argued that a key role in the acid resistance of $MCuSi_4O_{10}$ (M=Ca, Sr or Ba) is played by the high stability of Cu^{2+} in square planar coordination (Pabst 1959). However, the high stability of Cu^{2+}in square planar coordination is not the only explanation for the acid resistance of $MCuSi_4O_{10}$. In fact, effenbergerite is much more stable than colinowensite even if both have Cu^{2+} in square planar coordination. Another key role should thus be played by the high stability of the network of SiO_4 tetrahedra in the gillespite-group members.

Nevertheless, EB pigment in harsh environments and on very long-time exposure (i.e., in the order of a few thousand years) has been reported to suffer from acid or salt-induced forms of decay, such as copper chloride cancer (see also Sect. 3.3.11). In the case of EB and other ancient Egyptian vitreous materials containing copper (e.g., Egyptian green and Egyptian faience), this kind of degradation seems due to the devitrification of the glass phase that is rich in elements, such as Na^+ and K^+ (Kakoulli 2009; Moussa et al. 2009; Moussa and Ali 2013). Devitrification likely occurs in archaeological EB even as a simple consequence of washout (Pradell et al. 2006). It has also been observed in an archaeological octagonal stick made of CP (Doehne and Ma 2004) and arguably could happen also in CB. Even if cuprorivaite has antibacterial properties (Lamprecht et al. 1997; Tian et al. 2016) (see also Sect. 3.6), it has been suggested that a key role in the copper chloride cancer attack of EB could be played also by some fungal and bacterial species (Moussa et al. 2021). An attempt to artificially induce copper chloride cancer on EB has been reported with prolonged exposure to concentrated HCl (Abadir 2014). It seems unclear if copper chloride cancer can affect directly cuprorivaite, effenbergerite, and wesselsite but may be worth noting that the use of strong acids such as HCl has been exploited to produce their artificial exfoliation. However, in this case quite concentered HCl has been used in conjunction with an ultrasonic treatment that likely can greatly accelerate and amplify the process (Guo et al. 2015a, b, c). In this regard, it has been speculated that in the archaeological time scale, water-mediated delamination could take place even in archaeological samples of EB (Salguero et al. 2014; Orna and Fontani 2022). Indeed, some examples in the literature suggest the presence of nanoplatelets in various degrees of detachment in EB of archaeological sources (Canti and Heathcote 2002) and thus this possible pathway of decay should be taken into account by conservation scientists.

3.4.4 Stability in the alkaline environment

The stability of EB and CB in alkaline environments has been much less studied. However, it is possible to argue that they are very stable, since very well-preserved EB has been widely used in a highly alkaline environment (e.g., with slaked lime in fresco techniques or to paint on terracotta) both in the Early Middle Ages, in Roman times or even before (Riederer 1997; Coccato et al. 2017; Nicola et al. 2018a; Osanna and Rescigno 2022). At high temperatures, the presence of highly alkaline environment, e.g., due to soda or potash fluxes can decompose EB (Augusti 1967; Riederer 1997) and arguably CB, CP, and related 2D materials.

3.4.5 Effects of oxygen and light

Cuprorivaite, effenbergerite, wesselsite, and arguably also colinowensite are stable in oxidizing environments and are in general not affected by the presence of O_2. Actually, O_2 seems even necessary for the successful synthesis of EB, since it prevents the formation of Cu^+ (Kiss et al. 2022). Kendrick et al. point out that containing Cu^{2+}, it is unlikely that those species show air instability but point out a possible light instability. In this regard, they reported a discoloration in some of their samples caused by irradiation with a high-intensity laser during their attempted Raman experiments. They ascribed it to the formation of a small amount of CuO that they reported also in X-ray diffraction patterns acquired after exposing the samples to sunlight (Kendrick et al. 2007). This interesting hypothesis of Kendrick et al. would be consistent with the first accounts for EB blackening (Lucas 1934; Scott 2016) but deserves further confirmation, since it contradicts the general consensus as reported by Riederer that EB exposed for thousands of years to the sun and heat on monuments in Egypt has overall retained its blue color (Riederer 1997). No instability under laser irradiation seems to have been reported by other scholars that performed wide Raman studies (Baraldi et al. 2006) but it has been reported for high laser irradiation during upconversion experiments (Chen et al. 2015). Furthermore, it should be considered that explaining the blackening of archaeological EB with the formation of black CuO would also contradict the overall accepted conclusions of Lorna Lee (née Green) (Green 2001) and Daniels et al. (2004) who did not report significant amounts of CuO in samples of blackened EB.

Godet et al. recently assessed the effects of synchrotron X-ray on EB and Egyptian green. Notably, Egyptian green was found to be more sensitive to X-rays than EB, turning brown at the lowest doses tested, while no color change occurred on EB at that X-ray intensity. Increasing the irradiation, three types of radiation-induced defects arise: E', non-bonding oxygen hole, and aluminum hole centers (Godet et al. 2022).

3.5 Luminescence

3.5.1 NIR photoluminescence

All three Cu^{2+} members of the gillespite-group show a strong luminescence associated with the electronic transition $^2B_{2g} -> {}^2B_{1g}$ with emission in the NIR I region at 900–1000 nm. The NIR luminescence of $MCuSi_4O_{10}$ can be triggered by the absorption of visible light in the red (overall between 600 and 630 nm) and, to a lesser extent, in the green region (Li et al. 2014). It can be induced also by absorptions in the NIR-I region at about 780 nm (King et al. 2016) and in the UV (Binet et al. 2021). The three broadband absorptions in the VIS and NIR-I region are associated with parity-forbidden d–d transitions which are weakly allowed, despite approximate D_{4h} symmetry at the copper center, due to vibronic coupling (Kendrick et al. 2007). The d–d transitions are, respectively, $^2B_{1g} -> {}^2A_{1g}$ (~ 540 nm), $^2B_{1g} -> {}^2E_g$ (~ 630 nm), and $^2B_{1g} -> {}^2B_{2g}$ (~ 780 nm) (Pozza et al. 2000; Kendrick et al. 2007; Accorsi et al. 2009; Verri 2009; Li et al. 2014; King et al. 2016) and are schematized in Fig. 6 in Sect. 3.3.1. Binet et al. report that the emission is excited much more efficiently by a factor of about 60 in the UV with an excitation peak at 5 eV (i.e., about 250 nm), corresponding to the valence band-conduction band transition (Binet et al. 2021). NIR excitation is noteworthy due to its higher depth of penetration. According to Borisov et al., λ_{max} of emission of the NIR photoluminescence (PL) for the three $MCuSi_4O_{10}$ (M=Ca^{2+}, Sr^{2+}, and Ba^{2+}) are, respectively, at 909 nm, 914 nm, and 948 nm (Borisov et al. 2013), while according to Cheng et al., λ_{max} are at 932 nm, 936 nm, and 964 nm (Chen et al. 2015). Other authors report slightly different values with a general consensus on a red-shift in the Ca^{2+} to Ba^{2+} series (Pozza et al. 2000; Accorsi et al. 2009; Verri 2009; Li et al. 2014; King et al. 2016). The red-shift of the emission peak has been attributed to the increase of ionic radius from Ca^{2+} to Ba^{2+} which causes an expansion of the lattice resulting in a weaker crystal field (Pozza et al. 2000; Chen et al. 2015). The photoluminescence is based on the Cu^{2+} ion located on a fourfold axis, where, in square planar coordination, it links four SiO_4 tetrahedra (Pozza et al. 2000; Kriss et al. 2016; Chiari 2018). It seems correlated also with the fact that despite their high concentration in the host matrix, Cu^{2+} ions are, indeed, weakly antiferromagnetically coupled and can be considered to show properties as they were independent Cu^{2+}

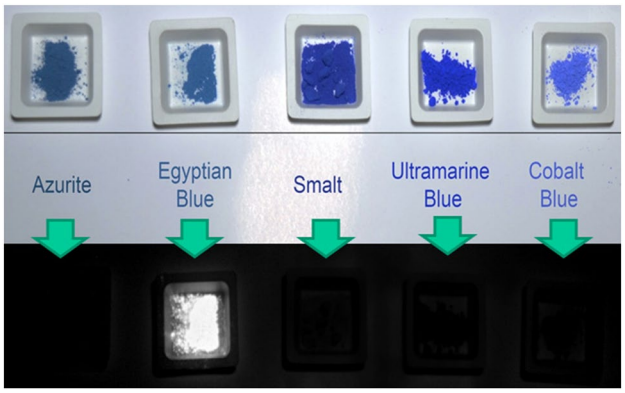

Fig. 11 (Top) Reflected Visible Light (VIS) of some blue pigments (bottom) Visible Induced Luminescence Imaging of the same pigments (colour figure online). Adapted from Nicola and Nicola (2018)

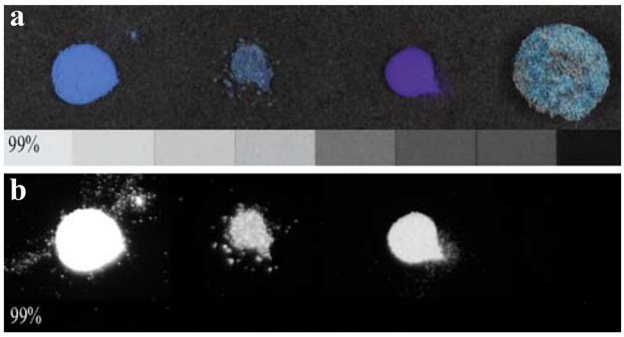

Fig. 12 First three samples (from the left) are EB, CB, CP. The fourth is Egyptian green used as reference. **a** Regular photo (i.e., reflected visible light); **b** Vis-induced NIR luminescence, under excitation from a red LED; The image was acquired in the 800–1000 nm range. In both images the grey scale contains a non-luminescent 99% reflectance standard. Reproduced with permission from Verri (2009)

centers (Warner 2011; Barbar et al. 2017; Binet et al. 2021). Cu^{2+} centers, being isolated, release the excitation energy mainly via radiative decay and not through non-radiative pathways. In this regard, Zhuang and Tanabe pointed out how in Yb^{3+} doped crystals of cuprorivaite, i.e., $Ca_{1-x}CuSi_4O_{10}:Yb_x$, there seems to be an energy transfer mechanism that reduces the PL of Cu^{2+} centers. In fact, with the increase of the concentration of Yb, the PL intensity of Yb^{3+} increases too, reducing though the PL intensity of the Cu^{2+} due to the increased possibility of non-radiative charge transfer between the adjacent centers Cu^{2+} and Yb^{3+} (Zhuang and Tanabe 2012a, b).

$BaCuSi_2O_6$ shows photoluminescence analogous to that of the three $MCuSi_4O_{10}$ (M=Ca, Sr, or Ba) (Pozza et al. 2000). According to Selvaggio et al. and Chen et al. its λ_{max} of emission is centered at 924–925 nm (Chen et al. 2014a; Selvaggio et al. 2021), while according to Pozza et al., it is at 980 nm (Pozza et al. 2000). It may be worth noting that $BaCu_2Si_2O_7$ (i.e., Chinese dark blue) does not seem to show any photo-induced luminesce in the visible and near-infrared spectral region (Chen et al. 2014b).

Photoluminescence of EB, CB, and CP has been discovered at the end of the 1990s (Ajò et al. 1996; Pozza et al. 2000). Since 2009, it is used to identify the presence and map the distribution of the three pigments through multispectral imaging, i.e., the Visible Induced Luminescence imaging method, shortened as VIL (Verri 2008, 2009; Dyer et al. 2013). An exemplifying image of the NIR photoluminescence of EB obtained through VIL is reported in Fig. 11, while the comparison with CB, CP, and Egyptian green is displayed in Fig. 12. In the last decade, VIL has been widely used in Conservation Science and beyond, becoming an almost indispensable method in many archaeological sites and conservation institutions (Kriss et al. 2016). VIL method will be one of the foci of Part B of this review.

3.5.2 Lifetime of emission

Selvaggio and Kruss report that the lifetimes of emission of the NIR photoluminescence are generally in the range of 100–150 µs for EB, 60–100 µs for CB, and 6–30 µs for CP (Selvaggio and Kruss 2022). Other authors reported values slightly different but in the same order of magnitude (Borisov et al. 2013; Chen et al. 2014a; Berdahl et al. 2018). Fluorescence lifetimes are reduced by grinding (Berdahl et al. 2018; Linn et al. 2018), likely due to the introduction of defects by mechanical stress as typically observed also for other phosphors (Borisov et al. 2013; Berdahl et al. 2018). According to Selvaggio et al., the lifetimes of emission decrease significantly after exfoliation in nanosheets due to defects or changes in symmetry that either enable non-radiative decay pathways or increase the radiative rate constants. In particular, EB-nanosheets have been reported to show a fluorescence lifetime of 17 µs, CB-nanosheets of 8 µs, and CP-nanosheets of 7 µs (Selvaggio et al. 2021). The route of synthesis seems also to impact the lifetime of emission although a systematic study is needed to clearly understand how synthesis affects the emission lifetime (as well as quantum yield, see the following paragraph) (Linn et al. 2018). The luminescence decay of CP produced via hydrothermal synthesis has been reported to be 5.6 µs (Chen et al. 2014b). The study of luminescence lifetimes has been pioneered by Comelli et al. and Linn et al. to obtain useful data for archaeometric study (Comelli et al. 2016; Linn et al. 2018).

3.5.3 Quantum yield

In 2009 Accorsi et al. tested commercially available EB (i.e., Kremer Pigmente) for the quantum yield of the NIR photoluminescence, reporting an outstanding result of $\Phi_{EM} = 10.5\%$ (Accorsi et al. 2009). The value is very high when compared with Φ_{EM} of other NIR fluorophores which is often < 2%. Furthermore, unlike EB, other NIR fluorophores often have low photostability and /or biocompatibility issues (Hong et al. 2017; Selvaggio et al. 2020; Selvaggio and Kruss 2022). The quantum yield of hydrothermally synthesized $SrCuSi_4O_{10}$ and $BaCuSi_4O_{10}$ has been reported to be, respectively, 8.5% and 6.9% (Chen et al. 2014a), while for $BaCuSi_2O_6$, a value of 0.9% has been measured. This latter lower level has been ascribed to the influence of Cu–Cu interaction within the CuO_4–CuO_4 dimers in CP (Chen et al. 2014b). Features that have been reported to influence the quantum yield (or at least the PL intensity) include the way of grinding (Sobik et al. 2021), the presence of CuO

(Berdahl et al. 2018), and the route of synthesis (Berdahl et al. 2018; Nicola et al. 2019). Using a technique based on temperature measurements in full sunlight instead of the traditional de Mello method, Berdahl et al. measured an even much higher value of quantum yield for EB and wesselsite (Berdahl et al. 2018; Selvaggio and Kruss 2022). Being highly promising as a means to simplify the procedure of acquiring quantum yield data, this interesting and less laborious method seems to deserve further in-depth. The aim could be the confirmation of the results obtainable, crossing them with more traditional methods.

3.5.4 Thermoluminescence and cathodoluminescence

EB shows the rather rare feature of being a thermoluminescent material. It follows that it is directly datable with the thermoluminescence technique (Schvoerer et al. 1988). It seems, however, unclear if this feature is purely relative to cuprorivaite or if it is due to quartz grains present withing EB (see Sect. 3.1.1). So far, EB thermoluminescence has hardly been exploited.

The cathodoluminescence of EB has been seldom investigated (Schvoerer et al. 1988; Binet et al. 2021; Yuryev et al. 2023). According to Kadikova et al. EB shows a characteristic peak at 874 nm when investigated through cathodoluminescence microspectroscopy. The technique is a promising method to identify pigments in cultural heritage (Kadikova et al. 2019; Yuryev et al. 2023).

3.5.5 Photothermal effect and photon up-conversion

EB nanosheets and wesselsite nanosheets have been reported to exhibit an excellent photothermal effect by absorbing energy in the NIR-II window, a region of electromagnetic radiation that is generally not absorbed by biological tissue, i.e., characterized by low self-heating of the tissues, maximum permissible high exposure and depth of penetration (He et al. 2021; Yang et al. 2021a, b; Dong et al. 2022). The feature has been exploited in innovative medical devices (see also Sect. 3.6).

Furthermore, Chen et al. reported a bright and broadband photon up-conversion from NIR-I to visible in $MCuSi_4O_{10}$ (M=Ca, Sr, Ba). The effect is obtained via off-resonance pumping with a NIR laser diode and is mainly ascribed to the synergic effect of the laser-driven blackbody radiation and the peak broadening due to electron–phonon coupling. They use NIR-I wavelengths of 808 nm, 976 nm, and 1064 nm to produce red to bright white broadband light with the increase of laser power (Chen et al. 2015). Gao et al. report that it is possible to enhance photocatalytic nitrogen fixation arguably thanks to the up-conversion capability of $CaCuSi_4O_{10}$, which they report to convert NIR into visible and UV light, thus improving the utilization efficiency of the full solar spectrum. $CaCuSi_4O_{10}$ nanosheet that they used for this purpose are produced from EB obtained using as raw materials palygorskite, egg shells, and 5–15% of K_2CO_3 as a flux (Gao et al. 2022). No other studies have been so far performed about the up-conversion features of EB and related 2D materials. Confirmation of the results and a further in-depth understanding of the mechanism seem promising opportunities for future research and innovative applications.

3.6 Biological effects and biocompatibility

3.6.1 General features

Many archaeological objects and papyri, e.g., the bust of Nefertiti, the Papyrus Berolina, and the Papyrus Ebers, have been observed to be less affected by biological decay in the parts painted with EB (Wiedemann et al. 1996; Lamprecht et al. 1997; Wiedemann and Berke 2001; Ramadan et al. 2019). The effects of EB, CB, and CP on the growth of lichens show that the three pigments, and especially EB, have a strong inhibitory effect on the growth of the algal component and to a minor extent of the fungal part (Lamprecht et al. 1997). CB has fungicidal properties similar to those of EB, while CP, being acid-sensitive, is purportedly less effective, since it can be decomposed by the oxalic acid produced by some microorganisms, e.g., lichens (Wiedemann and Berke 2001). A strong antibacterial effect of cuprorivaite has been reported by Tian et al. using the bacteriological plate count method to test it against the proliferation of Gram-negative *Escherichia coli* (Tian et al. 2016). The anti-microbial effect of EB, CB, and CP has been related to the Cu^{2+} ions resulting from their slow solubilization. The effect is evident even if their solubility is very low, i.e., EB: $3{\cdot}10^{-7}$ mol·l^{-1}; CB: $< 4{\cdot}10^{-8}$ mol·l^{-1}; CP: $< 6{\cdot}10^{-8}$ mol·l^{-1} (Lamprecht et al. 1997). The mechanisms besides the use of Cu^{2+} ions for the contrast of pathogenic microorganisms are well-known and have been treated by many authors (Thurman et al. 1989; Borkow and Gabbay 2009; Ramadan et al. 2019). In 2016, Tian et al., furthermore, report that Cu and Si ions from cuprorivaite have a synergistic effect on angiogenesis within a safe concentrations range. This can provide a better therapeutic activity and notably, it is free of cytotoxic effects for applications in the regeneration of human tissues (Tian et al. 2016). The angiogenic effect and the safety of cuprorivaite have subsequently received growing interest for application in regenerative medicine (Zhang et al. 2020; Yang et al. 2021b; Dong et al. 2022). Tian et al. conclude that cuprorivaite has great potential for the preparation of wound healing dressings, but may not be suitable for bone repair applications, since it could inhibit osteogenesis (Tian et al. 2016). However, more recently, He et al. reported that 3D-printed scaffolds coated with

cuprorivaite nanosheets can be used to fight osteosarcoma achieving also enhanced bone tissue regeneration (He et al. 2021). Similar results have been reported also for wesselsite nanosheets (Yang et al. 2021a). The safety and biocompatibility of cuprorivaite nanosheets are also at the base of their use as fluorescent material in bioimaging and biophotonics (Selvaggio et al. 2020, 2021).

3.6.2 Historical awareness

From an archaeological point of view, it is possible that the angiogenetic and antibacterial effects of EB have been historically known and used. According to the description given by Pliny the Elder in 77 CE in *Book XXXIII*—57 of *Naturalis Historia*, EB could have been used to clean ulcers. Pliny states that "*Caeruleum* has the medicinal property of acting as a detergent upon ulcers. Hence, it is, that it is used as an ingredient in plasters, as also in cauteries. However, it is very difficult to grind." (*vis in medicina ut purget ulcera; itaque et emplastris adiciunt, item causticis. Teritur autem difficillime*) (Bostock and Riley 1857). Nevertheless, the passage is somehow unclear, since the Latin word *caeruleum* generally means EB, but sometimes it refers simply to a blue pigment (Riederer 1997). Since the immediately preceding sentence in the text of Pliny is relative to indigo, it is not possible to state conclusively that the Romans were aware of the angiogenetic effect of EB even if it is very likely since the features reported by Pliny, i.e., healing ulcers and being difficult to grind seems more appropriate for EB than for indigo.

It cannot be ruled out that ancient Romans may have known the anti-algae properties of EB. Notably, in fact, between the first century BCE and the first century CE they used lumps of EB as mosaic tesserae that were almost exclusively used in environments rich in water, such as nymphaea and fountains (see also Fig. 15) (Boschetti 2011; Chiari 2018).

It may be worth noting that some authors on the basis of a translation of documents of the 18th dynasty of Egypt, i.e., 1550–1292 BCE (Sethe 1961; Wiedemann and Bayer 1997; Wiedemann and Berke 2001) seem to have incorrectly inferred that EB could have been used in antiquity to preserve bread. According to them, the production of "blue bread" would have been mentioned in the ancient text translated by Sethe (1961) and it could have denoted some knowledge about the conservation effect of EB that was possibly exploited to produce air-dried bread for emergency situations (Wiedemann and Bayer 1997; Wiedemann and Berke 2001). However, to a closer view, it seems that the text reported more specifically "loaves" of EB with the term reliably referring to the shape of balls or blocks made of EB, such as those in which it was produced and which are sometimes found in archeological sites (see also Sect. 4.2). The fact that no other foods are described in the same inscription but other goods such as precious materials and stones is consistent with this interpretation as well as the fact that the presence of EB has never been reported in any of the quite numerous archaeological remains of bread from the Egyptian era analyzed so far (Glabau and Goldman 1938; Leek 1972; Samuel 2002).

4 Production and use in antiquity

4.1 Egyptian blue: development and use

4.1.1 The origins

EB was at first used in glazes or as a solid material and only later in powdered form as a pigment (Forbes 1955; Riederer 1997). Although the hypothesis of a first development in Mesopotamia cannot be completely ruled out (Moorey 1985; Ullrich 1987; Cavassa 2018), the early development of EB most likely took place in Egypt during the 4th millennium BCE (Berke 2007; Delamare 2007). The earliest known findings of EB are as a constituent material of some beads and have been reported by Kaczmarczyk at the site of Abydos in a funerary context dating back to the period Naqada II in Hendrickx's classification, i.e., 3500–3300 BCE (Bouquillon et al. 2007; Cavassa 2018). The first use of EB as a pigment has been instead reported by Corcoran in the carving of a bowl of the late Egyptian predynastic period listed as Naqada IIIa1—roughly 3300 BCE (Corcoran 2016; Greco 2022). Since c. 2900 BCE, EB has been found also in Mesopotamia and Greece (Riederer 1997; Panagiotaki et al. 2004, 2015; Kakoulli 2009; Cavassa 2018).

The development of the manufacturing process of EB has been likely only possible thanks to the improvement of furnaces in the Early Bronze Age (Riederer 1997; Nicholson 2010). It occurred probably in parallel with the emergence of other furnace products, such as bronze (El Goresy et al. 1998; Gouda et al. 2020), lime (Gourdin and Kingery 1975; Philokyprou 2013), glazes, and at a later time glass that spread in Egypt only around 1500 BCE, i.e., roughly two millennia after the development of EB (Lilyquist et al. 1993; Paynter 2008; Nicholson 2012).

The ancient materials most closely related to EB are, indeed, vitreous materials. Notably, EB shares similar qualitative chemical composition, and likely kind of required raw materials with the following ancient vitreous substances ranging in color between blue, pale blue, turquoise, and green:

(a) the glaze on some stones (i.e., quartz and steatite) that were already produced in the 5th millennium BCE or earlier (Paynter 2008; Nicholson 2012)

(b) the copper-containing glazes of some Egyptian and Mesopotamian faience widespread since the 5th–4th millennium BCE (Kaczmarczyk and Hedges 1983; Tite and Shortland 2003, 2008; Paynter 2008; Moussa and Ali 2013; Masic and Nicola 2021). It has been speculated that the development of EB may derive from the efflorescence method of faience production in which the quartz body and glazing components are mixed together (Tite et al. 1987; Warner 2011). It may be worth noting that these glazes may consist not only of a colored glassy phase but also of a few embedded spicular crystals, similar but not identical to those in EB as observed in experiments on the incorporation of EB (Berke 2007). As shown in Fig. 13, these materials are so intimately linked to EB that both can have a very similar aspect (Masic and Nicola 2021)

(c) a peculiar ancient pigment referred to as Egyptian green, green frit, or turquoise frit and used mainly in Egypt since about 2200 BCE (Ullrich 1987; Pagès-Camagna et al. 2006; Hatton et al. 2008; Scott 2016). It may be worth noting that Egyptian green features and production has been highly debated (Pagès-Camagna and Colinart 2003, 2006; Schiegl and El Goresy 2006). It seems however widely accepted that Egyptian green has not to be simply considered a misfired EB but it is a distinct pigment (Pagès-Camagna and Colinart 2003; Schiegl and El Goresy 2006; Hatton et al. 2008; Scott 2016). According to Pagès-Camagna et Colinart Egyptian green is largely constituted by a widespread Cu-rich glass phase containing also wollastonite and high-temperature polymorphs of silica, while, in general, cuprorivaite is absent (Pagès-Camagna and Colinart 2003; Hatton et al. 2008). Egyptian green is overall considered to have been produced at higher temperatures than EB and with a higher amount of flux and possibly of Ca-bearing compounds (Hatton et al. 2008). Grifa et al. report that Egyptian green has been produced also outside of Egypt, e.g., in Roman times in the city of *Cumae* in Southern Italy (Grifa et al. 2016). Perez-Rodriguez et al. report an example of use in Spain during Roman times (Perez-Rodriguez et al. 2015)

(d) some types of glass colored with copper that are widespread since the mid-2nd millennium BCE (Lucas and Harris 1962; Lilyquist et al. 1993; Rehren et al. 2001; Paynter 2008; Boschetti 2011).

However, while those ancient vitreous materials are largely amorphous (Paynter 2008), EB is instead mainly crystalline having generally only a quite limited glassy matrix (Pagès-Camagna et al. 2006; Pradell et al. 2006) and exhibiting many characteristics similar to glass–ceramic materials (Chase 1971; Nicola 2019).

4.1.2 Use in Egypt, the Aegean, and the near East

Although EB was already present in Egypt since predynastic times, it was not until the 4th–5th dynasty (around 2500 BCE) that it became widespread. Examples of use in the 5th dynasty (c. 2494–2345 BCE) include the deeply etched hieroglyphs on the reliefs in the pyramid of Unas at Saqqara, which are filled with solid masses of EB, indicating its extensive manufacturing. At those times EB was almost the only blue pigment used in Egypt and the surrounding areas (Riederer 1997; Greco 2022).

As their ancient names suggest, it has been proposed that the ancient bluish vitreous materials may have been developed to replace precious stones such as the very expensive lapis lazuli which was to be imported from distant Afghanistan, and also other rare bluish stones like turquoise (Nicholson 2012). Indeed, in Egypt EB was known as *ḫśbd iryt*, meaning artificial lapis lazuli, or artificial blue (Quirke 2001; Corcoran 2016; Becker 2022), or occasionally "*mfkȝ.t*", meaning turquoise (Blom-Böer and Warburton 2020). In the Aegean, the term used was *kuwano* (*κύανος* also *kuanos* and *kyanos*), meaning dark blue or lapis lazuli (Delamare 2007). It may be worth noting that the Greek term became also the root of the Latin *cyanus* and the English word «cyan», the latter actually referring to a turquoise hue. Also related to lapis lazuli seems to be the term used in Mesopotamia for EB, i.e., *uqnû* (or *uknû*) *merku* meaning molded lapis lazuli (Delamare 2007). May be worth noting that *uqnŭ kūri,* meaning lapis lazuli from the kiln, is generally related to glass (Shortland 2012; Becker 2022), and *uqnû* and the related term *zagindurû* may also be translated as "gleaming" or "shining" (Busatta 2014; Thavapalan et al. 2016).

Hatton et al. described the extensive production of EB as almost the only blue pigment in Egypt and Mesopotamia during the second millennium BCE. To try to quantify the extent of this production, he estimated that the mass of EB required to paint a single typical temple of the 18th–20th dynasties (c. 1550–1075 BCE), e.g., Medinet Habu at Thebes, should have been roughly 1.4 tons (Hatton et al. 2008). It may be worth noting that another artificial blue vitreous material occasionally used also as a pigment appeared in Egypt around 1479–1370 BCE, sometimes referred to in the literature as Amarna blue (Tite and Shortland 2003; Shortland et al. 2006b; Scott 2016; Skovmøller et al. 2016). It was produced from cobalt alum found in the Western Desert but its use as a pigment was abandoned at the end of the New Kingdom, i.e., around 1069 BCE (Scott 2016). The use of cobalt as a coloring agent persisted for blue glass (Shortland et al. 2006b). It is noteworthy that EB produced from the New Kingdom seems less prone to turn green as a consequence of decay (Greco 2022). Possibly, the improved

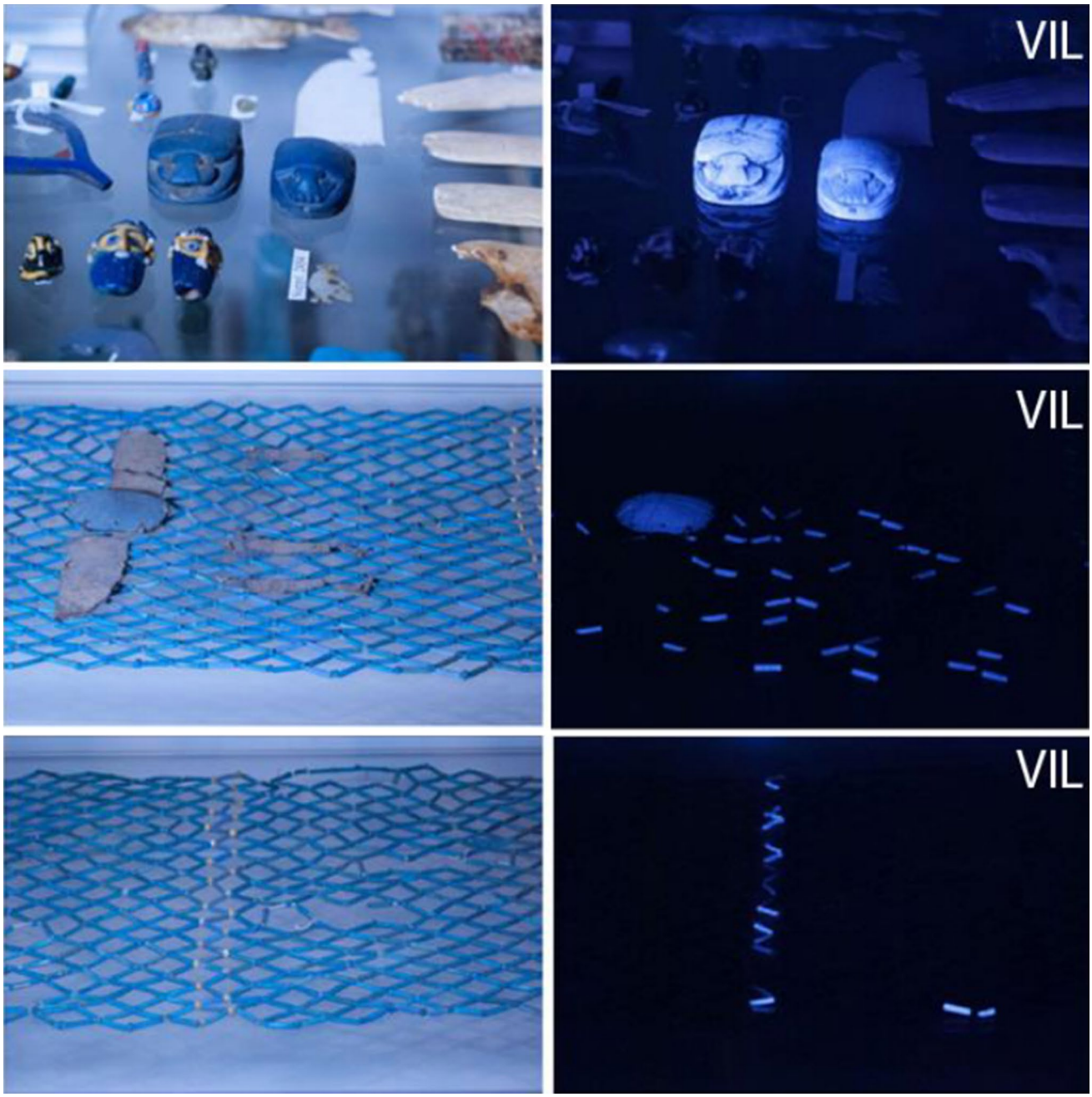

Fig. 13 Some scarabs and mummy nets in Museo Egizio in Turin. The VIL images on the left of each photo indicate the presence of EB as a glowing material. The top VIL shows that the scarabs are made of EB, while the central and the bottom VIL allow to recognize which tubular beads are made of EB and which of Egyptian faience within each net. Reproduced with permission from Masic and Nicola (2021)

resistance could be due to the optimization of the EB production technique as a consequence of the development of glass processing or to the strengthening of the glass matrix due to the use of natron as a fluxing agent (see also Sects. 3.3.11 and 4.2.3).

EB has been widely used also in the Aegean, where it has been found in sites of the Bronze Age in the 3rd and 2nd millennium BCE, such as Keros, Knossos, Thera, Mycenae, Pylos, and Tiryns (Kakoulli 2009; Skovmøller et al. 2016). After the era of the great buildings of the Bronze Age, the occurrences of EB seem to drop significantly in the Greek world, reappearing only in the Archaic period, i.e., from the sixth century BCE (Osanna and Rescigno 2022). An explanation can be the lack of massive orders for large buildings. In this regard, Osanna and Rescigno point out that likely in that period the use of EB was not abandoned

Fig. 14 Marble head of an unidentified figure from the classical Temple of Artemis in Ephesus (British Museum No. 18720405.121). **a** Visible image and **b** green-induced luminescence image, i.e., a specific variant of the VIL technique which will be detailed in part B of this review (see also Sect. 3.5). Reproduced with permission from Verri (2009)

but the pigment was mainly relegated to uses on materials of a labile nature, such as the largely lost wooden objects (Osanna and Rescigno 2022). In classical times, EB has been used to color marbles and statues not only in Egypt but also in the Near East, Greece, and Italy, a noteworthy case being, e.g., the Parthenon (Verri et al. 2010; Osanna and Rescigno 2022). As shown in Fig. 14, the polychromies on statues are very often lost or survive only in traces. However, if they contain EB, it is possible to detect them easily by exploiting its luminescence (Verri 2009; Verri et al. 2010; Skovmøller et al. 2016).

4.1.3 Manufacturing centers and trade in antiquity

EB was a valuable and widespread trade good in ancient times. Its production, use, and trade in antiquity have been the object of some reviews (Tite and Hatton 2007; Kakoulli 2009; Rodler and Kostomitsopoulou Marketou 2022). EB reached places quite far from its production centers. It has been found in the west in sites as old as the eighth century BCE or before, e.g., in Etruria (Baraldi et al. 2015), in Phoenician and Punic settlements including Sardinia (Hölbl 1986; Barnett and Mendleson 1987) and Spain or even in England (Needham and Bimson 1988; Gorton 1996; Cavassa 2018). In a more recent site, i.e., of the third century CE, EB has been detected also as far north as Norway, where it was used as a pigment on a shield of the Bo people (Rosenquist 1959; Scott 2016). The presence of EB in that place is probably due to the trade between the Romans and the northern populations (Rosenquist 1959; Canti and Heathcote 2002).

At first, the other ancient populations must have imported EB produced in Egypt, but over time the production technology spread (Delamare 2007; Rodler and Kostomitsopoulou Marketou 2022). Many manufacturing centers have, indeed, been proposed in various era and places both inside and outside Egypt. In Egypt, the major centers were identified in, e.g., the cities of Memphis (Hatton et al. 2008; Cavassa 2018), Amarna (Spurrell 1895; Nicholson 2007; Rodler and Kostomitsopoulou Marketou 2022), and Qantir-Piramesses (Rehren et al. 2001). Minor centers proposed are also a village near Karnak, Thebes, and Zawiyet Umm el-Rakham (Hatton et al. 2008; Skovmøller et al. 2016). Furthermore, *Vitruvius* also implicitly refers to production in Alexandria in the first century BCE (Rowland 1999). Outside Egypt, it has been suggested that many production sites have existed, e.g., in Mesopotamia (Hatton et al. 2008; Skovmøller et al. 2016; Zaina et al. 2019), the Urartian zone in Easter Turkey (Ingo et al. 2013; Zaina et al. 2019; Ormanci 2020), Persepolis (Oudbashi and Hessari 2020; Amadori et al. 2021), the Isle of Kos in the Aegean (Panagiotaki et al. 2015; Kostomitsopoulou Marketou et al. 2020; Kostomitsopoulou Marketou 2022), the Etruria area in Central Italy (Bordignon et al. 2007; Brøns et al. 2016), and overall, from roughly the first century BCE, the Phlegraean Fields in Southern Italy, i.e., the ancient cities of *Puteoli, Liternum,* and *Cumae* near Naples (Gargiulo 1998; Cavassa et al. 2010; Lazzarini and Verità 2015; Grifa et al. 2016; Cavassa 2018; Osanna

and Rescigno 2022). During the Roman Empire, EB could have been produced also in Spain (Rodler et al. 2017) as arguably meant also by Pliny the Elder in *Book XXXIII* of *Naturalis Historia* (Bostock and Riley 1857), and possibly in Gaul (Delamare 1997) and Britain (Canti and Heathcote 2002; Clegg 2014). It has been suggested that a significant spread of sites for the production of EB took place at least from the Hellenistic period (Kakoulli 2009), i.e., from 323 BCE onward. Furthermore, it has also been suggested that, analogously to glassmaking, only a few centers were actually in charge of the production of EB, while many other workshops processed likely a semi-finished material imported from there, e.g., as ingots (Panagiotaki et al. 2015; Cavassa 2018; Zaina et al. 2019). So far, only a few production sites have been found in archaeological excavation and have a completely reliable identification, e.g., Memphis in Egypt (Cavassa 2018), the Phlegraean area in Italy (Gargiulo 1998; Cavassa et al. 2010; Lazzarini and Verità 2015; Grifa et al. 2016) and probably the Isle of Kos in Greece (Kostomitsopoulou Marketou et al. 2020).

4.1.4 Ancient written sources on Egyptian blue production

No recipes for the production of EB have been found in all the Egyptian texts known so far (Panagiotaki et al. 2015; Fontana et al. 2020), and it has been advanced that the technique used was kept with some secrecy and was handed down orally from generation to generation (Delamare 2007; Greco 2022; Orna and Fontani 2022). Actually, the earliest known written source about EB production in antiquity has been found in Mesopotamia within cuneiform texts from the library of *Ashurbanipal* (seventh century BCE, but copy of original texts dating back to the mid-late 2nd millennium BCE) (Forbes 1966; Delamare 2007; Kakoulli 2009). The texts reported a recipe for making *uknû merku* (Kakoulli 2009). It has to be noted that this first recipe involved methods that seem more typical of glassmaking (Delamare 2007) and that some passages are not at all clear. Other pre-Roman sources report some data about EB (Kakoulli 2009), and among them, is the valuable description given in the fourth century BCE by *Theophrastus* in section 55 of *De Lapidibus* (Eichholz 1965; Katsaros et al. 2010). *Theophrastus* refers to EB using the still current terminology *egyptios kyanos* testifying that it was of Egyptian origin. He also used an adjective meaning «moldable» for EB (Katsaros et al. 2010; Rodler and Kostomitsopoulou Marketou 2022), likely related to the vitreous glass–ceramic features of the material. Furthermore, *Theophrastus* reports that EB was produced to imitate the native stone (i.e., lapis lazuli) and arguably that it was produced in four hues of blue (i.e., that different hues can be produced) from the darker to the lighter according to grain size (Katsaros et al. 2010) (see also Sect. 3.3.3). However, the by far most detailed and popular source available about the production of EB in antiquity is that by *Vitruvius* in *Book VII* of *De Architectura* written around 20–30 BCE (Davidovits 2003; Grifa et al. 2016). It will be described in detail in Sect. 4.2.

4.1.5 Roman times

Analogously to other blue pigments, EB was generally known in Rome as *caeruleum* (akin to the English adjective cerulean). The term is related to the Latin word *caelum* and means «the color of the sky» (Busatta 2014). *Vitruvius* reports within the *De Architectura* (around 20–30 BCE) that an EB production plant was set up in Italy by *Vestorius* (Rowland 1999), a wealthy banker and entrepreneur, correspondent of Cicero and Atticus (Davidovits 2003; Osanna and Rescigno 2022). According to *Vitruvius* the technology to manufacture EB was imported from Alexandria to *Puteoli* (modern Pozzuoli near Naples see also Sect. 4.2). The description given by *Vitruvius* is overall consistent with that reported roughly a century later by Pliny the Elder in *Book XXXIII* of *Naturalis Historia* (Bostock and Riley 1857). Pliny seems to refer to some typologies of EB, i.e., *caeruleum Aegyptios, caeruleum Vestorianum, and caeruleum Puteolanum,* calling the latter also *cylon* (spelled also *coelon* or *cyanon*) (Augusti 1967; Becker 2022; Osanna and Rescigno 2022). He also uses the term *lomentum* referring to a typology of light blue pigment obtained by washing and grinding EB (see also Sect. 3.3.3) and the term *tritum* referring to an EB of lower quality probably deriving from grinding leftovers (Becker 2022). Pliny describes the uses of EB as pigment and even seems to suggest its use as a remedy for ulcers. This latter use could be related to the recently discovered antibacterial and regenerative properties of cuprorivaite (see also Sect. 3.6). Pliny reported the prices of the different types of *caeruleum*, but he does not include any type of EB in the list of rare and expensive pigments that had to be supplied by the commissioner of a paint, i.e., *colores floridi*. The full list of *colores floridi* is provided in *Book XXXV* of *Naturalis Historia* and includes only *minium*, *Armenium*, *cinnabaris*, *chrysocolla*, *Indicum*, and *purpurissum* (Bostock and Riley 1857; Augusti 1967). However, EB has been often implicitly considered among *colores floridi* by many authors (Duran et al. 2010; Lazzarini and Verità 2015) that likely considered its price to be relatively high (Damiani et al. 2003). On the contrary, other authors conclude that EB has not at all to be considered among *colores floridi* and that it likely had to be considered a fairly inexpensive pigment in Rome, pointing out that it was a substitute for more expensive and exotic natural pigments and that it was used also for hidden parts, such as underdrawings (Skovmøller et al. 2016).

EB was widespread in Italy since before the Roman times, i.e., in Magna Graecia, e.g., the Tomb of the Diver

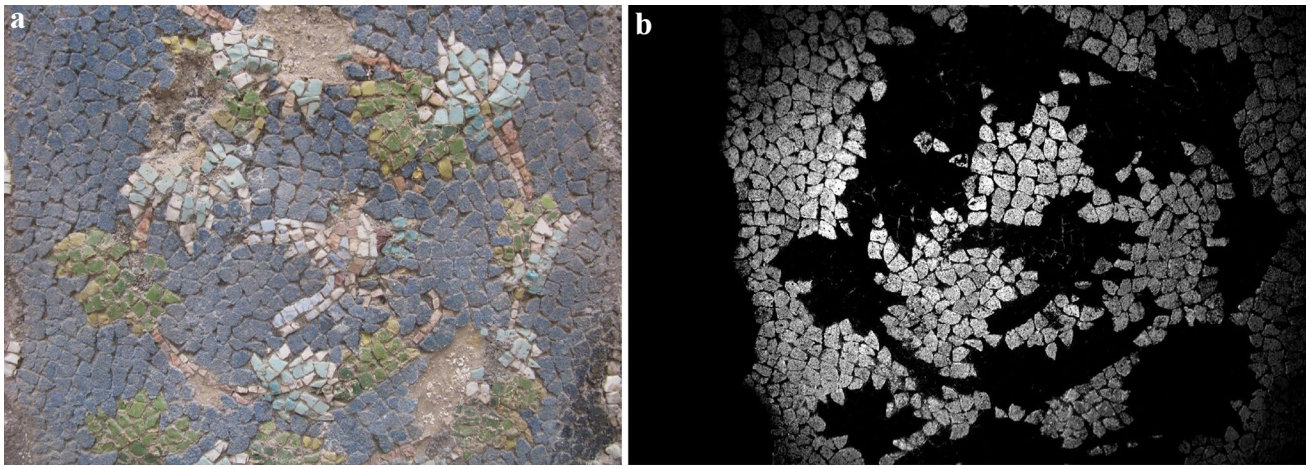

Fig. 15 House of Neptune and Amphitrite in Herculaneum. Nymphaeum. Use of lumps of EB in Roman times to produce mosaics. The centimeter sized tesserae are made of solid EB. **a** Visible light. **b** VIL image acquired in daylight using two NIR-free flashes. Reproduced with permission from Chiari (2018)

at *Paestum* (Zuchtriegel 2018; Osanna and Rescigno 2022) and extensively among the Etruscans (Bordignon et al. 2007; Baraldi et al. 2015, 2017; Brøns et al. 2016; Ceccarelli et al. 2020). Between the second century BCE and the end of the first century CE, the use of EB in Roman wall paintings has been thriving (Bracci et al. 2022). EB was widely used in Roman frescoes, but also in many other techniques and on a wide range of supports, e.g., wood, terracotta, and marbles (Rescigno and Sampaolo 2005; Osanna and Rescigno 2022). In mosaics it was used: (a) to paint preparatory underdrawings below mosaics (Verri et al. 2010); (b) to paint mosaic tesserae (Osanna and Rescigno 2022); and (c) from first century BCE as tesserae made of lumps of vitreous glass–ceramic material (generally used in wall mosaics inside Nymphaea and fountains, see Fig. 15), (Delamare 2007; Boschetti 2011; Chiari 2018).

Throughout the Roman Empire, EB has been almost the only blue pigment used in Europe, West Asia, and North Africa (Scott 2016; Sgamellotti and Anselmi 2022). In Italy, it reached possibly its highest diffusion at the end of the first century CE. In fact, from the second century CE, the presence of EB in the area of Rome (e.g., in Ostia Antica) seems to be limited to more simple uses than before, finding it mixed with other pigments only in contexts of great value (Blümich et al. 2021; Bracci et al. 2021; Falzone et al. 2021). Similar conclusions were drawn by Fermo et al. (2013) and also the use of lumps of EB in mosaics seems to end after the first century CE (Boschetti 2011). A fall in the use of EB in Italy at the end of the first century CE could have been due to many causes, such as local fashion or the troubled political and social period. It may be worth noting the concomitant eruption of Vesuvius near the main Italian sites producing EB. However, according to Delamare, the largest diffusion and use of EB was reached only in the third century CE (Delamare 2007). It has been reported that the price of EB dropped in time. In fact, in 301 CE Diocletian (referring to EB as *cyaninum vestorianus*) regulated its price in the Edict on Maximum Prices setting it at just about one-tenth of the parametrized price referred to by Pliny in first century CE (Delamare 2007; Cavassa 2018). In the fourth and fifth centuries, the availability of EB seems to decrease even if EB has been reported, e.g., in Roman villas (El Salam and Morgan 2006; Cristini et al. 2010; Piovesan et al. 2016) and catacombs (Delamare 2007; Iannaccone et al. 2015; Bracci et al. 2020; Bartolozzi et al. 2021).

4.1.6 Middle ages

Until quite recently it was a common belief that during the years leading to the collapse of the Western Roman Empire (i.e., during the 4th or fifth century CE) the technological know-how to produce EB got lost and consequently the use of EB quickly ended (Chase 1971; Orna et al. 1980; Lazzarini 1982). However, there is a significant number of identifications of EB in that period and beyond the classical Egyptian–Greek–Roman age, thus seems more appropriate to conclude that during the Early Middle Ages the use of EB dropped significantly but did not disappear completely (Delamare 2007; Skovmøller et al. 2016; Linn et al. 2017; Nicola et al. 2018a). However, only a limited number of occurrences seems to have been reported during the sixth century and even less during the seventh century, e.g., in some fourth–sixth century religious buildings in Romania (Iaţcu 2013), in a fifth–sixth century church in northern Italy (Dariz and Schmid 2021), in the fifth–sixth century chorus of the old Basilica Santa Maria *antiqua* in Rome (Raehlmann 1914; Riederer 1997), in the 6th-century wall paintings from a byzantine church in Israel (Linn et al. 2017), in

sixth century Byzantine encaustic mural paintings in Egypt (Gehad et al. 2015), in fifth–seventh century undercoloring of mosaics in Ravenna (Baraldi et al. 2016), in the seventh century Monument of Santalla de Boveda in Galicia (Blanco-Rotea et al. 2022) and in some illuminated manuscripts (Aceto et al. 2020; Hofmann et al. 2020; Aceto 2022). The reasons why the use of EB sharply declined during the Early Middle Ages are still debated. A possible explanation is related to the almost concurrent medieval crisis of glassmaking (Nicola et al. 2019). Notably, in fact, the discontinuation of EB production in the sixth–seventh century CE (Delamare 2007) seems to coincide with the early stages of the crisis of the closely related production of glass in the seventh–ninth century CE (Shortland et al. 2006a; Phelps et al. 2016). Analogously to what happened for glass, the disappearance of EB could have been related to a shortage of natron, i.e., a key ingredient for the production of both EB and glass (Nicola et al. 2019). The natron shortage could have been triggered by the paralysis of trade that followed the fall of the Western Roman Empire or by the political turmoil involving the main natron production sites (e.g., Wadi al Natrun and al-Barnuj) as a consequence of the surge of Islam (Shortland et al. 2006a). However, it has been pointed out that the Islamic conquest had little effect on people's everyday lives, with no destruction layers, no changes to settlement patterns and negligible changes in ceramic and glass production (Phelps et al. 2016).

Another hypothesis is that a natron shortage could have been due to a climatic change (Shortland 2004; Shortland et al. 2006a) triggered by long-term climatic dynamics (Phelps et al. 2016) or by disruptive events such as the three large volcanic eruptions in 536, 540 and 547 CE that led to the Late Antique Little Ice Age lasting between 536 and 660 CE (Büntgen et al. 2016).

Alternative explanations for the disappearance of EB have been expressed by some scholars, e.g., the decrease in the number and quality of newly produced works of art due to the troubled period (Delamare 2007) and the replacement with other pigments increasingly popular in the Middle Ages, such as lapis lazuli and azurite. Notably, in fact, the EB used in the Early Middle Ages and afterward is frequently found not in the pure form but together with another blue pigment, i.e., the very rare and expensive one obtained by lapis lazuli (Gaetani et al. 2004; Bredal-Jørgensen et al. 2011; Beeby et al. 2017; Hofmann et al. 2020). In any case, a certain use of EB has been observed also after the seventh century (Delamare 2007). The main occurrences of EB reported in the eighth to thirteenth century CE are listed in Table 1.

Some hypotheses have been put forward to explain this residual use. Some scholars argued that a limited EB production could have survived somewhere for a few centuries. It has been pointed out that some EB produced in the Middle Age seems of poor quality and low crystallinity (Lazzarini 1982). These features are consistent with a lack of natron (see Sect. 3.3.4). It has also been proposed that possibly some non-traditional manufacturing was developed to avoid or limit the use of natron, i.e., by replacing it with zinc from cementation brass (Nicola et al. 2018a, 2019; Aceto et al. 2020). An example of the ancient use of zinc-rich EB is shown in Fig. 16. Since many of the late finds of EB are in Northern Italy or close to its border (i.e., Müstair) it has been suggested that a certain production of EB could have survived in that area (Delamare 2007). It has been also pointed out that possibly such a production survived in the Eastern Roman Empire, a zone that was less touched by the political instability that affected the former Western Empire. In this case, EB could have reached Italy through painter-monks of oriental provenance, many of whom are known to have been active in Rome in the Middle Ages (Lazzarini 1982; Nicola et al. 2018a). In this regard, it is interesting to note that the term *Venetum* was then used to indicate a blue or bluish color (e.g., in the fourth–fifth century by the writer *Vegetius* in *De re militari*, *Book IV*, 37 referring to the camouflage color used for sails and sailors' clothes) (Spurrell 1895; Reeve 2004). Notably, also Isidore of Sevilla used this term in *Book XIX*, *Caput XVII* of *Etymologiae* which was written shortly before his death in 636 CE and is possibly the last medieval writer that described EB in a treatise. The use of the description of Vitruvius as a source is evident, but EB is referred to as *Venetum caeruleum* (Spurrell 1895; Riederer 1997; Barney et al. 2006). Since it was common to name a pigment or even a color from its place of origin (e.g., *Puteolanum,* see the previous paragraph) (Becker 2022), it seems possible that the use of the term *Venetum* can imply that a blue pigment was produced there or in the surrounding area, or that it arrived in Venice by sea from the mainland Roman Eastern Empire, maybe in raw form (Nicola 2019). At those times Venice was a glassmaking center rising in importance (Whitehouse 2014), and thus it seems possible that the name *Venetum* is related to a residual production of EB there, since generally EB production centers were bound to glass production centers (see also Sects. 4.2.3 and 4.2.4).

However, some other relevant theories exist to explain the use of EB in the Middle Ages. They are related to leftovers that could have remained in storage for some centuries or the pictorial reuse of EB found in excavations. It has to be noted that Hatton calculated that, for the elder fresco in the church of San Clemente in Rome, no less than 35 blue spheres would have been required (Hatton 2008). This would, therefore, imply the availability of fairly large deposits of unused EB (Cavassa 2018). Actually, the discovery of small groups of lumps of raw EB pigment is not uncommon in excavations of Roman sites (see also Sect 4.2.2) (Gaetani et al. 2004; Bensi 2017).

Table 1 Main occurrences of EB reported in the eighth to thirteenth century CE

Time (century CE)	Place	Support	References
7th–11th	St. Augustin's Abbey in Canterbury (England)	Polychrome capital	Brain and Welford (1991a; b) and Delamare (2007)
8th–12th	Various (mainly British)	Illuminated manuscripts	Roger et al. (2004), Delamare (2007), Roger (2007), Vezin and Roger (2007), Beeby et al. (2017, 2018) and Panayotova and Ricciardi (2017)
8th (first half)	Church of San Saba in Rome (Central Italy)	Wall paintings	Gaetani et al. (2004)
8th (781–783 CE)	The Godescalc Evangelistary (BNF Paris, France—made in Achen, North Rhine-Westphalia, Germany)	Illuminated manuscript	Denoël et al. (2018)
8th–9th	Church of Santa Susanna in Rome (Central Italy)	Wall paintings (fragments)	Marabelli et al. (2006)
8th–9th	Church of St. Benedict in Malles (Northern Italy)	Wall paintings	Cavallo et al. (2020)
8th–9th	Church of St. John and the chapel of the Holy Cross in Müstair (Switzerland)	Wall paintings	Emmenegger (1986), Mairinger and Schreiner (1986), Bläuer and Keller (2020) and Cavallo et al. (2020)
Before the half of 9th	St. Etienne oratory in the crypt of St. German Abbey in Auxerre (Burgundy, France)	Wall paintings (background)	Delamare (2007)
9th (824–842 CE)	Crypt of Epiphanius in the Abbey of San Vincenzo al Volturno (Southern Italy)	Wall paintings	Gherolodi and Marazzani (2018a; b)
9th	Excavations at San Vincenzo al Volturno (Southern Italy)	Painted plasters	Howard (2001)
9th and 11th	lower church of San Clemente in Rome (Central Italy)	Wall paintings (two different cycles)	Lazzarini (1982) and Santopadre et al. (2011)
9th–10th	Church of Santa Maria foris portas in Castelseprio (Northern Italy)	Wall paintings	ICR (1967) and Nicola et al. (2018a; b)
9th–10th	Church of Sant'Ambrogio at Montecorvino (Southern Italy)	Wall paintings	Lambert et al. (2018) and Dell'Acqua et al. (2018)
9th–12th (Middle Byzantine)	Church of St. Philip in Hierapolis of Phrygia (South-Western Anatolia, Turkey)	Painted plasters (fragments)	Vettori et al. (2019) and Nicola et al. (2019)
10th–11th	Church of Sant Pere de Terrassa (Catalonia)	Mural altarpiece	Lluveras et al. (2010)
11th–12th	parish church of Fossacaprara di Casalmaggiore (Northern Italy)	wall paintings	Bonazzi et al. (2012) and Milanesi (2017)
12th	The Last Judgment by Nicolaus and Johannes in Vatican Museum (Vatican)	Painting (tempera on wood)	Ajò et al. (1996) and Pozza et al. (2000)
12th (mid)	Chapter house of the St. Albans Abbey (England)	Polychrome sculpture	Howard (2003)
13th	Loggia dei Cavalieri in Treviso (Northern Italy)	Wall paintings	Gaetani et al. (2004)
13th	Portal of the Cathedral of Genoa (Northern Italy)	Polychrome lunette	Rotondi Terminiello (1978) and Bensi (1990, 2017)

EB in Middle Ages could have also been a recycled Roman material such as other building materials that were looted from Roman ruins (Lluveras et al. 2010). A large number of EB tesserae could be found, e.g., in Roman mosaics of the first century BCE-first century CE such as the one in Fig. 15, or EB may have also been scraped from earlier wall paintings (Settis 2022).

Fig. 16 Use of non-traditional EB in Middle Ages. The Apparizione dell'Angelo a Giuseppe scene. Church of Santa Maria foris portas in Castelseprio. On the right VIL image. The VIL was performed in daylight using two flashes with blocked IR component. Reproduced with permission from Nicola et al. (2018a, b)

Possibly, all explanations are valid, with residual production best explaining the most extensive uses of EB and leftovers or recycling for the occasional ones (Nicola et al. 2018a).

It should be noted that another area very rich in late EB findings is England, especially in terms of illuminated manuscripts (Beeby et al. 2018). However, the high number of occurrences of EB in the Middle Ages in both Northern Italy and England may be the result of a more focused search for EB that has been made in those zones (Delamare 2007). It is, therefore, hoped that wider future research also elsewhere, will fill important gaps in the general understanding of the use and trade of EB in the Middle Ages and help to improve the hypotheses expressed so far (Delamare 2007).

Finally, it is worth noting that the last reference to EB in a medieval treatise seems to date back to the eighth century CE as *Vestorianum*. It is in the recipe *XX Auri confectio* within *Mappae Clavicula*, likely related to the production of brass (Baroni et al. 2013; Settis 2022).

4.1.7 Renaissance

The use of EB did not stop in the thirteenth century. Some few but significant findings are reported in the sixteenth century, after more than two centuries of what seems complete oblivion. Actually, the findings of EB in the sixteenth century are all strictly related to the Italian Renaissance (Sgamellotti and Anselmi 2022). Baraldi et al. in 2001 reported the first of them, i.e., some evident traces of EB in Renaissance Bologna on the walls of a villa undergoing restoration (Baraldi et al. 2001b). In 2011 Bredal-Jørgensen identified for the first time the use of EB in an oil painting. It is a painting on wood (i.e., poplar) depicting St. Margaret by the artist Giovanni Battista Benvenuto known as "L'Ortolano" and active in the city of Ferrara, halfway between Bologna and Venice. EB is in a mixture with ultramarine (i.e., lapis lazuli) (Bredal-Jørgensen et al. 2011). Similar findings were made on two other paintings from the zone of Ferrara dating to the 1520–1530 period. They were both painted by the slightly younger and more famous painter Benvenuto Tisi known as "Il Garofalo" (de Vivo et al. 2019). The first depicts the *Holy Family with Saints Elizabeth, Zacharias, John the Baptist, and possibly Saint Francis* (Spring et al. 2019), while the second depicts the *Adoration of the Magi* (de Vivo et al. 2019). Garofalo was in touch with Titian, Giulio Romano, Ludovico Ariosto, and other leading humanists and notably had worked with Raphael in Rome (de Vivo et al. 2019). This is a key point, since the most surprising finding of EB occurred in 2020, i.e., on Raphael's fresco, the *Triumph of Galatea* painted around 1512 in Villa Farnesina, Rome (Anselmi et al. 2020, 2022), a detail of which is shown in Fig. 17. The reason for the use of EB in Renaissance has yet to find an explanation. It has been suggested that a new interest in an old pigment could have been triggered by Renaissance artists' attraction to classical Roman culture and materials, which were to be seen in the ruins and the excavations (Anselmi et al. 2020). EB was mentioned in the written testimonies of Pliny and *Vitruvius* and during Renaissance, a vivid interest surged around *Vitruvius De Architectura* following its full rediscovery in 1414, due to the Florentine humanist Poggio Bracciolini at Montecassino (Gaetani et al. 2004). It may be worth noting that Raphael had a very deep knowledge of *Vitruvius's* work (Anselmi et al. 2020). In fact, Raphael

Fig. 17 Left: detail of Raphael's Galatea. Villa Farnesina, Rome. Right: Red-Induced Luminescence showing EB distribution in white. Reproduced with permission from Sgamellotti and Anselmi (2022)

was in close touch with the elderly Fra 'Giocondo, publisher in 1511, of the first illustrated edition of *De Architectura* (Rowland 2011), and that Raphael in 1514 was also the commissioner of the translation in vernacular of *De Architectura* by the humanist Fabio Calvo from Ravenna (Fontana et al. 1975). It should also be noted that in 1515 Pope Leone X charged Raphael with the title of *praefectus marmorum et lapidum omnium,* i.e., prefect of all marbles and stones, a role that comprise the supervision of ancient monuments and ruins, which denotes Raphael's interest and familiarity in handling ancient and archaeological materials (Shearman and Staff 2003). Finally, it cannot be ruled out that Raphael directly obtained archaeological lumps of EB from the antiquity market, since he was also a collector of antiquities and was in touch with many other collectors such as his friend Agostino Chigi (Zuccari 2022).

No further reliable occurrence of EB has been reported so far beyond the Italian Renaissance until the development of the modern synthesis of the pigment in the nineteenth and twentieth centuries CE (Pisareva et al. 2021). The only exceptions seem to need confirmation, since in both cases, the authors infer the presence of EB by relying on techniques that are not conclusive. They are the following:

- two sculptural models, i.e., a papier-maché head and an unfired clay crucifix both attributed to the 17th-century workshop of Alessandro Algardi (Salerno 1997; Bensi 2017; de Vivo et al. 2019). In this case, the author refers to the identification of EB by polarized-light microscopy only, without supporting further analytical data (de Vivo et al. 2019)
- an 18th-century Coptic icon depicting the Angel Michael (Sakr et al. 2016). In this case, EB has been identified using SEM–EDX and FT-IR that in this situation seem however not sufficient for a univocal identification of EB.

Confirmation of these occurrences would be of high interest, since they could represent the last known preindustrial uses of EB.

The find of EB in Raphael's *Triumph of Galatea* constitutes the earliest known use of EB in a Renaissance painting (Anselmi et al. 2020). The enthusiastic discovery of EB in the palette of one of the most iconic Italian painters has been the starting point of new perspectives and brought to the birth of the BLUENET project, as a joint effort to improve the knowledge of the past use of EB and foster its applications in the present and the future (Sgamellotti and Anselmi 2022).

4.2 Egyptian blue: ancient production and *Vitruvius's*

4.2.1 Overview

Vitruvius's recipe to produce EB is included in *Book VII* of his *De Architectura* which was written around 20–30 BCE (Davidovits 2003). The passage is the following:

"Methods of making blue were first discovered in Alexandria, and afterwards Vestorius set up the making of it at Puzzuoli. The method of obtaining it from the substances of which it has been found to consist, is strange enough. Sand and the flowers of natron are brayed together so finely that the product is like meal, and copper is grated by means of coarse files over the mixture, like sawdust, to form a conglomerate. Then, it is made into balls by rolling it in the hands and thus bound together for drying. The dry balls are put in an earthen jar, and the jars in an oven. As soon as the copper and the sand grow hot and unite under the intensity of the fire, they mutually receive each other's sweat, relinquishing their peculiar qualities, and having lost their properties through the intensity of the fire, they are reduced to a blue color." (Riederer 1997).

Substantially, *Vitruvius*'s recipe implies that EB was obtained by mixing some water, a sand (i.e., *harena*), *flos nitri*, and filings of metallic copper. The paste produced by the mixture was then shaped in the form of balls that were then dried and fired in terracotta vessels.

There is general consensus about the fact that *Vitruvius*'s recipe is the most detailed literary source known about the ancient production of EB (Riederer 1997; Delamare 2007; Kakoulli 2009). However, it should be emphasized that, actually, *Vitruvius* does not give any information about the temperatures involved, does not describe the ingredient unambiguously nor indicate their quantity or ratio (Grifa et al. 2016; Dariz and Schmid 2021, 2022; Osanna and Rescigno 2022). He gives also no information about the dimensions of the "balls" of EB to be produced or if and how they have to be ground and reprocessed.

For this reason, some passages of the ancient method of production remain unclear or debated even though modern chemical analyses extensively carried out from the nineteenth century to the present day have significantly improved the understanding of the ancient technique of production.

In any case, it seems likely that the exact production technique changes quite significantly depending on the place and time. In this regard, it has to be noted that EB existed long before the founding of Alexandria (Augusti 1967), although possibly *Vitruvius* referred to a specific type of *caeruleum*.

4.2.2 Shape of the pellets

It seems that in the Roman Empire raw EB (at least the high-quality one) generally circulated in form of small spheres of around 15–20 mm in diameter (Dariz and Schmid 2022) called *pilae* (Augusti 1967; Osanna and Rescigno 2022) as, e.g., the EB found in some sunk cargoes (Delamare et al. 2004). However, EB has been found in archeological sites of a wide range of times and places as masses of various sizes. They have been defined, e.g., pellets (Kostomitsopoulou Marketou et al. 2020), lumps (Boschetti 2011), balls (Mirti et al. 1995), small blocks (Osanna and Rescigno 2022), cakes (Pagès-Camagna and Colinart 2003; Hatton et al. 2008; Ingo et al. 2013; Ormanci 2020), ingots of various shape (Panagiotaki et al. 2015; Zaina et al. 2019), "loaf of bread" (Bouquillon et al. 2007; Panagiotaki et al. 2015), disks, or spheres (Panagiotaki et al. 2015). Some irregularly shaped lumps of EB from Pompeii are shown in Fig. 18.

Fig. 18 Bowl containing EB pigment found in Pompeii excavations. First century CE. Soprintendenza Pompei, inv. 18106. Reproduced with permission from the Italian Ministry for Cultural Heritage and Activities

4.2.3 Temperature

The temperatures used in antiquity to produce EB have been estimated by many authors who generally agree on a range of 850–950 °C (Tite et al. 1987; Riederer 1997; Bianchetti et al. 2000; Mazzocchin et al. 2004). Pagès-Camagna and Colinart proposed a range slightly higher, i.e., 870–1080 °C (Pagès-Camagna and Colinart 2003). A temperature even higher, in the range of 950–1100 °C has been evaluated by Grifa et al. studying crucibles used in the manufacturing

center in *Cumae* (Grifa et al. 2016) and by Aliatis et al. (1000–1100 °C) studying Roman pigments of the Vesuvian area (Aliatis et al. 2010). On the opposite Jaksch et al. in a study on Egyptian EB deduced that the temperature of production should have been below 742 °C due to the presence of pyrite in some samples (Jaksch et al. 1983).

4.2.4 Natron and other fluxes

Notably, some disagreement exists about the translation of the Latin terminology «*flos nitri*», although it is generally accepted that it is associated with a typology of salt. The word «*flos*» (literally «flower») is generally understood as «high quality» or «refined» (Mottana 2006), but it cannot be ruled out that it simply means something like «efflorescences» (Crosland 2004). The term «*nitri*» is more debated. As suggested also by the description of *nitrum* given by Pliny the Elder in *Book XXXI* of *Naturalis Historia*, it is generally agreed that *flos nitri* refers reliably to natron (Gitton-Ripoll 2009), i.e., a salt mainly constituted by $Na_2CO_3{\cdot}10H_2O$ with minor amounts also of $NaHCO_3$, chlorides, sulfates, other carbonates and impurities (Shortland 2004; Shortland et al. 2011). Natron is a naturally occurring salt generally coming from the huge crusts that form in and around the periodic lakes (*sebka*) and rivers (*wadi*) in the desert, e.g., in Egypt at Wadi El Natrun (Lucas and Harris 1962) and al-Barnuj (Shortland 2004; Mottana 2006; Shortland et al. 2011). It has been pointed out that other exploitable sources were also at lake Van in Turkey (Dardeniz 2015) and maybe also elsewhere. Quite recently, e.g., it has been found as efflorescences in fumaroles at Mt. Vesuvius and in the Sicilian volcanoes (Mottana 2006). Natron was extensively produced in Egypt and used for many purposes, such as detergent, disinfectant, or desiccant (e.g., in mummification) (Abdel-Maksoud and El-Amin 2011; Dardeniz 2015). Its use for the production of glass spread from Egypt in the early 1st millennium BCE and has been widely exploited in Roman times (Shortland et al. 2006a). It was such an important commodity as to become a state monopoly in Ptolemaic times (Mottana 2006). In EB production, analogously to glassmaking, the role of natron is that of a flux, i.e., a substance that lowers the melting point of silica and allows the melt-flux synthesis (see also Sect. 3.3.4). The presence of appreciable amounts of potassium in addition to sodium in most of the ancient EB samples has been related to the use of other alkaline fluxes different from natron, such as plant ash or soda-rich plant ash, the latter from plants, such as *Salsola soda* and *Anabasis articulata*, growing in coastal, or salt-rich zones (Hatton et al. 2008). Similar uses of natron and other fluxes are well-known and established in the history of glassmaking (Shortland et al. 2006a; Hatton et al. 2008; Jackson et al. 2018). Other possible sources of potassium in EB are feldspar from the sand used (Hatton et al. 2008) or from terracotta crucibles (Grifa et al. 2016; Nicola et al. 2019). However, it is not possible to completely rule out that *nitri* in *Vitruvius*'s recipe referred actually to other salts different from natron and known in antiquity, such as saltpeter (KNO_3) (Pagès-Camagna et al. 1999; Barnum 2003; Skovmøller et al. 2016; Dariz and Schmid 2021). However, the translation with saltpeter would not only contradict the general consensus that relates *nitri* to natron (Mottana 2006; Gitton-Ripoll 2009) but would also seem inconsistent with the preponderant presence of sodium generally found in Roman EB (Hatton et al. 2008; Fontana et al. 2020). It may be worth noting that in some translations of *De Architectura,* i.e., the one of 1826 by Gwilt (still very widespread) «*flos nitri*» seems to be translated fairly loosely with «flower of sulphur» (Gwilt 1826). This type of interpretation seems erroneous and devoid of any foundation.

Natron was often impure due to chlorides, sulfates, and calcium carbonate (Turner 1956; Davidovits 2003; Pradell et al. 2006; Giménez et al. 2017). It is possible that such impurities played a key role in EB production. Calcium could be present as a natural impurity of natron but also as a consequence of the intentional adulteration of natron with lime as reported by Pliny the Elder in *Book XXXI* of *Naturalis Historia* (Bostock and Riley 1857; Davidovits 2003). The presence of chlorides has been pointed out as a possible cause of the formation of a green product as a result of the synthesis (Giménez et al. 2017), even if the production of the Egyptian green pigment has been generally related to other specific features, e.g., a higher temperature of production or an increased amount of flux (and possibly calcium) in comparison to EB (Hatton et al. 2008; Grifa et al. 2016).

4.2.5 Sand and source of calcium

The presence of calcium in natron could account for the lack of a calcium-bearing ingredient in *Vitruvius*'s recipe (Davidovits 2003). However, the general consensus is that, similar to what happened in glass production, the main source of calcium in *Vitruvius's* EB was a specific type of sand containing some $CaCO_3$ already in the proper ratio with SiO_2 (Mazzocchin et al. 2004; Lazzarini and Verità 2015; Fontana et al. 2020). Indeed, the two main sources of sand for glassmaking reported in Roman treaties are both relatable to siliceous sand, rich in calcium carbonate and low in iron (Turner 1956). The most famous of them is at the mouth of the River Belus on the Syrian coast and is referred to by *Strabo*, Pliny, *Josephus,* and *Tacitus,* while the other is found on the seashore deposit mentioned by Pliny near the mouth of the River Volturnus between *Cumae* and *Liternum*, north–west of the ancient harbors of Pozzuoli and Naples

(Turner 1956). The main sites for the production of EB in Italy have been found exactly in the same area. This fact strongly supports the hypothesis that the sand used to produce EB and referred to by *Vitruvius* was the same used for glassmaking and was the source of both calcium and silica (Lazzarini and Verità 2015; Rodler and Kostomitsopoulou Marketou 2022). The use in different places and periods of quartz pebbles or sand as a source of silica for EB has been taken into account and described diffusely by many authors (Jaksch et al. 1983; Pagès-Camagna and Colinart 2003; Tite and Shortland 2003; Hatton et al. 2008; Ingo et al. 2013; Panagiotaki et al. 2015).

4.2.6 Source of copper

The copper needed to produce EB could have been from copper metal, as reported by *Vitruvius,* but it has been pointed out that also copper ores may have been used (Jaksch et al. 1983; Hatton et al. 2008; Rodler and Kostomitsopoulou Marketou 2022). They could be, for example, malachite, e.g., from Sinai (Rademakers et al. 2017; Gouda et al. 2020) or roasted sulphidic copper ores (Dariz and Schmid 2021, 2022). Some specific studies to identify the source of the copper ore used have been recently performed using, e.g., lead isotopes data (Rademakers et al. 2017; Rodler et al. 2017). However, copper very likely has also been sourced from scraps of alloys as indicated by the presence of some peculiar elements reported in many archaeological samples of EB. The chronological succession of these occurrences fits well with the chronological development of metallurgy, i.e., meaningful amount of arsenic has been found in the most ancient samples of EB (related to arsenical bronzes), followed by tin (bronzes), lead (leaded bronzes) (Kaczmarczyk and Hedges 1983; El Goresy et al. 1998), and finally zinc (orichalcum or brass) (Nicola 2019).

4.3 Chinese blue and Chinese purple

Even if a technology transfer from Egypt to China could not be ruled out (Chiari and Scott 2004; Berke et al. 2010) it is most likely that the development of CB and CP occurred in China independently of EB, roughly two and a half millennia after the development of EB in Egypt (Berke 2007; Liu et al. 2007; Xia et al. 2014). Xia et al. conclude that CP and CB were developed in the southeast of Gansu province, China and that the trajectory of their usage follows the route of the development of the Qin State and Empire (Xia et al. 2014). It has been suggested that the diffusion of CB and CP could be connected with the developments of Taoism and alchemy, since the synthesis technology of barium–copper silicates could be related to the production of high refractive index glasses (artificial jades) by Taoist monks and alchemists (Thieme 2001; Liu et al. 2007; Li et al. 2015a, b).

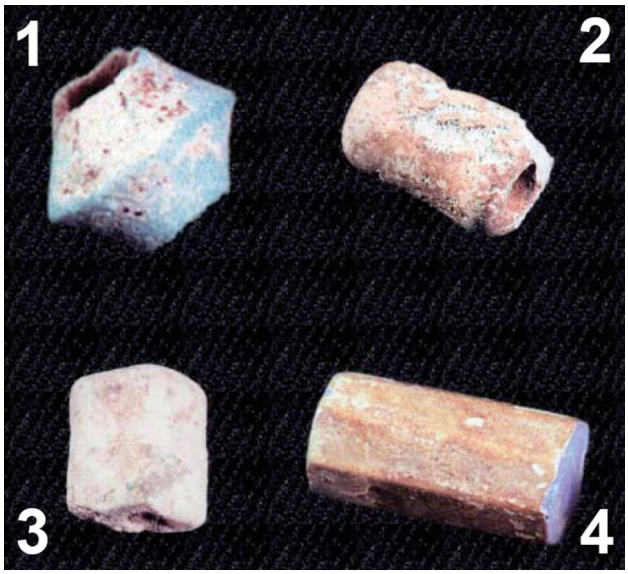

Fig. 19 Bead 1 (777–766 BCE) contains CP and lapis lazuli blue within a faience layer. Bead 2 (eighth–sixth century BCE) contains CB and lapis lazuli blue within a faience pigment layer. Origin: the archaeological excavation site Li County (Northwestern China). Bead 3 (770–476 BCE) is composed of a heterogeneous, compact blue body of CB. It is part of the class of the sinter minerals rich in lead and barium. Octagonal stick 4 (fifth–third century BCE) is composed of equally colored sinter material rich in lead and barium, partly crystallized and partly glassy with a decomposed, partly whitish surface (colour figure online). Reproduced with permission from Berke (2007)

The earliest occurrences of barium–copper silicate pigments known so far are from beads that date back to the beginning of the Spring and Autumn period (770–476 BCE) (Ma et al. 2006; Berke 2007; Qin et al. 2016; Zhang et al. 2019). The oldest known objects that contain artificial barium–copper silicates are, indeed, faience tubes, beads, and other decorative objects, such as octagonal sticks (see, e.g., Fig. 19). They date from the Eastern Zhou Dynasty (770–255 BCE) to the Warring States period (475–221 BCE) (Ma et al. 2006; Xia et al. 2014). CB and CP, analogously to EB, were actually at first used to mold small objects, having a production technology closely related to that of ancient faience, glazes, and glass (Ma et al. 2006; Li et al. 2015b; Wang et al. 2017). The fluxes used for the production of CB and CP were mainly lead compounds, e.g., lead metal, sulfides, oxides, or carbonates (Li et al. 2015a). It has been suggested that lead additives have been preferred likely because they can promote the thermal decomposition of the otherwise stable $BaSO_4$ (barite) that is one of the main natural sources of barium and is widespread in the area of production of ancient barium–copper silicates pigments (Wiedemann and Berke 2001; Xia et al. 2014). However, Qin et al. have pointed out with a series of simulation experiments how the most likely source of barium for the

production of barium–copper silicates should have been the rarer witherite deposits (i.e., $BaCO_3$) also present in the area (Qin et al. 2016). Analogously to what happened for EB the source of copper could have been sometimes also copper alloys such as bronze as suggested by the platelet-like crystals of $BaSnSi_3O_9$ detected on the mural painting of a tomb in Luoyang City, Henan Province, China, dated to Western Han Dynasty (206 BCE–8 CE) (Zhang et al. 2019).

It seems somehow unclear which appeared first between CP and CB. Currently, the general consensus seems to be that CP has been developed first (Xia et al. 2014; Qin et al. 2016). According to Xia et al. CP has been detected on finds dating to the beginning of the Spring and Autumn period (about 770 BCE), while CB should have appeared only during the early to mid-Warring States period (i.e., about three hundred years later) (Xia et al. 2014). However, Berke previously suggested that CB and CP appeared both around 800 BCE and that at first CB was used in preference, being replaced by CP as the preferred pigment around 400 BCE (Berke 2007; Berke et al. 2010). The difficulty of drawing a clear boundary between CB and CP production and use may be due to the fact that CB and CP are frequently found in the same sample. This is because the $BaO–CuO–SiO_2$ system is more complex than the $CaO–CuO–SiO_2$ one and can lead to the formation of multiple compounds. Actually, CB and CP are often found together and are occasionally found also in association with another blue copper–barium silicate pigment based on $BaCu_2Si_2O_7$ and named Chinese dark blue (Xia et al. 2008, 2014; Berke et al. 2009) (for further details see also Sect. 3.1.2 Composition of Chinese Blue and Chinese Purple). Since when CP has been developed blue pigments were quite available in China (i.e., azurite), Xia et al. proposed that CB and Chinese dark blue were developed as by-products of the production of CP (Xia et al. 2014). In this view, the fact that some CB has been reported also on more ancient findings could be explained, since CB (i.e., effenbergerite) is much more stable than CP (i.e., colinowensite) and also of Chinese dark blue, i.e., scottyite (Berke et al. 2009). Thus, the CB identified on ancient objects could be linked to the decay of CP (Berke 2007). Furthermore, it is anyway expected that effenbergerite can better survive in time on ancient objects in comparison with the other barium–copper silicates even in the case that, i.e., it was present only as a minor component in the ancient freshly produced CP pigment (Berke et al. 2009; Xia et al. 2014).

In the late Warring States period, both CP and CB start to be found in greater abundance as pigments in paintings as well as in glazed objects and as compact body artifacts (Xia et al. 2014; Zhang et al. 2019). The Terracotta Army of the first Emperor of the Qin dynasty, Qin Shi Huang, (about 220 BCE) was painted largely with CP, while azurite has been in general used for the blues (Herm et al. 1995; Thieme 2001; Blänsdorf and Xia 2006; Ma et al. 2006; Berke 2007; Bonaduce et al. 2008). Examples of warriors wearing robes painted with CP are reported, i.e., by Liu et al. (2007) and by Berke (2007). The use of barium–copper silicate pigments found its peak between the end of the Warring States period and the end of the Eastern Han Dynasty (220 BCE–220 CE) (Xia et al. 2014).

The use of CB and CP seems to be limited to some regions of China (i.e., Shaanxi, Henan, Gansu, Hebei, Shandong, and Jiangsu provinces) (Xia et al. 2014). Some occurrences of CB outside China were also reported, such as numerous tubular faience beads and a piece of glass unearthed in Japan, dating back to the centuries 1st BCE–2nd CE (Takayasu 2002). However, as there is no archaeological evidence of the use of CB and CP in the ancient Korean peninsula, they are likely related to travelers and trade (Xia et al. 2014).

The production and use of barium–copper silicate pigments seem to end with the end of the Han Dynasty when the Chinese Empire has been divided up again (Berke et al. 2009). According to Xia et al., after the fall of the Eastern Han Dynasty (220 CE) the lead barium glass industry declined and external lead silicate glass became the mainstream. The manufacture and use of CP and CB wane accordingly (Xia et al. 2014). Liu et al. suggest that a concomitant reason for the abandonment of CP and CB may also have been the coeval resurgence of Confucianism, a philosophy more focused on human society and with little interest in materials and natural science (Liu et al. 2007).

Contrary to what happened for EB, no further occurrences of CB or CP have ever been reported at any time. Their production technology and existence as pigments or material have been completely forgotten and lost for about 1750 years until their recent rediscovery, respectively, in the 1980s and 1990s (FitzHugh and Zycherman 1983, 1992).

Acknowledgements We are thankful to Enrico Ferraris, Egyptologist and Curator at the Museo Egizio in Turin, for his essential help in the understanding of Sethe's translation of the 18th dynasty text about "blue bread". We are also grateful to Daniela Comelli, (Physics Department of the Polytechnic University of Milan) and Paolo Tomassini (École française de Rome, Centro Studi Pittura Romana Ostiense) for valuable comments and discussion. We express our deep gratitude to the BLUENET project, to the Academia Nazionale dei Lincei—Centro linceo di ricerca sui beni culturali Villa Farnesina (CERIF), and to Antonio Sgamellotti, Director of CERIF.

Funding Open access funding provided by Università degli Studi di Torino within the CRUI-CARE Agreement.

Data availability The authors confirm that the data supporting the findings of this study are available within the article [and/or] in the articles in the reference list.

References

Abadir MI (2014) Experimental Study of the Egyptian blue degradation by the copper chloride cancer. Escola Tècnica Superior d'Enginyeria Industrial de Barcelona

Abdel-Maksoud G, El-Amin A-R (2011) A review on the materials used during the mummification processes in ancient Egypt. Mediterr Archaeol Archaeom 11:129–150

Accorsi G, Verri G, Bolognesi M et al (2009) The exceptional near-infrared luminescence properties of cuprorivaite (Egyptian blue). Chem Commun. https://doi.org/10.1039/b902563d

Aceto M (2022) Manuscript D23 sup Hystoria Adversos Paganos 7th century CE from Abbazia di Bobbio—Biblioteca Ambrosiana di Milano (**Personal Commun**)

Aceto M, Calà E, Fenoglio G et al (2020) New evidence of non-traditional Egyptian blue manufacture in the 6th century Ashburnham Pentateuch. J Archaeol Sci Rep. https://doi.org/10.1016/j.jasrep.2020.102487

AIRPA (2021) La peinture murale antique: méthodes et apports d'une approche technique—Actes du colloque international Louvain-la-Neuve 21 avril 2017. In: Cavalieri M, Tomassini P (eds) Associazione Italiana Ricerche Pittura Antica—Edizioni Quasar

Ajò D, Chiari G, De Zuane F, et al (1996) Photoluminescence of some blue natural pigments and related synthetic materials. In: 5th International conference on non-destructive testing, microanalytical methods and environmental evaluation for study and conservation of works of art. Budapest, pp 37–47

Aliatis I, Bersani D, Campani E et al (2010) Pigments used in Roman wall paintings in the Vesuvian area. J Raman Spectrosc 41:1537–1542. https://doi.org/10.1002/jrs.2701

Allenspach S, Biffin A, Stuhr U et al (2020) Multiple magnetic bilayers and unconventional criticality without frustration in $BaCuSi_2O_6$. Phys Rev Lett 124:177205. https://doi.org/10.1103/PhysRevLett.124.177205

Allenspach S, Puphal P, Link J et al (2021) Revealing three-dimensional quantum criticality by Sr substitution in Han purple. Phys Rev Res 3:1–18. https://doi.org/10.1103/PhysRevResearch.3.023177

Amadori ML, Vagnini M, Vivani R et al (2021) Advances in characterization of colourful residues unearthed in Persepolis West craft zone using microscopic and spectroscopic techniques. Microchem J 167:106304. https://doi.org/10.1016/j.microc.2021.106304

Anselmi C, Vagnini M, Seccaroni C et al (2020) Imaging the antique: unexpected Egyptian blue in Raphael's Galatea by non-invasive mapping. Rend Fis Acc Lincei 31:913–917. https://doi.org/10.1007/s12210-020-00960-4

Anselmi C, Azzarelli M, Vagnini M, et al (2022) Il Blu Egizio nel Trionfo di Galatea di Raffaello. In: Atti dei Convegni Lincei 343—Il blu egizio dall'antichità al Rinascimento. 25 febbraio 2021. Bardi Editore

Augusti S (1967) I Colori Pompeiani. De Luca Editore, Roma

Baraldi P, Bondioli F, Fagnano C et al (2001a) Study of the vibrational spectrum of cuprorivaite. Ann Chim 11–12:679–692

Baraldi P, Fagnano C, Giordani N, et al (2001b) Una testimonianza di blu egiziano nella Bologna del '500. In: 8a giornata "Archeometria e Mondo classico" Roma 22-24/2/2001b. p 1

Baraldi P, Fagnano C, Loschi Ghittoni A et al (2006) Vibrational spectra of some pigments from Pompeii. Automata 49–65

Baraldi P, Marchesini M, Rottoli M (2015) Analisi scientifiche dalle necropoli di Verucchio. Analisi chimiche e botaniche: risultati e prospettive di ricerca. In: Von Eles P, Bentini L, Poli P, Rodriguez E (eds) Immagini di uomini e di donne. pp 109–117

Baraldi P, Bracci S, Cristoferi E et al (2016) Pigment characterization of drawings and painted layers under 5th–7th centuries wall mosaics from Ravenna (Italy). J Cult Herit 21:802–808. https://doi.org/10.1016/j.culher.2016.03.001

Baraldi P, Natalucci M, Rossi A (2017) Il blu egiziano a Kainua: dai pigmenti alla policromia su terracotta. Quad della Sc di Spec Beni Archeol 25

Barbar SK, Patel KR, Kumar S (2017) Structural, optical and magnetic properties of $MCuSi_4O_{10}$ (M = Ba and Sr) blue pigments. J Mater Sci Mater Electron 28:3716–3724. https://doi.org/10.1007/s10854-016-5978-z

Barnett RD, Mendleson C (1987) Tharros; a catalogue of material in the British Museum from Phoenician and other Tombs at Tharros, Sardinia. BMP, London

Barney S, Lewis W, Beach J, Berghof O (eds) (2006) The Etymologies of Isidore of Seville. Cambridge University Press. https://doi.org/10.1017/CBO9780511482113

Barnum DW (2003) Some history of nitrates. J Chem Educ 80:1393. https://doi.org/10.1021/ed080p1393

Baroni S, Pizzigoni G, Travaglio P (2013) Mappae Clavicula. In: Mappae Clavicula—Alle origini dell'alchimia in Occidente. Testo, traduzione, note. Il Prato, pp 57–190

Bartolozzi G, Bracci S, Sacchi B et al (2021) Mural paintings of the cubicle "dei fornai" in Domitilla catacombs in Rome: a study via non-invasive techniques. Archaeol Anthropol Sci 13:1–11. https://doi.org/10.1007/s12520-021-01447-5

Batista CD, Schmalian J, Kawashima N et al (2007) Geometric frustration and dimensional reduction at a quantum critical point. Phys Rev Lett 98:1–4. https://doi.org/10.1103/PhysRevLett.98.257201

Bazin D, Rehr JJ (2003) Limits and advantages of X-ray absorption near edge structure for nanometer scale metallic clusters. J Phys Chem B 107:12398–12402. https://doi.org/10.1021/jp0223051

Becker H (2022) Pigment nomenclature in the ancient Near East, Greece, and Rome. Archaeol Anthropol Sci. https://doi.org/10.1007/s12520-021-01394-1

Beeby A, Gameson R, Nicholson C (2017) New light on old illuminations. Arch Rec 39:244–256. https://doi.org/10.1080/23257962.2017.1325729

Beeby A, Gameson R, Nicholson C (2018) Colour at canterbury; the pigments of canterbury illuminators from the tenth to twelfth centuries. In: Panayotova S, Ricciardi P (eds) Manuscripts in the making: art & science, vol 1. Brepols Publishers, Turnhout, pp 21–35

Belsky HL, Rossman GR, Prewitt CT, Gasparik T (1984) Crystal structure and optical spectroscopy (300 to 2200 nm) of $CaCrSi_4O_{10}$. Am Mineral 69:771–776

Bensch W, Schur M (1995) Crystal structure of calcium copper phyllodecaoxotetrasilicate, $CaCuSi_4O_{10}$. Zeitschrift Fur Krist New Cryst Struct 210:530. https://doi.org/10.1524/zkri.1995.210.7.530

Bensi P (1990) La pellicola pittorica nella pittura murale in Italia: materiali e tecniche esecutive dall'alto medioevo al XIX secolo. In: Danti C, Matteini M, Moles A (eds) Le pitture murali. Tecniche, problemi, conservazione. Centro Di, Firenze, pp 73–102

Bensi P (2017) Blu egiziano, il pigmento che visse due volte. Kermes 100:157

Berdahl P, Boocock SK, Chan GC-Y et al (2018) High quantum yield of the Egyptian blue family of infrared phosphors (MCuSi4O10, M = Ca, Sr, Ba). J Appl Phys 123:193103. https://doi.org/10.1063/1.5019808

Berke H (2007) The invention of blue and purple pigments in ancient times. Chem Soc Rev 36:15–30. https://doi.org/10.1039/B606268G

Berke H, Wiedemann HG (2000) The chemistry and fabrication of the anthropogenic pigments chinese blue and purple in ancient China. East Asian Sci Technol Med. https://doi.org/10.1163/26669323-01701006

Berke H, Corbiere T, Portmann A, et al (2009) Man-made Ancient Chinese Blue and Purple Barium Copper Silicate Pigments. Wen bo Reli Museol, pp 251–265

Berke H, Portmann A, Bouherour S et al (2010) The development of ancient synthetic copper-based blue and purple pigments. In: Agnew N (ed) Conservation of ancient sites on the silk road: proceedings of the second international conference on the conservation of grotto sites, Mogao Grottoes, Dunhuang, People's Repubblic of China. June 28–July 3, 2004. The Getty Conservation Institute, Los Angeles, pp 225–233

Bianchetti P, Talarico F, Vigliano MG, Ali MF (2000) Production and characterization of Egyptian blue and Egyptian green frit. J Cult Herit 1:179–188

Binet L, Lizion J, Bertaina S, Gourier D (2021) Magnetic and new optical properties in the UV–visible range of the Egyptian blue pigment cuprorivaite $CaCuSi_4O_{10}$. J Phys Chem C. https://doi.org/10.1021/acs.jpcc.1c06060

Blanco-Rotea R, Sanjurjo-sánchez J, Freire-lista DM, Benavides García R (2022) Absolute dating of construction materials and petrological characterisation of mortars from the santalla de bóveda monument (Lugo, Spain). In: Res. Sq. (PREPRINT—Version 1). https://www.researchsquare.com/article/rs-1891346/v1. Accessed 15 Sep 2022

Blänsdorf C, Xia Y (2006) A colourful world for the Emperor's soul: the polychromy of the terracotta sculptures at Qin Shihuang's Burial Complex. Stud Conserv 51:177–183. https://doi.org/10.1179/sic.2006.51.Supplement-2.177

Bläuer C, Keller AT (2020) Mainly red and a hidden blue—Laboratory and MSI investigations on the Carolingian wall paintings in the Chapel of the Holy Cross of Müstair (Switzerland). J Cult Herit 42:72–80. https://doi.org/10.1016/j.culher.2019.07.024

Bloise A (2018) Synthesis and characterization of gillespite. Appl Phys A Mater Sci Process. https://doi.org/10.1007/s00339-018-1756-5

Bloise A, Abd El Salam S, De Luca R et al (2016) Flux growth and characterization of cuprorivaite: the influence of temperature, flux, and silica source. Appl Phys A Mater Sci Process 122:1–8. https://doi.org/10.1007/s00339-016-0198-1

Blom-Böer I, Warburton DA (2020) The Composition of the colour palette and the socio-economic role of pigments used in Egyptian painting. In: Warburton DA, Thavapalan S (eds) The value of colour. Material and Economics aspects in the Ancient World—Berlin Studies of The Ancient World. Edition Topoi, Berlin, pp 231–253

Blümich B, Del FE, Jaschtschuk D et al (2021) Nondestructive analysis of wall paintings at Ostia Antica. Heritage 4:4421–4438. https://doi.org/10.3390/heritage4040244

Bonaduce I, Blaensdorf C, Dietemann P, Colombini MP (2008) The binding media of the polychromy of Qin Shihuang's Terracotta Army. J Cult Herit 9:103–108. https://doi.org/10.1016/j.culher.2007.08.002

Bonazzi A, Campana F, Ferrari F et al (2012) Il restauro del ciclo medievale della parrocchiale di Fossacaprara di Casalmaggiore (CR). In: Lo Stato dell'Arte 10. Atti del convegno (Roma, 22–24 novembre 2012). pp 211–218

Bordignon F, Postorino P, Dore P, Trojsi G (2007) Raman identification of green and blue pigments in Etruscan polychromes on architectural terracotta panels. J Raman Spectrosc 38:255–259. https://doi.org/10.1002/jrs

Borisov SM, Würth C, Resch-Genger U, Klimant I (2013) New life of ancient pigments: application in high-performance optical sensing materials. Anal Chem 85:9371–9377. https://doi.org/10.1021/ac402275g

Borkow G, Gabbay J (2009) Copper, an ancient remedy returning to fight microbial, fungal and viral infections. Curr Chem Biol. https://doi.org/10.2174/187231309789054887

Boschetti C (2011) Vitreous materials in early mosaics in Italy: Faience, Egyptian blue, and glass. J Glass Stud 53:59–91

Bostock J, Riley HT (1857) Pliny the Elder—Naturalis Historia. In: Natural History of Pliny, 77th–79 CE edn. H. G. Bohn, pp 141–143

Bouherour S, Berke H, Wiedemann H-G (2001) Ancient man-made copper silicate pigments studied by Raman microscopy. Chimia (aarau) 55:942–951

Bouquillon A, Caubet A, Kaczmarczyk A, Matoïan V (2007) Faïences et matières vitreuses de l'Orient ancien. Étude physico-chimique et catalogue des œuvres du département des Antiquités orientales. Musée du Louvre—Sonek, Paris

Bracci S, Magrini D, Manganelli Del Fà R et al (2020) Brightly colored to stay in the dark. Revealing of the polychromy of the Lot sarcophagus in the catacomb of San Sebastiano in Rome. Heritage 3:858–874. https://doi.org/10.3390/heritage3030047

Bracci S, Cantisani E, Falzone S et al (2021) Archaeometry and roman wall painting: the case of pre-hadrianic paintings in Ostia Antica. In: Cavalieri M, Tomassini P (eds) La peinture murale antique: méthodes et apports d'une approche technique—Actes du colloque international Louvain-la-Neuve 21 avril 2017. Associazione Italiana Ricerche Pittura Antica, Edizioni Quasar, pp 13–19

Bracci S, Cantisani E, Conti C et al (2022) Enriching the knowledge of ostia antica painted fragments: a multi-methodological approach. Spectrochim Acta Part A Mol Biomol Spectrosc 265:120260. https://doi.org/10.1016/j.saa.2021.120260

Brain D, Welford PM (1991a) The conservation of a stone capital from St Augustine's Abbey, Canterbury—Ancient Monuments Laboratory Report 121/91. 1–32

Brain D, Welford PT (1991b) Composite capital, in The making of England: Anglo-Saxon Art and Culture AD 600-900. University of Toronto

Bredal-Jørgensen J, Sanyova J, Rask V et al (2011) Striking presence of Egyptian blue identified in a painting by Giovanni Battista Benvenuto from 1524. Anal Bioanal Chem 401:1433–1439. https://doi.org/10.1007/s00216-011-5140-y

Brøns C, Hedegaard SS, Sargent ML (2016) Painted faces: investigations of polychromy on Etruscan Antefixes in the Ny Carlsberg Glyptotek. Etruscan Stud 19:23–67. https://doi.org/10.1515/etst-2015-0012

Bruni S, Cariati F, Casadio F, Toniolo L (1999) Spectrochemical characterization by micro-FTIR spectroscopy of blue pigments in different polychrome works of art. Vib Spectrosc 20:15–25

Büntgen U, Myglan VS, Ljungqvist FC et al (2016) Cooling and societal change during the Late Antique Little Ice Age from 536 to around 660 AD. Nat Geosci 9:231–236. https://doi.org/10.1038/ngeo2652

Burzo E (2009) Gillespite Group of Silicates. In: Landolt-Bornstein (ed) New Series, Group III, Volume 27: magnetic properties of non-metallic inorganic compounds based on transition elements,

subvolume I 5a: Phyllosilicates—Part 1. Springer, Berlin, pp 1–15
Busatta S (2014) The perception of color and the meaning of brilliance among archaic and ancient populations and its reflections on language. Cult Anthropol 10:309–347
Cairncross B, Rumsey MS (2022) Cuprorivaite and papagoite from the messina mine, Limpopo Province, South Africa. Rocks Miner 97:134–141. https://doi.org/10.1080/00357529.2022.2004512
Canti MG, Heathcote JL (2002) Microscopic Egyptian blue (synthetic cuprorivaite) from sediments at two archaeological sites in west central England. J Archaeol Sci 29:831–836. https://doi.org/10.1006/jasc.2001.0717
Cavaleri T, Buscaglia P, Migliorini S et al (2017) Pictorial materials database: 1200 combinations of pigments, dyes, binders and varnishes designed as a tool for heritage science and conservation. Appl Phys A Mater Sci Process 123:1–15. https://doi.org/10.1007/s00339-017-1031-1
Cavallo G, Aceto M, Emmenegger R et al (2020) Preliminary non-invasive study of Carolingian pigments in the churches of St. John at Müstair and St. Benedict at Malles. Archaeol Anthropol Sci. https://doi.org/10.1007/s12520-020-01024-2
Cavassa L (2018) La production du bleu égyptien durant l'époque hellénistique et l'Empire romain (IIIe av. J.-C.-Ier s. apr. J.-C.). In: Jockey P (ed) Bulletin de correspondance hellénique-supplément, 2018, Les arts de la couleur en Grèce ancienne..et ailleurs Approches interdisciplinaires. pp 13–34
Cavassa L, Delamare F, Repoux M (2010) La fabrication du bleu égyptien dans les Champs Phlégréens (Campanie, Italie) durant le Ier siècle de notre ère. In: Aspects de l'artisanat en milieu urbain: Gaule et Occident romain. pp 235–249
Ceccarelli S, Guarneri M, Romani M et al (2020) Are the blue daemons really blue? Multidisciplinary study for the colours characterization of the mural paintings inside the Blue Daemons Etruscan tomb. J Cult Herit. https://doi.org/10.1016/j.culher.2020.09.002
Chakoumakos BC, Fernandez-Baca JA, Boatner LA (1993) Refinement of the structures of the layer Silicates $MCuSi_4O_{10}$ (M = Ca, Sr, Ba) by rietveld analysis of neutron powder diffraction data. J Solid State Chem 103:105–113
Chase WT (1971) Egyptian blue as a pigment and ceramic material. In: Brill RH (ed) Science and archaeology. MIT Press, Cambridge, pp 80–90
chemtube3d.com ChemTube3D. https://www.chemtube3d.com/sscacusi4o10-2/. Accessed 16 Sep 2022
Chen Y, Shang M, Wu X, Feng S (2014a) Hydrothermal synthesis, hierarchical structures and properties of blue pigments $SrCuSi_4O_{10}$ and $BaCuSi_4O_{10}$. CrystEngComm 16:5418–5423. https://doi.org/10.1039/c3ce42394h
Chen Y, Zhang Y, Feng S (2014b) Hydrothermal synthesis and properties of pigments Chinese purple $BaCuSi_2O_6$ and dark blue BaCu2Si2O7. Dye Pigment 105:167–173. https://doi.org/10.1016/j.dyepig.2014.01.017
Chen W, Shi Y, Chen Z et al (2015) Near-infrared emission and photon energy upconversion of two-dimensional copper silicates. J Phys Chem C 119:20571–20577. https://doi.org/10.1021/acs.jpcc.5b04819
Chen Y, Kan M, Sun Q, Jena P (2016) Structure and Properties of Egyptian Blue Monolayer Family: XCuSi4O10 (X = Ca, Sr, and Ba). J Phys Chem Lett. https://doi.org/10.1021/acs.jpclett.5b02770
Chiari G (2018) Photoluminescence of Egyptian blue. SAS Encycl Archaeol Sci. https://doi.org/10.1002/9781119188230.saseas0453
Chiari G, Scott D (2004) Pigment analysis: potentialities and problems. Period Di Mineral 73:227–237
Chopin T, Macaudiere P (1994) Alkaline-earth metal-, copper-, and optionally titanium-based silicates, blue or violet pigments based on these silicates, process for their preparation and their use
Clegg S (2014) Blue shade hues: a study of blue pigments used by Romano-British Wall-Painters. University of Sussex
Coccato A, Moens L, Vandenabeele P (2017) On the stability of mediaeval inorganic pigments: a literature review of the effect of climate, material selection, biological activity, analysis and conservation treatments. Herit Sci 5:1–25. https://doi.org/10.1186/s40494-017-0125-6
Coccato A, Mazzoleni P, Spinola G, Barone G (2021) Two centuries of painted plasters from the Lateran suburban villa (Rome): investigating supply routes and manufacturing of pigments. J Cult Herit 48:171–185. https://doi.org/10.1016/j.culher.2020.11.010
color-name.com color-name. https://www.color-name.com/egyptian-blue.color#color-codes. Accessed 7 Sep 2022
colour-index.com The Colour Index™—Published online by Society of Dyers and Colourists and American Association. colour-index.com. Accessed 7 Sept 2022
Comelli D, Capogrosso V, Orsenigo C, Nevin A (2016) Dual wavelength excitation for the time-resolved photoluminescence imaging of painted ancient Egyptian objects. Herit Sci 4:21. https://doi.org/10.1186/s40494-016-0090-5
Corbiere T (2009) Preparation and Methods of Characterisation of the Barium Copper Silicates $BaCuSi_4O_{10}$ (Chinese Blue), $BaCuSi_2O_6$ (Chinese Purple), $Ba_2CuSi_2O_7$, $BaCu_2Si_2O_7$ used as blue and purple pigments. Universität Zürich
Corcoran L (2016) The color blue as an animator in ancient Egyptian art. In: Goldman RB (ed) Essays in global color history: interpreting the ancient spectrum. Gorgias Press, Piscataway, pp 43–63. https://doi.org/10.31826/9781463236632-008
Cosentino A (2014) FORS spectral database of historical pigments in different binders. e-Conserv J. https://doi.org/10.18236/econs2.201410
Cosentino A (2015) Effects of different binders on technical photography and infrared reflectography of 54 historical pigments. Int J Conserv Sci 6:287–298
Cristini O, Kinowski C, Jarry T et al (2010) Micro-Raman spectroscopic identification of pigments of 4th century Roman wall paintings. AIP Conf Proc 1267:313–314. https://doi.org/10.1063/1.3482530
Crosland MP (2004) Historical studies in the language of chemistry. Dover Publications, Mineola
Damiani D, Gliozzo E, Turbanti IM, Spangenberg JE (2003) Pigments and plasters discovered in the House of Diana (Cosa, Grosseto, Italy): an integrated study between art history, archaeology and scientific analyses. Archaeometry 45:341–354. https://doi.org/10.1111/1475-4754.00112
Daniels V, Stacey R, Middleton A (2004) The blackening of paint containing Egyptian blue. Stud Conserv 49:217–230. https://doi.org/10.2307/25487699
Dardeniz G (2015) Was ancient Egypt the only supplier of natron? New research reveals major anatolian deposits. Anatolica 41:191–202
Dariz P, Schmid T (2021) Trace compounds in Early Medieval Egyptian blue carry information on provenance, manufacture, application, and ageing. Sci Rep 11:1–13. https://doi.org/10.1038/s41598-021-90759-6
Dariz P, Schmid T (2022) Raman focal point on Roman Egyptian blue elucidates disordered cuprorivaite, green glass phase and trace compounds. Sci Rep. https://doi.org/10.1038/s41598-022-19923-w
Davidovits F (2003) Vitruvius recipe for the manufacture of the pigment "Egyptian blue." In: Piccioli C, Sogliani F (eds) Il vetro in Italia meridionale e insulare. Atti del Secondo Convegno Multidisciplinare, Settime Giornate Nazionali di Studio Comitato

Nazionale AIHV (Napoli, 5-6-7 dicembre 2001). Napoli, pp 297–302
de Vivo GS, van Loon A, Noble P et al (2019) An unusual pigment in 16th century Ferrara: "Egyptian blue" in Garofalo's Adoration of the Magi and Ortolano's St. Margaret. In: Christensen AH, Jager A (eds) Trading paintings and painters' materials 1550–1800. Archetype Publications Ltd in association with CATS, London, pp 136–148
Delamare F (1997) Sur les processus physiques intervenant lors de la synthèse du bleu égyptien : réflexion à propos de la composition de pigments bleux gallo-romains. Rev D'archéométrie 21:103–119
Delamare F (2007) Bleus en poudres. De l'Art à l'Industrie 5000 ans d'innovations. Presses de l'École des mines de Paris, Paris
Delamare F, Monge G, Repoux M (2004) À la recherche de différentes qualités marchandes dans les blues égyptiens trouvés à Pompéi. Riv Di Stud Pompeiani 15:89–107
Dell'Acqua F, Gheroldi V, Marazzani S, et al (2018) La chiesa altomedievale di Sant'Ambrogio a Montecorvino Rovella (Sa). Prima campagna di studi archeologici e storico-artistici. Hortus Artium Mediev J Int Res Cent Late Antiq Middle Ages 24
Denoël C, Roger Puyo P, Brunet AM, Siloe NP (2018) Illuminating the Carolingian era: new discoveries as a result of scientific analyses. Herit Sci 6:1–19. https://doi.org/10.1186/s40494-018-0194-1
Doehne E, Ma Q (2004) Rediscovering ancient technology: microbeam analysis of Han Purple. Microsc Microanal 10:910–911. https://doi.org/10.1017/S1431927604887257
Dong C, Yang C, Younis MR et al (2022) Bioactive NIR-II light-responsive shape memory composite based on cuprorivaite nanosheets for endometrial regeneration. Adv Sci 2102220:1–11. https://doi.org/10.1002/advs.202102220
Du JM, Zeng HY, Song LJ et al (2003) Synthesis and structure of a new polymorph $Ba_2CuSi_2O_7$. Jiegou Huaxue 22:33–36
Duran A, Jimenez De Haro MC, Perez-Rodriguez JL et al (2010) Determination of pigments and binders in Pompeian Wall paintings using synchrotron radiation - high-resolution X-Ray powder diffraction and conventional spectroscopy - chromatography. Archaeometry 52:286–307. https://doi.org/10.1111/j.1475-4754.2009.00478.x
Dyer J, Verri G, Cupitt J (2013) Multispectral imaging in reflectance and photo-induced luminescence modes: a user manual
Eastaugh N, Walsh V, Chaplin T, Siddall R (2004) The pigment compendium a dictionary of historical pigments. Elsevier, New York
Edreira MC, Feliu MJ, Fernández-Lorenzo C, Martín J (2003) Spectroscopic study of Egyptian blue mixed with other pigments. Helv Chim Acta 86:29–49. https://doi.org/10.1002/hlca.200390017
Eichholz DE (1965) Theophrastus—De Lapidibus. Oxford University Press, Oxford
El Goresy A, Jaksch H, Razek MA, Weiner KL (1986) Ancient pigments in wall paintings of Egyptian tombs and temples: an archaeometric project (Farbpigmente in altägypschen Wandmalereien in Gräbern und Tempeln: ein archïsches Projekt). Max Planck Institute für Kernphysik, Heidelberg
El Goresy A, Schiegl S, Weiner KL (1998) A chronological scheme for the technological evolution of copper in ancient Egypt. In: Ismael FA (ed) Proceedings of the first international conference on ancient Egyptian mining and metallurgy and conservation of metallic artifacts. Egyptian Antiquities Organization Press, Cairo, pp 215–234
El Salam SA, Morgan G (2006) Scientific examination of wall plaster from brading Roman Villa: isle of wight. In: Moreau J-F, Auger R, Chabot J, Herzog A (eds) The 36h international symposium on archaeometry, ISA 2006, 2–6 May 2006, Quebec City, Canada. Quebec City, pp 207–214
Emmenegger M (1986) Deterioration and preservation of Carolingian and medieval mural paintings in the Müstair Convent (Switzerland)—part III: techniques and materials used and past restorations. In: Bromelle NS, Smith P (eds) Case studies in the conservation of stone and wall paintings: contributions to the 1986 IIC Congress. International Institute for Conservation, London, pp 197–199
Etcheverry MP, Schvoerer M, Bechtel F (2001) Bleu égyptien: mise en évidence de deux processus de formation de la cuprorivaïte. Rev D'archéométrie 25:87–100
Falzone S, Marano M, Tomassini P (2021) Painters of Ostia: Reconstructing Production Dynamics and Craftsmanship of Ostian Wall Paintings. In: Thomas R (ed) Local styles or common pattern books in roman wall painting and mosaics. Archaeology and Economy in the Ancient World—Proceedings of the 19th International Congress of Classical Archaeology (2018). Cologne/Bonn, pp 49–63
Fang C, Van Blaaderen A, Van Huis MA (2015) Two-dimensional hydrous silica: nanosheets and nanotubes predicted from first-principles simulations. J Phys Chem C 119:14343–14350. https://doi.org/10.1021/jp512590z
Fermo P, Piazzalunga A, De Vos M, Andreoli M (2013) A multi-analytical approach for the study of the pigments used in the wall paintings from a building complex on the Caelian Hill (Rome). Appl Phys A Mater Sci Process 113:1109–1119. https://doi.org/10.1007/s00339-013-7754-8
Finger LW, Hazen RM, Hemley RJ (1989) $BaCuSi_2O_6$: a new cyclosilicate with four-membered tetrahedral rings. Am Mineral 74(7–8):952–955
FitzHugh EW, Zycherman LA (1983) An early man-made blue pigment from China—barium copper silicate. Stud Conserv 28(1):15–23
FitzHugh EW, Zycherman LA (1992) A purple barium copper silicate pigment from early china. Stud Conserv 37(3):145–154
Fontana V, Calvi MF, Morachiello P (1975) Vitruvio e Raffaello: il De architectura di Vitruvio nella traduzione inedita di Fabio Calvo Ravennate, vol 13. Officina
Fontana R, Baraldi P, Fedi ME et al (2020) Notes on Vestorius' Blue—new findings and investigations. J Cult Herit. https://doi.org/10.1016/j.culher.2020.03.002
Forbes RJ (1955) Studies in ancient technology—vol III. E.J Brill, Leiden
Forbes RJ (1966) Studies in ancient technologies—vol V. E. J. Brill, Leiden
Ford RJ, Hitchman MA (1979) Single crystal electronic and EPR spectra of $CaCuSi_4O_{10}$, a synthetic silicate containing copper(II) in a four-coordinate, planar ligand environment. Inorg Chim Acta 33:167–170. https://doi.org/10.1016/S0020-1693(00)89436-0
Fouqué F (1889) Sur le bleu Égyptien ou vestorien. Bull La Société Française Minéralogie 12:36–38
Frondel C (1979) Crystalline silica hydrates from leached silicates. Am Mineral 64:799–804
Gaetani MC, Santamaria U, Seccaroni C (2004) The use of Egyptian blue and lapis lazuli in the Middle Ages: the wall paintings of the San Saba church in Rome. Stud Conserv 49:13–23
Gaines RV, Skinner HCW, Foord EE et al (1997) Dana's new mineralogy, the system of mineralogy of James Dwight and Edward Salisbury Dana, 8th edn. Wiley, New York
Gao R, Shi A, Cao Z et al (2022) Construction of 2D up-conversion calcium copper silicate nanosheet for efficient photocatalytic nitrogen fixation under full spectrum. J Alloys Compd 910:164869. https://doi.org/10.1016/j.jallcom.2022.164869
García-Fernández P, Moreno M, Aramburu JA (2015) Origin of the exotic blue color of copper-containing historical pigments. Inorg Chem 54:192–199. https://doi.org/10.1021/ic502420j
García-Fernández P, Moreno M, Aramburu JA (2016) Origin of the anomalous color of Egyptian and han blue historical pigments: going beyond the complex approximation in ligand field theory. J Chem Educ. https://doi.org/10.1021/acs.jchemed.5b00288

Gargiulo P (1998) Contenitori con depositi di colore blu egiziano e officine vetrarie nell'area dell'antica Liternum e nel territorio flegreo. Aspetti tecnologici e prospettive di studio. In: Il vetro dall'antichità all'età contemporanea: aspetti tecnologici, AIHV—Comitato nazionale italiano, 14–15 dicembre 1996, Milano. Comune di Milano, Settore cultura e musei, Civiche raccolte archeologiche, Milano, pp 61–65

Gehad B, Aly MF, Marey H (2015) Identification of the Byzantine encaustic mural painting in Egypt. Mediterr Archaeol Archaeom 15:243–256. https://doi.org/10.5281/zenodo.16612

Gheroldi V, Marazzani S (2018a) Usi dell'azzurro egizio. Due esempi di ricostruzione storica. In: Giostra C (ed) Città e campagna: culture, insediamenti, economia (secc. VI-IX) - II Incontro per l'Archeologia barbarica. Milano, 15 maggio 2017. SAP Società Archeologica s.r.l., Mantova, pp 351–359

Gheroldi V, Marazzani S (2018b) I dipinti murali della cripta: nuove indagini, nuove acquisizioni. In: Marazzi F (ed) Molise Medievale Cristiano. Edilizia religiosa e territorio (secoli IV–XIII). Volturnia Edizioni, pp 257–276

Giester G, Rieck B (1994) Effenbergerite, $BaCu[Si_4O_{10}]$, a new mineral from the Kalahari Manganese Field, South Africa: description and crystal structure. Mineral Mag 58:663–670. https://doi.org/10.1180/minmag.1994.058.393.17

Giester G, Rieck B (1996) Wesselsite, SrCu[Si4O10], a further new gillespite-group mineral from the Kalahari Manganese Field, South Africa. Mineral Mag 60:795–798. https://doi.org/10.1180/minmag.1996.060.402.09

Giménez J (2015a) Finding hidden chemistry in ancient Egyptian artifacts: pigment degradation taught in a chemical engineering course. J Chem Educ 92:456–462. https://doi.org/10.1021/ed500327j

Giménez J (2015b) Egyptian blue and/or atacamite in an ancient Egyptian coffin. Int J Conserv Sci 6:747–749

Giménez J, Espriu-Gascon A, Bastos-Arrieta J, de Pablo J (2017) Effect of NaCl on the fabrication of the Egyptian blue pigment. J Archaeol Sci Rep 14:174–180. https://doi.org/10.1016/j.jasrep.2017.05.055

Gitton-Ripoll V (2009) Pourquoi il ne faut pas traduire natrum par «nitre»: emplois thérapeutiques de ce minéral dans la médecine humaine et vétérinaire des romaines (Pline, NH 31, 106–117, Scribonius largus, Pelagonius). Bull Société Hist La Médecine Des Sci Vétérinaires 9:5–16

Glabau CA, Goldman PF (1938) Some physical and chemical properties of Egyptian bread. Cereal Chem. https://doi.org/10.4172/2471-2728.1000161

Glazkov VN, Smirnov AI, Revcolevschi A, Dhalenne G (2005) Magnetic resonance study of the spin-reorientation transitions in the quasi-one-dimensional antiferromagnet $BaCu_2Si_2O_7$. Phys Rev B Condens Matter Mater Phys. https://doi.org/10.1103/PhysRevB.72.104401

Glazkov VN, Dhalenne G, Revcolevschi A, Zheludev A (2011) Multiple spin-flop phase diagram of $BaCu_2Si_2O_7$. J Phys Condens Matter. https://doi.org/10.1088/0953-8984/23/8/086003

Godet M, Binet L, Schoder S et al (2022) X-ray irradiation effects on Egyptian blue and green pigments. J Anal at Spectrom. https://doi.org/10.1039/d2ja00020b

Gorton AF (1996) Egyptian and Egyptianizing scarabs. A typology of steatite, faience and paste scarabs from punic and other mediterranean sites. Oxford University School of Archaeology, Oxford

Gouda VK, Angelini E, Abouelata AMA et al (2020) Survey of copper base alloys used in ancient Egypt. In: Eurocorr 2019—the annual event of the European Federation of Corrosion—Seville, Spain, September 9-13 2019. pp 1–10

Gourdin WH, Kingery WD (1975) The beginnings of pyrotechnology: neolithic and egyptian lime plaster. J F Archaeol 2:133–150. https://doi.org/10.1179/009346975791491277

Greco C (2022) Il colore delle cose. In: Atti dei Convegni Lincei 343 - Il blu egizio dall'antichità al Rinascimento. 25 febbraio 2021. Bardi Edizioni, pp 25–32

Green L (2001) Colour transformations in ancient Egyptian pigments. In: Davies WV (ed) Colour and painting in ancient Egypt. British Museum Press, London, pp 43–48

Grifa C, Cavassa L, De Bonis A et al (2016) Beyond vitruvius: new insight in the technology of egyptian blue and green frits. J Am Ceram Soc 99:3467–3475. https://doi.org/10.1111/jace.14370

Guo Q, Liu X, Qiu J (2015a) Method for preparing $CaCuSi_4O_{10}$ two-dimensional crystals. 1–6

Guo Q, Liu X, Qiu J (2015b) $SrCuSi_4O_{10}$ two-dimensional crystal and preparation method thereof. 1–7

Guo Q, Liu X, Qiu J (2015c) Method for preparing $BaCuSi_4O_{10}$ two-dimensional crystal. 1–6

Gwilt J (1826) Vitruvius—De Architectura. In: The architecture of marcus vitruvius pollio. Priestley and Weale

Hallmann A, Rickerby S, Shekede L (2021) Blue and green in the decoration of a Kushite chapel in Karnak, Egypt: technical evaluation using low-tech, non-invasive procedures. J Archaeol Sci Rep 39:103190. https://doi.org/10.1016/j.jasrep.2021.103190

Harrison N, Sebastian SE, Batista CD et al (2006) Bose-Einstein condensation in $BaCuSi_2O_6$. J Phys Conf Ser 51:9–14. https://doi.org/10.1088/1742-6596/51/1/002

Hassanein M (1969) Substitution effect on structure and colour in Egyptian blue system. Indian J Chem 7(3):269

Hatton GD (2008) Production of Egyptian blue and green frits. In: Tite MS, Shortland AJ (eds) Production technology of Faïence and related early vitreous materials. Oxford University School of Archeology, Oxford, pp 147–185

Hatton GD, Shortland AJ, Tite MS (2008) The production technology of Egyptian blue and green frits from second millennium BC Egypt and Mesopotamia. J Archaeol Sci 35:1591–1604. https://doi.org/10.1016/j.jas.2007.11.008

Hazen RM, Burnham CW (1974) The crystal structures of gillespite I and II: a structure determination at high pressure. Am Mineral 59(11–12):1166–1176

Hazen RM, Finger LW (1983) High-pressure and high-temperature crystallographic study of the gillespite I-II phase transition. Am Mineral 68:595–603

He C, Dong C, Yu L et al (2021) Ultrathin 2D inorganic ancient pigment decorated 3D-printing Scaffold enables photonic hyperthermia of osteosarcoma in NIR-II biowindow and concurrently augments bone regeneration. Adv Sci 2101739:1–10. https://doi.org/10.1002/advs.202101739

Hedegaard SB, Delbey T, Brøns C, Rasmussen KL (2019) Painting the Palace of Apries II: ancient pigments of the reliefs from the Palace of Apries, Lower Egypt. Herit Sci. https://doi.org/10.1186/s40494-019-0296-4

Herm C, Thieme C, Emmerling E et al (1995) Analysis of painting materials of the polychrome terracotta army of the first emperor Qin Shi Huang. Ceram Cult Herit Proc Int Symp "The Ceram Heritage''' 8th CIMTEC-World Ceram Congr Forum New Mater Florence, Italy, June 28–July 2, 1994" 675–684

Hofmann C, Rabitsch S, Malissa A et al (2020) The miniatures of the Vienna Genesis: colour identification and painters ' palettes. In: Hofmann C (ed) The vienna genesis: material analysis and conservation of a late antique illuminated manuscript on purple parchment. Bohlau Verlag GmbH u, Company KG, p 2020

Hölbl G (1986) Agyptisches Kulturgut im phonikischen und punischen Sardinien. Etudes Prelim aux Relig Orient dans l'Empire romain 102

Hong G, Antaris AL, Dai H (2017) Near-infrared fluorophores for biomedical imaging. Nat Biomed Eng 1:1–22. https://doi.org/10.1038/s41551-016-0010

Howard H (2001) An analysis of the painted plasters. In: Mitchell J, Hansen I (eds) San Vincenzo al Volturno 3: the findings from the 1980–86 excavations. Centro Italiano di Studi sull'Alto Medioevo, Spoleto, pp 287–295

Howard H (2003) Pigments of english medieval wall painting. Archetype Publications Ltd, London

Hughes EM, Pack MJ, Dann SE, Weller MT (1997) Preparation and structural characterisation of alkaline earth sheet silicates containing copper by powder neutron diffraction, EXAFS and UV–visible spectroscopy. An Quim 93:233–236

Huheey JE (1978) Inorganic chemistry: principles of structure and reactivity, 2nd edn. Harper and Row, New York

Iannaccone R, Bracci S, Cantisani E, Mazzei B (2015) An integrated multimethodological approach for characterizing the materials and pigments on a sarcophagus in St. Mark, Marcellian and Damasus catacombs. Appl Phys A Mater Sci Process 121:1235–1242. https://doi.org/10.1007/s00339-015-9495-3

Iaţcu I (2013) The painting of Roman Dobruja (5th -6th AD): a General View. Cercet Istor (serie Noua) 32:113–129

ICR (1967) Relazione dell'Istituto Centrale per il Restauro, faldone, "Castelseprio, Santa Maria foris portas", Archivio della Soprintendenza per i Beni Stori e Artistici, Milano

Ingo GM, Çilingiroğlu A, Di Carlo G et al (2013) Egyptian Blue cakes from the Ayanis fortress (Eastern Anatolia, Turkey): Micro-chemical and -structural investigations for the identification of manufacturing process and provenance. J Archaeol Sci 40:4283–4290. https://doi.org/10.1016/j.jas.2013.06.016

Inoue M, Uematsu K, Ishigaki T, et al (2009) Synthesis of Gillespite related silicate phosphor for a white LED. In: 216th ECS Meeting. The Electrochemical Society

irug.org IRUG Spectral Database—IRUG The Infrared and Raman Users Group. www.irug.org. Accessed 15 Sept 2022

Jackson CM, Paynter S, Nenna MD, Degryse P (2018) Glassmaking using natron from el-Barnugi (Egypt); Pliny and the Roman glass industry. Archaeol Anthropol Sci 10:1179–1191. https://doi.org/10.1007/s12520-016-0447-4

Jaime M, Correa VF, Harrison N et al (2004) Magnetic-field-induced condensation of triplons in Han Purple pigment $BaCuSi_2O_6$. Phys Rev Lett 93:6–9. https://doi.org/10.1103/PhysRevLett.93.087203

Jaksch H, Seipel W, Weiner KL, El Goresy A (1983) Egyptian blue—cuprorivaite a window to ancient Egyptian technology. Naturwissenschaften 70:525–535. https://doi.org/10.1007/BF00376668

Janczak J, Kubiak R (1992a) Refinement of the structure of barium copper silicate BaCu[Si4O10] at 300 K. Acta Crystallogr Sect C 48:1299–1301. https://doi.org/10.1107/S0108270191014580

Janczak J, Kubiak R (1992b) Structure of the cyclic barium copper silicate $Ba_2Cu_2[Si_4O_{12}]$ at 300 K. Acta Crystallogr 48:8–10

Johnson-Mcdaniel D, Barrett CA, Sharafi A, Salguero TT (2012) Nanoscience of an ancient pigment. J Am Chem Soc 135:1677–1679. https://doi.org/10.1021/ja310587c

Johnson-McDaniel D, Salguero TT (2014) Exfoliation of Egyptian blue and Han blue, two alkali earth copper silicate-based pigments. J vis Exp. https://doi.org/10.3791/51686

Johnson-McDaniel D, Comer S, Kolis JW, Salguero TT (2015) Hydrothermal formation of calcium copper tetrasilicate. Chem A Eur J 21:17560–17564. https://doi.org/10.1002/chem.201503364

Kaczmarczyk A, Hedges REM (1983) Ancient Egyptian faience: an analytical survey of Egyptian faience from predynastic to Roman Times. Aris and Phillips Ltd, Warminster

Kadikova IF, Malyhin SA, Morozova EA et al (2019) Cathodoluminescence microspectroscopy as a new method in the study of art pigments. In: Technart 2019: The European Conference on the Use of Analytical Techniques for Characterization of ArtworksAt: Bruges, Belgium, 7–10 May 2019. Bruges, Belgium, pp 2–3

Kakoulli I (2002) Late Classical and Hellenistic painting techniques and materials: a review of the technical literature. Stud Conserv 47:56–67. https://doi.org/10.1179/sic.2002.47.supplement-1.56

Kakoulli I (2009) Egyptian blue in Greek painting between 2500 and 50 BC. In: Shortland A, Freestone I, Rehren T (eds) From mine to microscope: advances in the study of ancient technology. Oxbow Books, Oxford, pp 101–112

Katsaros T, Liritzis I, Laskaris N (2010) Identification of Theophrastus' Pigments egyptios kyanos and psimythion from archaeological excavations: a case study. ArchéoSciences. https://doi.org/10.4000/archeosciences.2632

Kendrick E, Kirk CJ, Dann SE (2007) Structure and colour properties in the Egyptian blue Family, M1-xM′xCuSi4O10, as a function of M, M′ where M, M′ = Ca, Sr and Ba. Dye Pigment 73:13–18. https://doi.org/10.1016/j.dyepig.2005.10.006

King RSP, Hallett PM, Foster D (2016) NIR−NIR fluorescence: a new genre of fingermark visualisation techniques. Forensic Sci Int 262:e28–e33

Kiss A, Stretz HA, Ueda A, Mu R (2022) Synthesis of Egyptian blue and mechanisms. J Phys Chem Solids. https://doi.org/10.1016/j.jpcs.2022.110738

Knight KS, Henderson CMB (2007) Structural basis for the anomalous low-temperature thermal expansion behaviour of the gillespite-structured phase Ba0.5Sr0.5CuSi4O10. Eur J Mineral 19:189–200. https://doi.org/10.1127/0935-1221/2007/0019-1711

Knight KS, Henderson CMB, Clark SM (2010) Structural variations in the wesselsite-effenbergerite (Sr 1-xBaxCuSi4O10) solid solution. Eur J Mineral 22:411–423. https://doi.org/10.1127/0935-1221/2010/0022-2025

Kostomitsopoulou Marketou A (2022) The materialisation of colour: reconstructing Egyptian blue manufacture on late Hellenistic Kos. Nor Archaeol Rev 55:21–37. https://doi.org/10.1080/00293652.2022.2052746

Kostomitsopoulou Marketou A, Andriulo F, Steindal C, Handberg S (2020) Egyptian blue pellets from the first century BCE Workshop of Kos (Greece): microanalytical investigation by optical microscopy, scanning electron microscopy-X-ray energy dispersive spectroscopy and micro-Raman Spectroscopy Ariadne. Minerals 10:1–31. https://doi.org/10.3390/min10121063

Kostomitsopoulou Marketou A, Giannici F, Handberg S et al (2021) Synchrotron radiation-based micro-XANES and micro-XRF study of unsuccessfully produced Egyptian blue from the late hellenistic production site of Kos (Dodecanese, Greece). Anal Chem 93:11557–11567. https://doi.org/10.1021/acs.analchem.1c02063

Krämer S, Stern R, Horvatić M et al (2007) Nuclear magnetic resonance evidence for a strong modulation of the Bose–Einstein condensate in $BaCuSi_2O_6$. Phys Rev B Condens Matter Mater Phys 76:1–4. https://doi.org/10.1103/PhysRevB.76.100406

Kriss D, Serotta A, Chiari G, et al (2016) Visible-Induced Luminescence (VIL) Imaging: Past, Current and Future Applications in Conservation Research. In: AIC's 44th Annual Meeting

Lambert C, Torino M, Perciante F, et al (2018) Montecorvino Rovella (SA), chiesa di S. Ambrogio. Revisione di vecchi scavi—analisi paleopatologiche—prospezioni geognostiche - indagini multispettrali sui dipinti murali. In: Sogliani F, Gargiulo B, Annunziata E, Vitale V (eds) VIII Congresso Nazionale di Archeologia Medievale—Chiesa del Cristo Flagellato (ex Ospedale di San Rocco) Matera, 12—15 settembre 2018. All'Insegna del Giglio, pp 74–79

Lamprecht I, Reller A, Riesen R, Wiedemann HG (1997) Ca-oxalate films and microbiological investigations of the influence of

ancient pigments on the growth of lichens: thermogravimetric/thermomicroscopic analyses. J Therm Anal 49:1601–1607
Lazzarini L (1982) The discovery of Egyptian blue in a Roman Fresco of the Mediaeval Period (Ninth Century). Sour Stud Conserv 27:84–86
Lazzarini L, Verità M (2015) First evidence for 1st century AD production of Egyptian blue frit in Roman Italy. J Archaeol Sci 53:578–585. https://doi.org/10.1016/j.jas.2014.11.004
Lee L, Quirke S (2000) Painting materials. In: Nicholson PT, Shaw I (eds) Ancient Egyptian materials and technology. pp 104–120
Lee HC, Siew KW, Gimbun J, Cheng CK (2013) Application of cement clinker as Ni-catalyst support for glycerol dry reforming. Bull Chem React Eng Catal 8:137–144. https://doi.org/10.9767/bcrec.8.2.5023.137-144
Leek FF (1972) Teeth and bread in ancient Egypt. J Egypt Archaeol 58:126–132
Li Y-J, Ye S, Wang C-H et al (2014) Temperature-dependent near-infrared emission of highly concentrated Cu^{2+} in $CaCuSi_4O_{10}$ phosphor. J Mater Chem C 2:10395–10402. https://doi.org/10.1039/C4TC01966K
Li M, Wang J, Ma Q (2015a) The effect of lead additives on ancient Chinese purple pigment synthesis. J Cult Herit 16:575–578. https://doi.org/10.1016/j.culher.2014.09.007
Li QH, Yang JC, Li L et al (2015b) Identification of the man-made barium copper silicate pigments among some ancient Chinese artifacts through spectroscopic analysis. Spectrochim Acta Part A Mol Biomol Spectrosc 138:609–616. https://doi.org/10.1016/j.saa.2014.11.060
Lilyquist C, Brill RH, Wypyski MT (1993) Studies in early Egyptian glass. Metropolitan Museum of Art, New York
Lin Y (2018) Reconstruction of ancient production technology of Chinese blue pigment and synthesis of Chinese Blue nanoscrolls as a novel optical material. University of California, Los Angeles
Linn R, Tepper Y, Bar-Oz G (2017) Visible induced luminescence reveals invisible rays shining from Christ in the early Christian wall painting of the Transfiguration in Shivta. PLoS One 12:1–16. https://doi.org/10.1371/journal.pone.0185149
Linn R, Comelli D, Valentini G et al (2018) Egyptian blue pigment in East Mediterranean wall paintings: a study of the lifetime of its optical infrared emission. Strain. https://doi.org/10.1111/str.12277
Liu Z, Mehta A, Tamura N et al (2007) Influence of Taoism on the invention of the purple pigment used on the Qin terracotta warriors. J Archaeol Sci 34:1878–1883. https://doi.org/10.1016/j.jas.2007.01.005
Lluveras A, Torrents A, Giráldez P, Vendrell-Saz M (2010) Evidence for the use of Egyptian Blue in an 11th century mural altarpiece by sem-eds, FTIR and SR XRD (Church Of Sant Pere, Terrassa, Spain). Archaeometry 52:308–319. https://doi.org/10.1111/j.1475-4754.2009.00481.x
Lucas A (1934) Ancient Egyptian materials and industries. Edward Arnold, London
Lucas A, Harris JR (1962) Ancient Egyptian materials and industries. Edward Arnold, London
Ma Q, Portmann A, Wild F, Berke H (2006) Raman and SEM studies of man-made barium copper silicate pigments in ancient Chinese artifacts. Stud Conserv 51:81–98. https://doi.org/10.1179/sic.2006.51.2.81
Ma Q, Zhang Z, Scott DA et al (2016) Microstructure and composition of Ancient Chinese octagonal sticks from the warring states period (475–221 BC). In: Gan F, Li Q, Henderson J (eds) Recent advances in the scientific research on ancient glass and glaze, vol 2. World Century Publishing Corp., pp 455–488. https://doi.org/10.1142/9341
Mairinger F, Schreiner M (1986) Deterioration and preservation of Carolingian and medieval mural paintings in the Müstair Convent (Switzerland)—Part II: materials and rendering of the Carolingian wall paintings. In: Bromelle NS, Smith P (eds) Case studies in the conservation of stone and wall paintings: contributions to the 1986 IIC Congress. International Institute for Conservation, London, pp 195–196
Marabelli M, Santopadre P, Bianchetti P (2006) I frammenti dipinti altomedievali di Santa Susanna in Roma: nota analitica sui materiali e sulla tecnica. Boll ICR Nuova Ser 13:64–72
Marler B, Gies H (2012) Hydrous layer silicates as precursors for zeolites obtained through topotactic condensation: a review. Eur J Mineral 24:405–428. https://doi.org/10.1127/0935-1221/2012/0024-2187
Martín D, Moro D, Ulian G, Valdrè G (2020) Monte Carlo SEM-EDS nano-microanalysis strategy of historical mineral pigments: the simulation of the Egyptian blue from Pompeii (Italy) as an example. Minerals 10:1–17. https://doi.org/10.3390/min10090807
Masic A, Nicola M (2021) NIR luminescence and composition of Egyptian blue as markers in archaeometric evaluations. Microsc Microanal 27:3004–3006. https://doi.org/10.1017/s1431927621010448
Masse S, Boch P, Vaissière N (1999) Trapping of nickel and cobalt in $CaNiSi_2O_6$ and $CaCoSi_2O_6$ diopside-like phases in heat-treated cement. J Eur Ceram Soc 19:93–98. https://doi.org/10.1016/S0955-2219(98)00114-9
Masunaga SH, Rebello A, Schye AT et al (2015) Heat capacity, thermal expansion and heat transport in the Han Blue ($BaCuSi_4O_{10}$): observation of structural phase transitions. J Phys Chem Solids 85:69–74. https://doi.org/10.1016/j.jpcs.2015.04.021
Mazurenko VV, Valentyuk MV, Stern R, Tsirlin AA (2014) Nonfrustrated interlayer order and its relevance to the bose-einstein condensation of magnons in $BaCuSi_2O_6$. Phys Rev Lett 112:1–5. https://doi.org/10.1103/PhysRevLett.112.107202
Mazzi F, Pabst A (1962) Reexamination of cuprorivaite. Am Mineral 47:409–411
Mazzocchin GA, Agnoli F, Mazzocchin S, Colpo I (2003) Analysis of pigments from Roman wall paintings found in Vicenza. Talanta 61:565–572. https://doi.org/10.1016/S0039-9140(03)00323-0
Mazzocchin GA, Rudello D, Bragato C, Agnoli F (2004) A short note on Egyptian blue. J Cult Herit 5:129–133. https://doi.org/10.1016/j.culher.2003.06.004
McKeown DA, Bell MI (1997) Four-membered silicate rings: vibrational analysis of and implications for glass structure. Phys Rev B Condens Matter Mater Phys 56:3114–3121. https://doi.org/10.1103/PhysRevB.56.3114
McKeown DA, Bell MI (1998) Linked four-membered silicate rings: vibrational analysis of Gillespite. Phys Chem Miner 25:273–281. https://doi.org/10.1007/s002690050114
Milanesi G (2017) Qualche riflessione sull'architettura e sull'affresco di San Lorenzo a Fossacaprara (Cremona). In: Schiavi LC, Caldano S, Gemelli F (eds) La lezione gentile. Scritti di storia dell'arte per Anna Maria Segagni Malacart—Storia dell'architettura e della città antica, medievale e moderna. Franco Angeli, Milan, pp 403–412
Miletich R, Allan DR, Angel RJ (1997) The synthetic Cr^{2+} silicates $BaCrSi_4O_{10}$ and $SrCrSi_4O_{10}$: the missing links in the gillespite-type $ABSi_4O_{10}$ series. Am Mineral 82:697–707
Minguzzi C (1938) Cuprorivaite: un nuovo minerale. Period Di Mineral 3:333–345
Mirti P, Appolonia L, Casoli A et al (1995) Spectrochemical and structural studies on a roman sample of Egyptian blue. Spectrochim Acta Part A Mol Spectrosc 51:437–446. https://doi.org/10.1016/0584-8539(94)E0108-M
Moorey PRS (1985) Materials and Manufacture in Ancient Mesopotamia. The evidence of Archaeology and Art. Metals and metalwork, glazed materials and glass. BAR Int Ser 237

Mottana A (2006) Storia delle scienze sperimentali. Đ Nicander on stones and inorganic materials. Rend Fis Acc Lincei 17:333–353
Moussa A, Ali MF (2013) Color alteration of ancient Egyptian blue faience. Int J Archit Herit 7:261–274. https://doi.org/10.1080/15583058.2011.634960
Moussa AMA, Kantiranis N, Voudouris KS et al (2009) The impact of soluble salts on the deterioration of pharaonic and coptic wall paintings at Al Qurna, Egypt: mineralogy and chemistry. Archaeometry 51:292–308. https://doi.org/10.1111/j.1475-4754.2008.00422.x
Moussa A, Badawy M, Saber N (2021) Chromatic alteration of Egyptian blue and Egyptian green pigments in pharaonic late period tempera murals. Sci Cult 7:1–15. https://doi.org/10.5281/zenodo.4465458
Needham SP, Bimson M (1988) Late bronze age Egyptian blue at Runnymede. Antiq J 2:314–315
Nicholson PT (2007) Brilliant things for Akhenaten—the production of glass, vitreous materials and pottery at Amarna. Short Run Press Ltd, Exeter
Nicholson PT (2010) Kilns and firing structures. UCLA Encycl Egyptol 1:1–10
Nicholson PT (2012) "Stone … That Flows": Faience and Glass as Man-Made Stones in Egypt. J Glass Stud 54:11–23
Nicholson PT, Henderson J (2000) Glass. In: Nicholson PT, Shaw I (eds) Ancient Egyptian materials and technology. Cambridge University Press, Cambridge
Nicola M (2019) Ancient materials inspiring new technologies: the Egyptian blue. Università di Torino, Turin
Nicola M, Nicola A (2018) Study of the Egyptian blue pigment through the visible induced luminescence photography (VIL) on different artifacts. In: Conservation of cultural heritage international bursa symposium 2017. Bursa Metropolitan Municipality, Bursa, Turkey, pp 119–134
Nicola M, Aceto M, Gheroldi V et al (2018a) Egyptian blue in the Castelseprio mural painting cycle. Imaging and evidence of a non-traditional manufacture. J Archaeol Sci Rep 19:465–475. https://doi.org/10.1016/j.jasrep.2018.03.031
Nicola M, Musso S, Petacchi S (2018b) Non invasive diagnostic techniques in the authentication and study of Egyptian coffins The case of the anthropoid coffin of Pakharu, son of Panehesy and the cartonnage of Asetirdis in the Stibbert Museum, Florence. In: Dawson J, Strudwick H (eds) Ancient Egyptian coffins: past–present–future. Oxbow Books, Oxford, pp 135–144
Nicola M, Seymour LM, Aceto M et al (2019) Late production of Egyptian blue: synthesis from brass and its characteristics. Archaeol Anthropol Sci 11:5377–5392. https://doi.org/10.1007/s12520-019-00873-w
Nicola M, Scalesse R, Coluccia S (2006) Elaborazione ed applicazione di un sistema di pulitura per l'assottigliamento di strati di carbonatazione su superficie murale dipinta sensibile, realizzato mediante soluzioni acquose addensate a pH debolmente acido. In: IV Congresso Nazionale IGIIC—Lo Stato dell'Arte—Siena 28–30 Settembre 2006. pp 133–140
Nicolini L, Porta P (1970) Preparation, X-ray and magnetic investigations of some silicates containing transition metal ions. Gazetta Chim Ital 79:923–930
Onoratini G, Conrad G, Michaud L (1987) Identification de deux silicates de cuivre de synthese, confondus sous l'appellation generique de "bleu egyptien", et definition des ceramiques "bleu antique" retrouvees dans les fresques. Comptes Rendus L'acad Des Sci 304(2):651–655
Ormanci O (2020) Non-destructive characterization of Egyptian Blue cakes and wall painting fragments from the east of Lake Van, Turkey. Spectrochim Acta Part A Mol Biomol Spectrosc 229:117889. https://doi.org/10.1016/j.saa.2019.117889
Orna MV, Fontani M (2022) The modernity of ancient pigments: a historical approach. Colorants 1:307–346
Orna MV, Low MJD, Baer NS (1980) Synthetic blue pigments: ninth to sixteenth centuries. I. Literature. Stud Conserv 25:53–63
Orsega EF, Agnoli F, Mazzocchin GA (2006) An EPR study on ancient and newly synthesised Egyptian blue. Talanta 68:831–835. https://doi.org/10.1016/j.talanta.2005.06.001
Osanna M, Rescigno C (2022) Il blu egizio in età classica: fonti e testimonianze. In: Atti dei Convegni Lincei 343—Il blu egizio dall'antichità al Rinascimento. 25 febbraio 2021. Bardi Edizioni, pp 33–51
Oudbashi O, Hessari M (2020) A "Western" imported technology: an analytical study of the Achaemenid Egyptian blue objects. J Cult Herit 47:246–256. https://doi.org/10.1016/j.culher.2020.11.001
Pabst A (1943) Crystal structure of gillespite, $BaFeSi_4O_{10}$. Am Mineral 28:372–390
Pabst A (1958) The structure of leached gillespite, a sheet silicate. Am Mineral 43:970–980
Pabst A (1959) Structures of some tetragonal sheet silicates. Acta Crystallogr 12:733–739. https://doi.org/10.1107/S0365110X59900216X
Pagès-Camagna S, Colinart S (2003) The Egyptian green pigment: its manufacturing process and links to Egyptian Blue*. Archaeometry 45:637–658
Pagès-Camagna S, Colinart S (2006) Reply to comments on the article "The Egyptian Green Pigment: Its Manufacturing Process and Links to Egyptian Blue" in Archeometry 45(4), 2003. Archaeometry 48:710–713
Pagès-Camagna S, Colinart S, Coupry C (1999) Fabrication processes of archaeological Egyptian blue and green pigments enlightened by Raman microscopy and scanning electronic microscopy. J Raman Spectrosc 30:313–317
Pagès-Camagna S, Reiche I, Brouder C et al (2006) New insights into the colour origin of archaeological Egyptian blue and green by XAFS at the Cu K-edge. X-Ray Spectrom 35:141–145. https://doi.org/10.1002/xrs.885
Pagès-Camagna S, Laval E, Vigears D, Duran A (2010) Non-destructive and in situ analysis of Egyptian wall paintings by X-ray diffraction and X-ray fluorescence portable systems. Appl Phys A Mater Sci Process 100:671–681. https://doi.org/10.1007/s00339-010-5667-3
Panagiotaki M, Maniatis Y, Kavoussanaki D et al (2004) The production technology of Aegean Bronze age vitreous materials. In: Bourriau J, Phillips J (eds) Invention and innovation. The social context of technological change 2: Egypt, the Aegean and the Near East, 1650–1150 BC. Oxbow Books, Oxford, pp 149–175
Panagiotaki M, Tite M, Maniatis Y (2015) Egyptian Blue in Egypt and Beyond. The Aegean and the Near East
Panagopoulou A, Karanasios K, Xanthopoulou G (2016) Ancient Egyptian blue ($CaCuSi_4O_{10}$) pigment by modern solution combustion synthesis method. Eurasian Chem J 18:31–37. https://doi.org/10.18321/ectj390
Panayotova S, Ricciardi P (2017) Painting the Trinity Hrabanus: materials, techniques and methods of production. Trans Camb Bibliogr Soc 2:227–262. https://doi.org/10.17863/CAM.31749
Pascualini ME, Di Russo NV, Thuijs AE et al (2015) A high-spin square-planar Fe(ii) complex stabilized by a trianionic pincer-type ligand and conclusive evidence for retention of geometry and spin state in solution. Chem Sci 6:608–612. https://doi.org/10.1039/C4SC02634A
Paynter S (2008) Links between glazes and glass in mid-2nd millennium BC Mesopotamia and Egypt. In: Tite MS, Shortland A (eds) Production technology of faience and related early vitreous materials. Oxford U. School of Archaeology, Oxford, pp 93–108

Perez-Rodriguez JL, de Haro MCJ, Siguenza B, Martinez-Blanes JM (2015) Green pigments of Roman mural paintings from Seville Alcazar. Appl Clay Sci 116–117:211–219. https://doi.org/10.1016/j.clay.2015.03.016

Phelps M, Freestone IC, Gorin-Rosen Y, Gratuze B (2016) Natron glass production and supply in the late antique and early medieval Near East: the effect of the Byzantine-Islamic transition. J Archaeol Sci 75:57–71. https://doi.org/10.1016/j.jas.2016.08.006

Philokyprou M (2013) The earliest use of lime and gypsum mortars in Cyprus. In: Válek J, Hughes JJ, Groot CJWP (eds) Historic mortars: characterisation, assessment and repair. RILEM Bookseries, Berlin, pp 25–35

Piovesan R, Maritan L, Amatucci M et al (2016) Wall painting pigments of Roman Empire age from Syria Palestina province (Israel). Eur J Mineral 28:435–448. https://doi.org/10.1127/ejm/2015/0027-2500

Pisareva SA, Shibanova IN, Kadikova IF et al (2021) Identification of $CaCuSi_4O_{10}$ (Egyptian blue) in the "Birch. Spring" painting by Robert Falk (1907) using photoluminescence. J Cult Herit 50:126–138. https://doi.org/10.1016/j.culher.2021.05.005

Plesters J (1966) Ultramarine blue, natural and artificial. Stud Conserv 11:62–75. https://doi.org/10.1179/sic.1966.009

Pozza G, Ajò D, Chiari G et al (2000) Photoluminescence of the inorganic pigments Egyptian blue, Han blue and Han purple. J Cult Herit 1:393–398. https://doi.org/10.1016/S1296-2074(00)01095-5

Pradell T, Salvado N, Hatton GD, Tite MS (2006) Physical processes involved in production of the ancient pigment, Egyptian blue. J Am Ceram Soc 89:1426–1431. https://doi.org/10.1111/j.1551-2916.2005.00904.x

Prieto-Taboada N, Fdez-Ortiz de Vallejuelo S, Santos A et al (2021) Understanding the degradation of the blue colour in the wall paintings of Ariadne's house (Pompeii, Italy) by non-destructive techniques. J Raman Spectrosc 52:85–94. https://doi.org/10.1002/jrs.5941

Puphal P, Sheptyakov D, Van Well N et al (2016) Stabilization of the tetragonal structure in $(Ba1\text{-}xSrx)CuSi_2O_6$. Phys Rev B 93:1–9. https://doi.org/10.1103/PhysRevB.93.174121

Qin Y, Wang YH, Chen X et al (2016) A discussion on the emergence and development of ancient Chinese artificial barium copper silicate pigments from simulation experiments. Archaeometry 58:796–806. https://doi.org/10.1111/arcm.12205

Quirke S (2001) Colour vocabulary. In: Davies WV (ed) Colour and painting in ancient Egypt. British Museum Press, London, pp 186–192

Rademakers FW, Rehren T, Pernicka E (2017) Copper for the Pharaoh: Identifying multiple metal sources for Ramesses' workshops from bronze and crucible remains. J Archaeol Sci 80:50–73. https://doi.org/10.1016/j.jas.2017.01.017

Raehlmann E (1914) Mikroskopische Untersuchungen iiber die in den verschiedenen Kunstperioden der Malerei verwendeten Farbstoffe. Miinchener Kunsttechnische Blatter 10:1–38

Ramadan S, Mahgoub G, Abdel-Aziz MS et al (2019) Study of the antifungal effects of copper-based pigments and synthesized nanomaterial on mural painting-deteriorated fungi in the Egyptian museum in Tahrir. J Archit Arts Humanist Sci 4:46–68. https://doi.org/10.12816/mjaf.2019.11995.1138

Rehren T (2008) A review of factors affecting the composition of early Egyptian glasses and faience: alkali and alkali earth oxides. J Archaeol Sci 35:1345–1354. https://doi.org/10.1016/j.jas.2007.09.005

Rehren T, Pusch EB, Herold A (2001) Qantir-Piramesses and the organisation of the Egyptian glass industry. In: Shortland A (ed) The social context of technological change: Egypt and the Near East, 1650–1150 BC. Oxbow Books, Oxford, pp 223–238

Rendón-Angeles JC, Quiñones-Gurrola JR, López-Cuevas J et al (2021) Rapid one-pot hydrothermal reaction for preparing $BaCu_2Si_2O_7$ fine particles with controlled blue colour tonality. Ceram Int 47:9354–9365. https://doi.org/10.1016/j.ceramint.2020.12.066

Rescigno C, Sampaolo V (2005) Note sull'utilizzo del colore nelle terrecotte architettoniche di Capua. Mediterr II 133–163

Rieck B, Pristacz H, Giester G (2015) Colinowensite, $BaCuSi_2O_6$, a new mineral from the Kalahari Manganese Field, South Africa and new data on wesselsite, $SrCuSi_4O_{10}$. Mineral Mag 79:1769–1778. https://doi.org/10.1180/minmag.2015.079.7.04

Riederer J (1997) Egyptian Blue. In: FitzHugh EW (ed) Artists' Pigments: a handbook of their history and characteristics, vol 3. National Gallery of Art, Washington, pp 23–45

Rodler AS, Artioli G, Klein S et al (2017) Provenancing ancient pigments: lead isotope analyses of the copper compound of egyptian blue pigments from ancient mediterranean artefacts. J Archaeol Sci Rep 16:1–18. https://doi.org/10.1016/j.jasrep.2017.09.008

Rodler AS, Matthys SM, Brøns C et al (2021) Investigating the provenance of Egyptian blue pigments in ancient Roman polychromy. Archeometriai Muh 18:97–108. https://doi.org/10.55023/issn.1786-271x.2021-008

Rodler AS, Kostomitsopoulou Marketou A (2022) Supplying the Mediterranean world with Egyptian blue: an archaeometric perspective

Roger P (2007) Étude des couleurs et de la pratique picturale. Art L'enluminure L'évangéliaire Charlemagne 20:46–65

Roger P, Barrandon JN, Bos A (2004) Discovering of the Egyptian blue employment for the decoration in a 10th century manuscript, characterised by absorption in diffuse reflectance spectrometry. In: Arantegui P (ed) Proceedings of 34th International Symposium on Archaeometry, Zaragoza, 3–7 May 2004. Institución Ferrando el Católico, Zaragoza, pp 341–345

Rösch O, Vojta M (2007) Reduced dimensionality in layered quantum dimer magnets: frustration vs. inhomogeneous condensates. Phys Rev B Condens Matter Mater Phys 76:1–21. https://doi.org/10.1103/PhysRevB.76.224408

Rosenquist AM (1959) Analyser av sverd og skjold fra bo-funnet = Analysis of sword and shield from the Bo-find. Viking 23:29–34

Rotondi Terminiello G (1978) Il restauro della lunetta del portale maggiore. In: Floriani A De, Fusconi G, Mazzino E (eds) Restauri in Liguria. Genova, pp 224–226

Rowland ID (1999) Vitruvius—De Architectura. In: Ten Books on Architecture. Cambridge University Press, Cambridge

Rowland I (2011) The Fra Giocondo Vitruvius at 500 (1511–2011). J Soc Archit Hist 70:285–289. https://doi.org/10.1080/03632415.2013.813484

Sakr AA, Ghaly MF, Geight ESF, Abdel-Haliem MEF (2016) Characterization of grounds, pigments, binding media, and varnish coating of the Angel Michael' icon, 18th century. Egypt J Archaeol Sci Rep 9:347–357. https://doi.org/10.1016/j.jasrep.2016.08.039

Salerno CS (1997) "Cartapeste d'autore" berniniane e algardiane, contributo alla storia, alla tecnica e al restauro della cartapesta nelle botteghe rinascimentali e barocche. Boll D'arte 99:67–98

Salguero TT, Johnson-McDaniel D, Barrett CA et al (2014) Nanoscience of metal silicate-based pigments. MRS Proc. https://doi.org/10.1557/opl.2014.465

Samuel D (2002) Bread in archaeology. Civilisations. https://doi.org/10.4000/civilisations.1353

Samulon EC, Islam Z, Sebastian SE et al (2006) Low-temperature structural phase transition and incommensurate lattice modulation in the spin-gap compound $BaCuSi_2O_6$. Phys Rev B Condens Matter Mater Phys 73:2–5. https://doi.org/10.1103/PhysRevB.73.100407

Santopadre P, Tamanti G, Bianchetti P, Sidoti G (2011) Studio delle tracce di pigmenti azzurri in due affreschi della chiesa inferiore di San Clemente a Roma. Boll ICR Nuova Ser 22–23:85–95

Schaller WT (1922) Gillespite, a new mineral. J Washingt Acad Sci 12(1):7–8
Schaller WT (1929) The properties and associated minerals of gillespite. Am Mineral 14(9):319–322
Schiegl S, El Goresy A (2006) Comments on S. Pages-Camagna and S. Colinart, "The Egyptian green pigments: Its manufacturing process and links to Egyptian blue, Archaeometry, 45(4) (2003). Archaeometry 48:707–709. https://doi.org/10.1111/j.1475-4754.2006.282_1.x
Schiegl S, Weiner KL, El GA (1989) Discovery of copper chloride cancer in ancient Egyptian polychromic wall paintings and faience: a developing archaeological disaster. Naturwissenschaften 76:393–400. https://doi.org/10.1007/BF00366160
Schiegl S, Weiner KL, El Goresy A (1992) The diversity of newly discovered deterioration patterns in ancient egyptian pigments: consequences to entirely new restoration strategies and to the egyptological colour symbolism. In: Vandiver PB, Druzik JR, Wheeler JR (eds) Materials issues in art and archaeology III. Materials Research Society, Pittsburgh, pp 831–858
Schippa G, Torraca G (1957) Contributo alla conoscenza del bleu egiziano. Boll Dell'istituto Cent per Restauro 31–32:97–107
Schofield PF, Van Der Laan G, Henderson CMB, Cressey G (1998) A single crystal, linearly polarized Fe 2p X-ray absorption study of gillespite. Mineral Mag 62:65–75
Schvoerer M, Delavergne M-C, Chapoulie R (1988) The thermoluminescence (TL) of Egyptian Blue. Int J Radiat Appl Instrum Part D Nucl Tracks Radiat Meas 14:321–327. https://doi.org/10.1016/1359-0189(88)90083-0
Scott DA (2016) A review of ancient Egyptian pigments and cosmetics. Stud Conserv 61:185–202. https://doi.org/10.1179/2047058414Y.0000000162
Sebastian SE, Harrison N, Batista CD et al (2006a) Dimensional reduction at a quantum critical point. Nature 441:617–620. https://doi.org/10.1038/nature04732
Sebastian SE, Tanedo P, Goddard PA et al (2006b) Role of anisotropy in the spin-dimer compound $BaCuSi_2O_6$. Phys Rev B Condens Matter Mater Phys 74:2–5. https://doi.org/10.1103/PhysRevB.74.180401
Selvaggio G, Kruss S (2022) Preparation, properties and applications of near-infrared fluorescent silicate nanosheets. Nanoscale 14:9553–9575. https://doi.org/10.1039/d2nr02967g
Selvaggio G, Chizhik A, Nißler R et al (2020) Exfoliated near infrared fluorescent silicate nanosheets for (bio)photonics. Nat Commun. https://doi.org/10.1038/s41467-020-15299-5
Selvaggio G, Weitzel M, Oleksiievets N et al (2021) Photophysical properties and fluorescence lifetime imaging of exfoliated near-infrared fluorescent silicate nanosheets. Nanoscale Adv 3:4541–4553. https://doi.org/10.1039/d1na00238d
Sethe K (1961) Urkunden der 18. Dynastie. Band 3. 636/638. Akademie-Verlag Berlin und Verlagsanstalt Graz
Settis S (2022) Galatea dagli occhi blu egizio. In: Atti dei Convegni Lincei 343 - Il blu egizio dall'antichità al Rinascimento. 25 febbraio 2021. Bardi Edizioni, pp 63–66
Seymour LM, Nicola M, Kessler M et al (2020) On the production of ancient Egyptian blue: multi-modal characterization and micron-scale luminescence mapping. PLoS One 15:1–13. https://doi.org/10.1371/journal.pone.0242549
Sgamellotti A, Anselmi C (2022) An evergreen blue. Spectroscopic properties of Egyptian blue from pyramids to Raphael, and beyond. Inorg Chim Acta 530:120699. https://doi.org/10.1016/j.ica.2021.120699
Shearman JK, Staff BH (2003) Raphael in early modern sources (1483–1602), vol 1. Yale University Press, New Haven
Sheptyakov DV, Pomjakushin VY, Stern R et al (2012) Two types of adjacent dimer layers in the low-temperature phase of $BaCuSi_2O_6$. Phys Rev B Condens Matter Mater Phys. https://doi.org/10.1103/PhysRevB.86.014433
Shortland AJ (2004) Evaporites of the Wadi Natrun: seasonal and annual variation and its implication for ancient exploitation. Archaeometry 46:497–516. https://doi.org/10.1111/j.1475-4754.2004.00170.x
Shortland AJ (2012) Lapis lazuli from the kiln: glass and glassmaking in the Late Bronze Age. Leuven University Press, Leuven
Shortland A, Schachner L, Freestone I, Tite MS (2006a) Natron as a flux in the early vitreous materials industry: sources, beginnings and reasons for decline. J Archaeol Sci 33:521–530. https://doi.org/10.1016/J.JAS.2005.09.011
Shortland AJ, Tite MS, Ewart I (2006b) Ancient exploitation and use of cobalt alums from the Western Oases of Egypt. Archaeometry 48:153–168. https://doi.org/10.1111/j.1475-4754.2006.00248.x
Shortland AJ, Degryse P, Walton M et al (2011) The evaporitic deposits of lake fazda (Wadi Natrun, Egypt) and their use in Roman glass production. Archaeometry 53:916–929. https://doi.org/10.1111/j.1475-4754.2010.00573.x
Skovmøller A, Brøns C, Sargent ML (2016) Egyptian blue: modern myths, ancient realities. J Rom Archaeol 29:371–387. https://doi.org/10.1017/S1047759400072184
Sobik P, Jeremiasz O, Nowak P et al (2021) Towards efficient luminescent solar energy concentrator using cuprorivaite infrared phosphor ($CaCuSi_4O_{10}$)—effect of dispersing method on photoluminescence intensity. Mater MDPI. https://doi.org/10.3390/ma14143952
Song XQ, Xie MQ, Du K et al (2019) Synthesis, crystal structure and microwave dielectric properties of self-temperature stable Ba1-xSrxCuSi$_2$O$_6$ ceramics for millimeter-wave communication. J Mater 5:606–617. https://doi.org/10.1016/j.jmat.2019.07.005
Sparta KM, Roth G (2004) Reinvestigation of the structure of $BaCuSi_2O_6$—evidence for a phase transition at high temperature. Acta Crystallogr Sect B Struct Sci 60:491–495. https://doi.org/10.1107/S0108768104011644
Spring M, Billinge R, Verri G (2019) A note on an occurrence of Egyptian blue in Garofalo's the holy family with Saints Elizabeth, Zacharias, John the Baptist (and Francis?). Natl Gall Tech Bull 40:74–85
Spurrell FJC (1895) Notes on Egyptian colours. Archaeol J 52:223–239
Stebbins JF (2017) Toward the wider application of 29Si NMR spectroscopy to paramagnetic transition metal silicate minerals: copper(II) silicates. Am Mineral 102:2406–2414. https://doi.org/10.2138/am-2017-6176
Stern R, Heinmaa I, Joon E et al (2014) Low-temperature high-resolution solid-state (cryoMAS) NMR of Han Purple $BaCuSi_2O_6$. Appl Magn Reson 45:1253–1260. https://doi.org/10.1007/s00723-014-0597-4
Strens RGJ (1966) Pressure-induced spin-pairing in gillespite, BaFe(II) Si_4O_{10}. Chem Commun (London) (21):777–778
Sun F, Yan Q, Wang L, Sun Z (2021) Study on the conditions of hydrothermal synthesis of Chinese purple $BaCuSi_2O_6$ and the analysis of its products. Spectrosc Spectr Anal 41:2284
Švarcová S, Hradil D, Hradilová J, Čermáková Z (2021) Pigments—copper-based greens and blues. Archaeol Anthropol Sci. https://doi.org/10.1007/s12520-021-01406-0
Szubka M, Zajdel P, Fijałkowski M et al (2022) Revisiting properties of CaCoSinO2n+2. Crystal and electronic structure. J Magn Magn Mater 546:168858. https://doi.org/10.1016/j.jmmm.2021.168858
Takayasu K (2002) Investigation of ancient glass found in Japan-Historical evolution of ancient glass systems. In: Proceedings of International congress on the conservation and restoration for archaeological objects. Independent Adminstrative Institution

e Nara National Research Institute for Cultural Properties. pp 147–157

Thavapalan S, Stenger J, Snow C (2016) Color and meaning in ancient Mesopotamia: the case of Egyptian blue. Zeitschrift Fur Assyriologie Und Vor Archaeol 106:198–214. https://doi.org/10.1515/za-2016-0014

Thieme C (2001) Paint layers and pigments on the Terracotta Army: A comparison with other cultures of antiquity. In: Yongqi W, Tingbao Z, Petzet M et al (eds) The Polychromy of antique sculptures and the terracotta Army of the first Chinese emperor: studies on materials, painting techniques, and conservation. International conference in Xi'an, Shaanxi museum, march 22–28, 1999. Bayerisches Landesamt für Denkmalpflege, München, pp 52–58

Thurman RB, Gerba CP, Bitton G (1989) The molecular mechanisms of copper and silver ion disinfection of bacteria and viruses. Crit Rev Environ Control 184:295–315. https://doi.org/10.1080/10643388909388351

Tian T, Wu C, Chang J (2016) Preparation and in vitro osteogenic, angiogenic and antibacterial properties of cuprorivaite ($CaCuSi_4O_{10}$, Cup) bioceramics. RSC Adv 6:45840–45849. https://doi.org/10.1039/C6RA08145B

Tite MS, Hatton GD (2007) The production technology of, and trade in, Egyptian blue pigment in the Roman World. In: Godsen C, Hamerow H, de Jersey P, Lock G (eds) Communities and connections: essays in honour of Barry Cunliffe. Oxford University Press, Oxford, pp 75–92

Tite MS, Shortland AJ (2003) Production technology for copper- and cobalt-blue vitreous materials from the New Kingdom site of Amarna—a reappraisal. Archaeometry 45:285–312. https://doi.org/10.1111/1475-4754.00109

Tite MS, Shortland AJ (2008) Production technology of faience and related early vitreous materials. Oxford U. School of Archaeology, Oxford

Tite MS, Bimson M, Cowell MR (1984) Technological examination of Egyptian blue. In: Archaeological chemistry III. American Chemical Society, pp 215–242

Tite MS, Bimson M, Cowell MR (1987) The technology of Egyptian blue. In: Bimson M, Freestone I (eds) Early vitreous materials. British Museum Occasional Paper 56. British Museum Press, London, pp 39–46

Toropov NA (1962) Barium dimetasilicates with layer structures: $MgBaSi_4O_{10}$ and $Ba_2Si_4O_{10}$. Russ J Inorg Chem 2:172–177

Tsukada I, Sasago Y, Uchinokura K et al (1999) $BaCu_2Si_2O_7$: a quasi-one-dimensional S = 1/2 antiferromagnetic chain system. Phys Rev B Condens Matter Mater Phys 60:6601–6607. https://doi.org/10.1103/PhysRevB.60.6601

Turner WES (1956) Studies in ancient glasses and glassmaking processes, part V. Raw materials and melting processes. J Soc Glas Technol 40:277–300

Ullrich D (1979) Ägyptisch Blau. Bildungsbedingungen und Rekonstruktionsversuch der antiken Herstellungstechniken. Freie Universität, Berlin

Ullrich D (1987) Egyptian blue and green frit: characterization, history and occurrence, synthesis. In: Delamanre F, Hackens T, Helly B (eds) PACT vol 17. Datation-Caractérisation des peintures pariétales et murales

van Well N, Puphal P, Wehinger B et al (2016) Influence of the oxygen concentration on crystal growth and structure of the $BaCuSi_2O_6{\pm}\delta$ and Ba1-xSrxCuSi$_2$O$_6{\pm}\delta$ spin dimer compounds. Acta Crystallogr Sect A Found Adv 72:s325–s326. https://doi.org/10.1107/s2053273316095140

Verri G (2008) The use and distribution of Egyptian blue: a study by visible-induced luminescence imaging. In: Uprichard K, Middleton A (eds) The Nebamun Wall Paintings. Archetype, pp 41–50

Verri G (2009) The spatially resolved characterisation of Egyptian blue, Han blue and Han purple by photo-induced luminescence digital imaging. Anal Bioanal Chem 394:1011–1021. https://doi.org/10.1007/s00216-009-2693-0

Verri G, Saunders D, Ambers J, Sweek T (2010) Digital maping of Egyptian Blue: conservation implications. Stud Conserv 55:220–224. https://doi.org/10.1179/sic.2010.55.supplement-2.220

Vettori S, Bracci S, Cantisani E et al (2019) Archaeometric and archaeological study of painted plaster from the Church of St. Philip in Hierapolis of Phrygia (Turkey). J Archaeol Sci Rep 24:869–878. https://doi.org/10.1016/j.jasrep.2019.03.008

Vezin MJ, Roger P (2007) Étude des matériaux de la couleur dans les manuscrits médiévaux: Emploi inédit de bleu égyptien dans trois manuscrits des VIIIe et Xe siècles. Comptes Rendus Des Séances L'acad Des Inscr B Lett 1:67–87. https://doi.org/10.3406/crai.2007.87610

Wang Y, Ma H, Chen K et al (2017) Identification of PbO (BaO) faience from an early and middle Warring States period cemetery at Zhaitouhe, northern Shaanxi, China. Archaeometry 61:43–54. https://doi.org/10.1111/arcm.12401

Warner TE (2011) Artificial cuprorivaite $CaCuSi_4O_{10}$ (Egyptian blue) by a salt-flux method. In: Synthesis, properties and mineralogy of important inorganic materials. Wiley, Chichester(UK), pp 26–49

Wei S, Ma Q, Schreiner M (2012) Scientific investigation of the paint and adhesive materials used in the Western Han dynasty polychromy terracotta army, Qingzhou, China. J Archaeol Sci 39:1628–1633. https://doi.org/10.1016/j.jas.2012.01.011

Wenerstrom B, Kantardzic M (2011) Enhanced visualization for web-based summaries. CEUR Workshop Proc 880

Whitehouse D (2014) The "proto-history" of Venetian glassmaking. In: Keller D, Price J, Jackson C (eds) Neighbours and successors of Rome. Traditions of glass production and use. Oxbow Books, Oxford, pp 73–78

Wiedemann HG, Bayer G (1997) Formation and stability of Chinese barium copper-silicate pigments. In: Agnew N (ed) Conservation of ancient sites on the Silk Road: proceedings of an International Conference on the Conservation of Grotto Sites. The Getty Conservation Institute, Los Angeles, pp 379–387

Wiedemann HG, Bayer G (1982) The bust of Nefertiti. Anal Chem 54:619–628. https://doi.org/10.1021/ac00241a001

Wiedemann H-G, Berke H (2001) Chemical and physical investigations of Egyptian and Chinese blue and purple. In: The polychromy of antique sculptures and the terracotta army of the first Chinese emperor: studies on materials, painting techniques and conservation: international conference in Xi'an, Shaanxi History Museum, March 22–28, 1999. pp 147; 154--171

Wiedemann HG, Reller A, Lamprecht I (1996) Investigation on the influence of some ancient pigments on the growth of lichens as artifact-deterioration agents. In: II. Internat. Symposium: The Oxalate Films in the Conservation of Works of Art, March 25–27, Milan 1996. pp 355–358

Xia Y, Wu S, Cui S et al (2008) Study on the Pigments in Polychrome Potteries of West Han Dynasty Tomb in Weishan, Shandong Province. Sci Conserv Archaeol 20:12–20

Xia Y, Ma Q, Zhang Z et al (2014) Development of Chinese barium copper silicate pigments during the Qin Empire based on Raman and polarized light microscopy studies. J Archaeol Sci 49:500–509. https://doi.org/10.1016/j.jas.2014.05.035

Yang H, Downs RT, Evans SH, Pinch WW (2013) Scottyite, the natural analog of synthetic BaCu2Si2O7, a new mineral from the Wessels mine, Kalahari Manganese Fields, South Africa. Am Mineral 98:478–484. https://doi.org/10.2138/am.2013.4326

Yang C, Ma H, Wang Z et al (2021a) 3D printed wesselsite nanosheets functionalized scaffold facilitates NIR-II photothermal therapy and vascularized bone regeneration. Adv Sci 2100894:1–11. https://doi.org/10.1002/advs.202100894

Yang C, Zheng R, Younis MR et al (2021b) NIR-II light-responsive biodegradable shape memory composites based on cuprorivaite

nanosheets for enhanced tissue reconstruction. Chem Eng J 419:129437. https://doi.org/10.1016/j.cej.2021.129437

Yuan B, Huang Y, Yu YM et al (2012) A new blue-emitting phosphor of Eu2 +-doped $BaMgSi_4O_{10}$. Mater Lett 70:57–59. https://doi.org/10.1016/j.matlet.2011.11.061

Yuryev VA, Yuryeva TV, Kadikova IF et al (2023) Photoluminescence and cathodoluminescence of $CaCu(Si_2O_5)_2$. SSRN Electron J. https://doi.org/10.2139/ssrn.4362577

Zaina F, Baraldi P, Cardini V, et al (2019) Archaeometric characterization of a blue ingot from the palace of Sargon II at Karkemish (Turkey) and the distribution and function of egyptian blue in the near east during the iron age. Mesopotamia Riv di Archaeol Epigr e Stor Orient Antica LIV, Univ di Torino 181–196.

Zhang Y, Zhang Y, Zhao X, Zhang Y (2016) Sol-gel synthesis and properties of europium-strontium copper silicates blue pigments with high near-infrared reflectance. Dye Pigment 131:154–159. https://doi.org/10.1016/j.dyepig.2016.04.011

Zhang C, Zhang N, Wang X, Zhang L (2018) Novel preparation of an ancient ceramic pigment $BaCuSi_4O_{10}$ and its performance investigation. Mater Res Bull 101:334–339. https://doi.org/10.1016/j.materresbull.2018.02.002

Zhang Z, Ma Q, Berke H (2019) Man-made blue and purple barium copper silicate pigments and the pabstite ($BaSnSi_3O_9$) mystery of ancient Chinese wall paintings from Luoyang. Herit Sci 7:1–9. https://doi.org/10.1186/s40494-019-0340-4

Zhang Z, Dai Q, Zhang Y et al (2020) Design of a multifunctional biomaterial inspired by ancient Chinese medicine for hair regeneration in burned skin. ACS Appl Mater Interfaces. https://doi.org/10.1021/acsami.9b22769

Zhong J, Zhuo Y, Hariyani S et al (2020) Thermally Robust and Color-Tunable Blue-Green-Emitting $BaMgSi_4O_{10}$:Eu2+, Mn2+Phosphor for Warm-White LEDs. Inorg Chem 59:13427–13434. https://doi.org/10.1021/acs.inorgchem.0c01803

Zhuang Y, Tanabe S (2012a) Forward and back energy transfer between Cu2+ and Yb3+ in Ca1-xCuSi4O10: Ybx crystals. J Appl Phys. https://doi.org/10.1063/1.4765013

Zhuang Y, Tanabe S (2012b) Interactive energy transfer between Cu2+ and Yb3+ in Ca1-x CuSi4O10: Yb x. Phys Status Solidi 9:2304–2307. https://doi.org/10.1002/pssc.201200281

Zuccari A (2022) Raffaello, l'Antico e la Policromia. In: Atti dei Convegni Lincei 343—Il blu egizio dall'antichità al Rinascimento. 25 febbraio 2021. Bardi Editore, pp 13–24

Zuchtriegel G (2018) Bringing the diver home: local élites, artisans, and esotericism in late archaic Paestum. Archeologia classica. L'Erma di Bretschneider, Rome, pp 1–35